WOOD-POLYMER COMPOSITES UTILIZING DEGRADED POLYOLEFINS AS COMPATIBILIZERS

by

Sibusiso Sibongiseni Ndlovu (B.Sc. Hons.)

Submitted in accordance with the requirements for the degree

MASTER OF SCIENCE (M.Sc.)

Department of Chemistry

Faculty of Natural and Agricultural Sciences

at the

UNIVERSITY OF THE FREE STATE (QWAQWA CAMPUS)

SUPERVISOR: PROF A.S. LUYT
CO-SUPERVISOR: PROF A.J. VAN REENEN

December 2011

DECLARATION

I declare that this thesis is my own independent work and that it has not been previously submitted at another university in order to obtain a degree. I furthermore cede copyright of the dissertation in favour of the University of the Free State.

_____ _____

S.S. Ndlovu (Mr) Prof A.S. Luyt (Prof)

DEDICATIONS

Kubobonke ngifisa ukudlulisa ukubonga okukhulu ngendima abayidlalile ukuzengizithole sengiphumelele. Kumathishela namathishelakazi nabo bonke abangivule amehlo, ngithi imbewu eniyitshalile ayiwelanga ematsheni. Mina ngingumvuzo wenu nonke. Ngiyabonga.

I dedicate this work to my whole family of Ndlovu, as well as to my daughter Nomusa Ndlovu and her mom Nokuphiwa Ndlovu.

ABSTRACT

The effect of degraded LDPE (dLDPE) as compatibilizer on the morphology, as well as thermal, mechanical, and thermo-mechanical properties, of LDPE/wood flour (WF) composites was investigated in this study. The composites were prepared through melt mixing in a Brabender Plastograph internal mixer, while the LDPE was thermally degraded in an air oven at 80 °C for different periods of time. The formation of functional groups on the polyethylene chains during the degradation enables the dLDPE to be used as a compatibilizer. Composites with different amounts of WF, compatibilized with dLDPEs having different carbonyl indices, were characterized with scanning electron microscopy (SEM), Fourier-transform infrared (FTIR) spectroscopy, gel permeation chromatography (GPC), differential scanning calorimetry (DSC), thermogravimetric analysis (TGA) and dynamic mechanical analysis (DMA), as well as tensile, impact and hardness testing. Addition of dLDPE as compatibilizer generally enhanced the mechanical properties of the composites. The SEM images show smooth surfaces with fewer voids and fibre pullout for the dLDPE modified composites. The FTIR results show an increase in carbonyl index up to 7 weeks degradation, and the GPC results show that the molecular weight decreased significantly with increasing degradation time. The DSC results show that the presence of WF particles, and increasing filler loading, had very little influence on the melting and crystallization behaviour of the untreated LDPE/WF composites. However, in the dLDPE treated composites a nucleating effect of the fibres gave rise to increased LDPE melting and crystallization enthalpies. There was no significant improvement in the thermal stability of the dLDPE treated composites. The DMA results show that the presence of dLDPE (especially the 7 weeks dLDPE with a carbonyl index of 0.90) observably influenced the viscoelastic properties of the composites. In summary, it was found that the higher carbonyl index dLDPEs are more efficient compatibilizers in LDPE/WF composites, despite their significantly reduced molecular weights.

ABBREVIATIONS

BF	Bamboo fibres
CRYSTAF	Crystallization analysis fractionation
ΔH_m^{obs}	Observed melting enthalpy
ΔH_m^{calc}	Calculated melting enthalpy
DBP	Dibenzoyl-peroxide
dLDPE	Degraded LDPE
DMA/DMTA	Dynamic mechanical analysis/thermal analysis
DSC	Differential scanning calorimetry
EPR-g-MA	Ethylene-propylene rubber grafted with maleic anhydride
f-EPR	Functionalized ethylene propylene rubber
GPC	Gel permeation chromatography
HCl	Hydrochloric acid
HDPE	High-density polyethylene
HDPE-g-MA	High-density polyethylene grafted with maleic anhydride
LDPE	Low-density polyethylene
LLDPE	Linear low-density polyethylene
LLDPE-g-MA	Linear low-density polyethylene grafted with maleic anhydride
LMFI	Low melt flow index
MAH	Maleic anhydride
MA-g-wax	Maleic anhydride grafted Fischer-Tropsch wax
MAPE	Maleic anhydride grafted polyethylene
MFI	Melt flow index
MMFI	Medium melt flow index
nf-EPR	Non-functionalized ethylene-propylene rubber
PE	Polyethylene
PE-EPDM	Polyethylene/ethylene-propylene-diene terpolymer blend
PP	Polypropylene
PP-g-MA	Polypropylene grafted with maleic anhydride
SEM	Scanning electron microscopy
SEC-FTIR	Size exclusion chromatography - Fourier transform infrared spectroscopy

TGA	Thermogravimetric analysis
T_m	Melting temperature
UV	Ultraviolet
WF	Wood fibres

TABLE OF CONTENTS

LIST OF TABLES

LIST OF FIGURES

Chapter 1

Historical information and background

1.1 Introduction

Composites are not a new concept, they combine two or more components of very different properties to form a single new structural product. One of the materials acts as a filler, while the other acts as a matrix. The names as well as the properties of this new structural product depend upon the properties of the each constituent; the interface between the constituents plays a very important role in the ultimate properties of the final composite product.

Composites are widely used in many industries such as in automotives, construction, marine, electronics, and aerospace industries [1-4]. The field of composite materials has grown rapidly in recent years in terms of both industrial applications and fundamental research. Addition of wood in a wood-polymer composites offers more and more advantages.

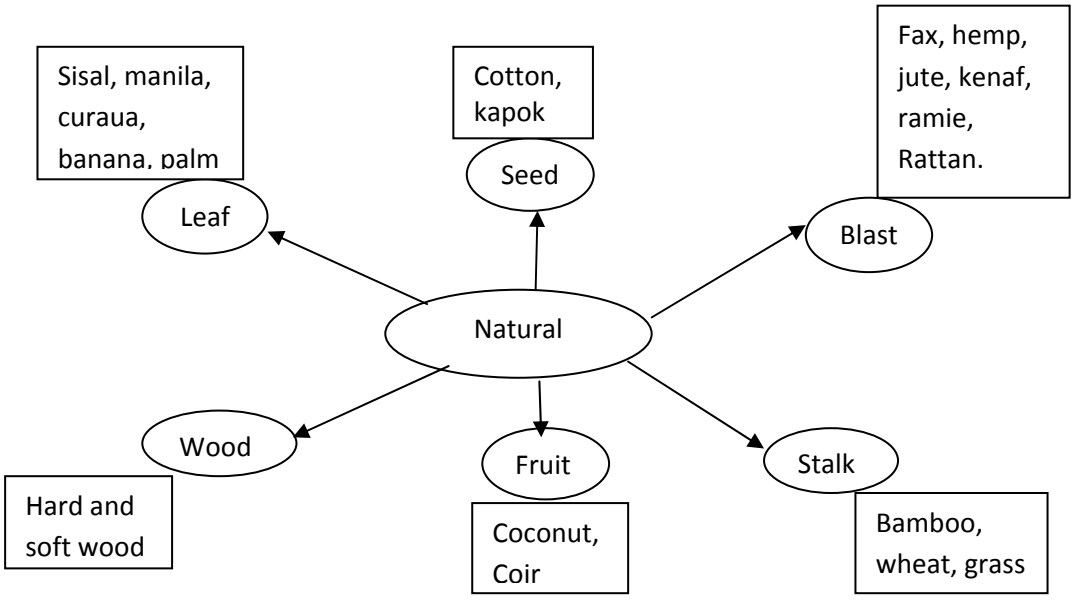

Figure 1.1 Classification of natural fibres [26]

Wood is a natural fibre (see classification in Figure 2). The degree polymerization of natural polymers depends on the part of the plant from which the fibre was extracted.

Man made composites either use ceramics, metals or polymers containing mostly inorganic fibres [5]. These fibres include glass, carbon, aramid (Kevlar), silicon carbide, and aluminium oxide. Table 1.1 compares the properties of natural and synthetic fibres. Synthetic fibres are non-biodegradable and they pollute the environment at the end of their life service, while natural fibres are biodegradable. Natural fibre just decomposes easily preventing environmental pollution compared to synthetic conventional fibres.

Table 1.1 Comparison between natural and glass fibres [8]

Parameter	Natural fibre	Glass fibre
Density	Low	Twice that of natural fibres
Cost	Low	Low but higher than that of natural fibres.
Renewability	Yes	No
Recyclability	Yes	No
Energy consumption	Low	High
Distribution	Wide	Wide
CO_2 neutrality	Yes	No
Abrasion to machines	No	Yes
Health risk when inhaled	No	Yes
Disposable	Biodegradable	Non-biodegradable

These days polymers are the most common matrix for fibre-containing composites. Polymer matrix composites consist of thermoplastic or thermosetting polymers reinforced mostly by natural fibres (e.g. wood fibre). Thermosetting polymers are plastics that once cured, cannot be molded into another shape by melting. These include resins such as epoxies, phenolics, novolacs, polyamides and polyersters. Thermoplastics are plastics which can be repeatedly melted and molded into different shapes. The advantages of thermoplastics over thermosets is that they require low processing cost, they are flexible and easily moldable. Polypropylene (PP), poly(vinyl chloride) (PVC), and polyethylene (PE) are the three thermoplastics that are mostly reinforced by natural fibres such as wood fibre [5].

Wood fibre reinforcement of polymer matrix is attractive due to the fact that wood is generally lightweight, abundantly available, cheap, has no skin irritation, and is user friendly and non toxic. Wood fibre allows easy fibre modification due to the presence of the reactive

groups like hydroxyls, and it can be added to commodity matrices in considerable amounts, thus offering economically and ecologically advantageous solutions.

Wood-polymer composites (WPCs) are produced at low cost. They have low densities, good mechanical properties combined with renewability, reasonable processibility and biodegradability when compared to the neat polymer matrix. This is because wood is obtained from natural resources, available in various forms and in large quantities. The presence of synthetic polymers in WPCs provides better moisture and decay resistance [6-10].

The use of wood in polymer-wood composites does have some drawbacks. The use of wood as a filler or reinforcement in thermoplastics has been hampered by the limited thermal stability of wood, and by the difficulties in obtaining good filler-matrix dispersion and strong interfacial adhesion [5-6]. Other disadvantages are that wood absorbs water, and is less thermally stable (above 150 °C it starts to degrade). Furthermore, WPCs are often more brittle than the neat polymers, which limits their use in applications where these composites are likely to be subjected to impact forces. Some of these disadvantages are due to the natural incompatibility between the hydrophilic wood and hydrophobic polymers. In order to address these drawbacks, the polymer must be fully compatible with lignocellulosic wood fibre. The compatibility or the interfacial adhesion can be improved by using compatibilizers or coupling agents or by modifying the wood surface. Improvement of wood-polymer adhesion is done either physically or chemically [2,7-18]. Physical treatments include methods such as electric discharge, corona, and cold plasma. These treatments can clean the fibre surfaces, and generate some oxygen containing functional groups, like carbonyl, hydroperoxide, and hydroxyl groups, that improve adhesion between polymer matrices and natural fibres. They can also create free radical surface crosslinking between the fibre and the polymer matrices [2]. Chemical treatments include mercerization, acetylation, and treatment with silane, acrylonitriles, iscocyanates, peroxides, and maleated coupling agents [8]. By using these methods, the interface between natural fibres and polymer matrices can be improved significantly *via* formation of real chemical bonds, which take place through grafting and/or crosslinking, acetylation, and esterfication [19-24].

Recently degraded polyolefins seems also to improve interfacial adhesion between filler and polymer matrix due to functional groups on polymer backbone. Heating in air atmosphere

oxidizes polyethylenes and adds functional groups (such as carbonyls, hydroxyls, hydroperoxides, and acids) onto the polymer backbone. These functional groups should then interact more strongly with the cellulose hydroxyls in wood fibre, while the non-polar part of the degraded LDPE should be miscible with the non-degraded polyethylene matrix. Polymers such as polyethylene are semicrystalline consisting of a well ordered crystalline phase and a less ordered amorphous phase. The crystalline lamellae are interconnected by tie chains passing through amorphous interlamellar regions [25-28]. The crystalline lamellae do not absorb oxygen during oxidative degradation, and the degradation is therefore assumed to occur primarily in the amorphous phase [20]. During thermal degradation the tie chains break up and leave chain segments free to recrystallise, which should increase the crystallinity of the polyethylene matrix, but decrease the average molecular weight [29-36].

1.2 Objective of the study

The objective of this study was to investigate the morphology and properties of LDPE-pine wood fibre composites using degraded LDPE as a compatibilizer. The LDPE was thermally degraded at 80 ºC for 5, 7 and 9 weeks. Part of the investigation was to see which degradation period gives the optimally improved properties. The LDPE-wood composites (with and without degraded LDPE as compatibilizer) were then characterized using scanning electron microscopy (SEM), thermogravimetric analysis (TGA), differential scanning calorimetry (DSC), dynamic mechanical analysis (DMA), Fourier-transform infrared spectroscopy (FTIR), as well as tensile, impact and hardness testing.

1.3 Outline of the thesis

This thesis comprises of five chapters.

Chapter 1: Background and objectives
Chapter 2: Literature survey
Chapter 3: Experimental
Chapter 4: Results and discussion
Chapter 5: Conclusions

1.3 References

1. A. Ashori. Wood-plastic composites as promising green-composites for automotive industries. Bioresource Technology 2008; 99:4661-4667.
   DOI: 10.1016/j.biortech.2007.09.043
2. A.K. Bledzi, J. Gassan. Composites reinforced with cellulose based fibres. Progress in Polymer Science 1999; 24:221-274.
   DOI: 10.1016/S0079-6700(98)00018-5
3. http://www.binhaitimes.com/history.html (accessed 14 April 2011).
4. http://www.binhaitimes.com/composite.html (accessed 14 April 2011).
5. S. Taj, M.A. Munawar, S. Khan. Natural fiber-reinforced polymer composites. Proceedings of the Pakistan Academy of Science 2007; 44:129-144.
6. G. Kalaprasad, P. Pradeep, M. George, C. Pavithran, T. Sabu. Thermal conductivity and thermal diffusivity analyses of low-density polyethylene composites reinforced with sisal, glass and intimately mixed sisal/glass fibres. Composites Science and Technology 2000; 60:2967-2977.
   DOI: 10.1016/S0266-3538(00)00162-7
7. S. Mishra, A.K. Mohanty, L.T. Drzal, M. Misra, G.Hinrichsen. A review on pineapple leaf fibers, sisal fibers and their biocomposites. Macromolecular Materials and Engineering 2004; 289:955-974.
   DOI: 10.1002/mame.200400132
8. P. Wambua, J. Ivens, I. Verpoest. Natural fibres: Can they replace glass in fibre reinforced plastics? Composites Science and Technology 2003; 63:1259-1264.
   DOI: 10.1016/S0266-3538(03)00096-4.
9. D. N. Saheb, J.P. Jog. Natural fiber polymer composites: A review. Advances in Polymer Technology 1999; 18:351-363.
   DOI: 10.1002/(SICI)1098-2329(199924)18:4<351
10. E. Chiellini, A. Corti, G. Swift. Biodegradation of thermally-oxidised, fragmented low density polyethylenes. Polymer Degradation and Stability 2003; 81:341-351.
    DOI: 10.1016/S0141-3910(03)00105-8
11. J. Weon. Effect of thermal ageing on the mechanical and thermal behaviors of linear low density polyethylene pipe. Polymer Degradation and Stability 2010; 95:14-20.
    DOI: 10.1016/j.polymdegradstab.2009.10.016

12. I. Ghasemi, M. Farsi. Interfacial behaviour of wood plastic composites: Effect of chemical treatment on wood fibres. Iranian Polymer Journal 2010; 19:811-818.
13. A. Kaboorani. Effect of formulation design on thermal properties of wood / thermoplastic composites. Journal of Composite Materials 2010; 44:2205-2215. DOI: 10.1177/0021998309360938.
14. D.D. Stokke, D.J. Gardner. Fundamental aspects of wood as a component of thermoplastic composites. Journal of Vinyl & Additive Technology 2003; 9:96-104. DOI: 10.1002/vnl.10069
15. Y. Li, Y.W. Mai, L. Ye. Sisal fibre and its composites: A review of recent developments. Composites Science and Technology 2000; 60:2037-2055. DOI: 10.1016/S0266-3538(00)00101-9
16. D.G. Dikobe, A.S. Luyt. Morphology and properties of polypropylene/ethylene vinyl acetate copolymer/wood powder blend composites. eXPRESS Polymer Letters 2009; 3:190-199. DOI: 10.3144/expresspolymerlett. 2009.24
17. M.E. Malunka, A.S. Luyt, H. Krump. Preparation and characterization of EVA-sisal fiber composites. Journal of Applied Polymer Science 2006; 100:1607-1617. DOI: 10.1002/app.23650.
18. K. Van De Velde, P. Kiekens. Influence of fibre surface characteristics on the flax/polypropylene interface. Journal of Thermoplastic Composite Materials 2001; 14:244-260. DOI: 10.1106/13PW-MYJU-8HCJ-B1TI
19. X. Li, L.G. Tabil, S. Panigrahi. Chemical treatments of natural fibre for use in natural fiber-reinforced composites: A review. Journal of Polymers and the Environment 2007; 15:25-33. DOI: 10.1007/s10924-006-0042-3
20. M.J. John, R.D. Anandjiwala. Recent developments in chemical modification and characterization of natural fiber-reinforced composites. Polymer Composites 2008; 29:187-207. DOI: 10.1002/pc.20461
21. S. Kalia, B.S. Kaith, I. Kaur. Pretreatments of natural fibers and their application as reinforcing material in polymer composites: A review. Polymer Engineering and Science 2009; 49:1253-1272. DOI: 10.1002/pen.21328

22. M.A. Sawpan, K.L. Pickering, A. Fernyhough. Effect of various chemical treatments on the fibre structure and tensile properties of industrial hemp fibres. Composites: Part A 2011; 42:888-895.
DOI: 10.1016/j.compositesa.2011.03.008

23. K. Joseph, S. Thomas, C. Pavithran. Effect of chemical treatment on the tensile properties of short sisal fibre-reinforced polyethylene composites. Polymer 1996; 37:5139-5149.
DOI: 10.1016/0032-3861(96)00144-9

24. J. George, M.S. Sreekala, S. Thomas. A review on interface modification and characterization of natural fibre reinforced plastic composites. Polymer Engineering and Science 2001; 41:1471-1485.
DOI: 10.1002/pen.10846

25. P.A. Dilara, D. Briassoulis. Degradation and stabilization of low-density polyethylene films used as greenhouse covering material. Journal of Agricultural Engineering Research 2000; 76:309-321.
DOI: 10.1006/jaer.1999.0513

26. D. Oldak, H. Kaczmarek, T. Buffeteau, C. Sourisseau. Photo and biodegradation processes in polyethylene, cellulose and their blends studied by ATR-FTIR and Raman spectroscopies. Journal of Materials Science 2005; 40:4189-4198.
DOI: 10.1007/s10853-005-2821-y

27. N. Olaru, L. Olaru, G.H. Cobiliac. Plasma-modified wood fibres as fillers in polymeric materials. Romanian Journal of Physics 2005; 50:1095-1101.

28. G. Davis. Characterization and characteristics of degradable polymer sacks. Materials Characterization 2003; 51:147–157.
DOI: 10.1016/j.matchar.2003.10.008

29. M. Liu, A.R. Horrocks, M.E. Hall. Correlation of physicochemical changes in UV-exposed low density polyethylene films containing various UV stabilizers. Polymer Degradation and Stability 1995; 49:151-161.
DOI: 10.1016/0141-3910(95)00008-A

30. J.H. Khan, S.H. Hamid. Durability of HALS-stabilized polyethylene film in a greenhouse environment. Polymer Degradation and Stability 1995; 48:137-142.
DOI: 10.1016/0141-3910(95)00015-E

31. A.J. Peacock, A.R. Calhoun. Polymer Chemistry: Properties and Applications. Carl Hanser Verlag: Munich 2006; 171-181.

32. J.K. Pandey, S.H. Ahn, C.S. Lee, A.K. Mohanty, M. Misra. Recent advances in the application of natural fibre based composites. Macromolecular Materials and Engineering 2010; 295:975-989.
DOI: 10.1002/mame.201000095

33. A.K. Mohanty, M. Misra, G. Hinrichsen. Biofibres, biodegradable polymers and biocomposites: An overview. Macromolecular Materials and Engineering 2000; 276:1-24.
DOI: 10.1002/(SICI)1439-2054(20000301)

34. R. Kozlowski, M. Wladyka-Przybylak. Flammability and fire resistance of composites reinforced by natural fibers. Polymers for Advanced Technologies 2008; 19:446-453.
DOI: 10.1002/part.1135

35. A.S. Herrmann, J. Nickel, U. Riedel. Construction materials based upon biological renewable resources – from components to finished parts. Polymer Degradation and Stability 1998; 59:251-261.
DOI:10.1016/S0141-3916(97)00169-9

36. U. Riedel. Natural fibre-reinforced biopolymers as construction materials – new discoveries. 2nd International Wood and Natural Fibre Composites Symposium, Kassel, Germany (1999) p.28-29.

Chapter 2

Literature review

2.1 Brief introduction

Composites refer to a combination of two or more materials with different forms or composition. When two or more constituencies are mixed they retain their identities in the composite. The do not dissolve into each other, but reinforce each other. Composite may have a ceramic, metallic or polymeric (thermoset or thermoplastic) matrix, whilst the fibres can be ceramic, metallic, or polymeric [1-13]. Fibres are also either synthetic (i.e glass, Kevlar or carbon) or natural (sisal, hemp, jute, pine wood, etc.). Fibres offer the strength to the composite, because they have high strength and modulus. The matrix holds them in a certain location and direction, also acting as a load transfer medium between fibres. The main problem encountered by polymer scientists is that natural fillers are hydrophilic in nature whereas polymer matrices are hydrophobic. Therefore there is an incompatibility between the two constituencies which leads to poor mechanical properties. In moist environments, because natural fiber is hydrophilic, there occurs water uptake and swelling, resulting in micro-cracks and water degradation of natural fibre composites [2-3]. Therefore the use of a compatibilizer or coupling agent plays a prominent role to promote the adhesion between fibre and matrix, and also by reducing the interfacial tension between hydrophobic polymers and hydrophilic natural fibres [3-6].

2.2 Natural fibres

2.2.1 Composition and structure

Natural fibres have been extensively investigated and studied by both scientists and engineers as reinforcements in polyolefins. They are comprised of cellulose, hemi-cellulose, lignin, extractives, fatty acid (acetic acid), pectin, sterols (alcohols), and waxes. These components are distributed throughout the cell wall at varying degrees depending on various factors such as species, variety, type of soil used, weather conditions, part from which the fibres are extracted, and age of the plants. All plant fibres consist of cellulose while animal fibres (hair,

silk, and wool) have proteins. The mechanical properties of some natural lignocellulosic and conventional fibres are shown in Tables 2.1. It appears from the table that natural fibres have low densities compared to synthetic fibres [14-16].

Table 2.1 Comparison of mechanical properties of some natural fibres with those of conventional fibres [7-8]

Fibres	Density / g cm^{-3}	Elongation at break / %	Tensile strength / MPa	Young's modulus / GPa
Natural fibres				
Cotton	1.5-1.6	7.0-8.0	287-800	5.5-12.6
Jute	1.3	1.5-1.8	393-773	26.5
Flax	1.5	2.7-3.2	3451035	27.6
Hemp	1.5	1.6	690	70
Ramie	1.5	1.2-3.8	400-938	61.4-128
Sisal	1.5	2.0-2.5	511-635	9.4-22.0
Coir	1.2	30.0	175	4.0-6.0
Viscose (cord)	-	11.4	593	11
Softwood (pine)	1.5	-	1000	40
Synthetic conventional fibres				
E-glass	2.5	2.5	2000-3500	70.0
S-glass	2.5	2.8	4570	86.0
Aramide	1.4	3.3-3.7	3000-3150	63.0-67.0
Carbon	1.4	1.4-1.8	4000	230-240

2.2.2 Cellulose

Cellulose is the principal component of natural fibres cinsisting about 50-90% of natural fibre. Cellulose is an organic compound with the formula $(C_6H_{10}O_5)_n$ and is highly crystalline (Figure 2.1). It is a high molecular weight carbohydrate polymer forming a linear condensed polymer of D-anhydroglucopyranose (abbreviated as the anhydroglucose unit or glucose

unit). It is arranged in an ordered arrangement called fibrils and is joined together by β-1,4-glycosidic bonds or 1,4-β-D-glucan, having a degree polymerization between 10000 and 14000. It contains three hydroxyl groups per unit [4]. Many properties of natural fibres depend on cellulose chain length or degree of polymerization. Hydrogen bonding (through the –OH groups of cellulose) can occur within the cellulose macromolecule itself, and it is referred to as *intramolecular* hydrogen bonding. If the hydrogen bonding is between different cellulose units, we call it *intermolecular* hydrogen bonding [17].

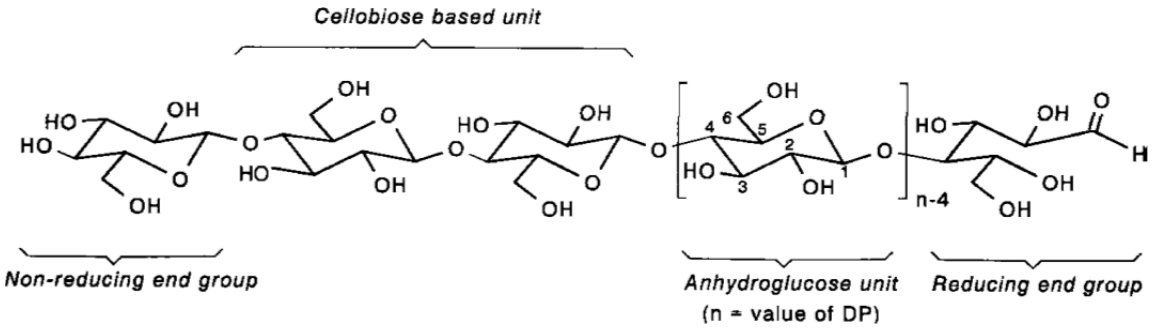

Figure 2.1 Molecular structure of cellulose [4-5,14-16]

2.2.3 Hemicellulose

Hemi-celluloses (Figure 2.2) is regarded as the second most abundant class of non-cellulosic polysaccharides in natural fibres. Mostly they make up about 25 to 35% of the natural fibre. Their general formula are either $(C_5H_8O_4)_n$ or $(C_6H_{10}O_5)_n$, called pectosans and hexosans respectively. Hemicellulose differ from cellulose in three aspects. Firstly, they contain several different sugar units (such as α-pyranose, α-furanose, and α-D-glucuronic acid), whereas cellulose contains only a 1,4-β-D-glucopyranose type sugar unit. Secondly, they exhibit a considerable degree of chain branching containing pendant side groups that gives rise to its non-crystalline amorphous nature, whereas cellulose is a linear polymer. Thirdly, the degree of polymerization of native cellulose is 10-100 times higher than that of hemicellulose [4,16-18].

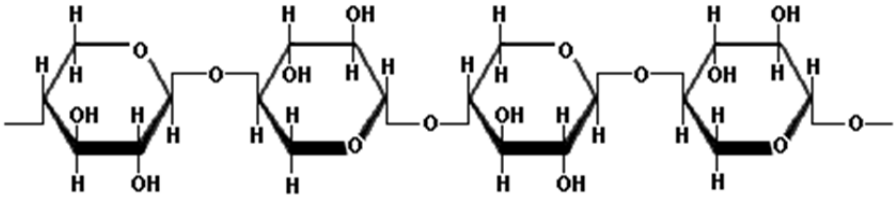

Figure 2.2 Molecular structure of hemicelluloses [16]

2.2.4 Lignin

The molecular structure of lignin is shown on Figure 2.4. Lignin is a random polymer composed mainly of aromatic rings with short (up to three) aliphatic carbon chains connecting the rings. It has a disordered structure, and is formed through ring opening polymerization of phenyl propane monomers. This also provides rigidity, hydrophobicity and decay resistance to the cell walls of lignocellulosic fibres. Lignin polymers are often found in most plant structures in association with cellulose. The structure of lignin is not well defined, but lignin appears to be made up of polymers of propylbenzene with hydroxyl and methoxy groups attached. Lignin is primarily hydrocarbon in nature and makes up a major portion of insoluble dietary fibre. It contains subunits derived from *p*-coumaryl alcohol, coniferyl alcohol, and sinapyl alcohol, and is unusual among biomolecules in that it is racemic i.e. it is not optically active. The lack of optical activity is because the polymerization of lignin occurs *via* free radical coupling reactions in which there is no preference for either configuration at a chiral centre [3-5].

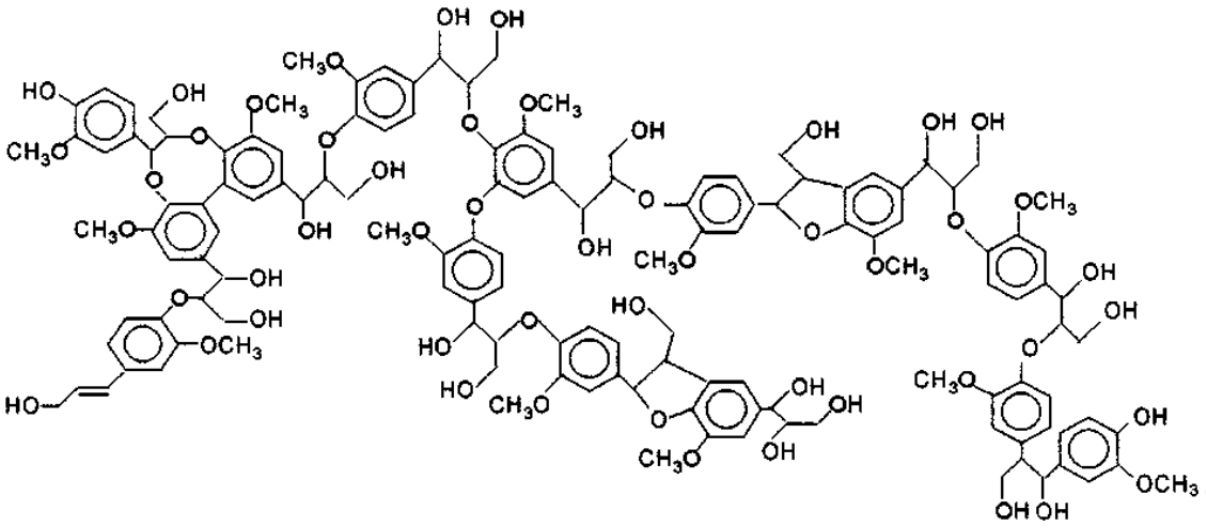

Figure 2.3 Molecular structure of lignin [3]

2.2.5 Wood extractives

Although wood extractives do not contribute too much to the properties of natural fibre as a whole, they are present. Extractives include fats, waxes, fatty acids, sugars, starches, resins, phenolic compounds, and sterols. Extractives can be removed by either polar or non-polar solvents such as ethanol, water, benzene, ethanol/cyclohexane [3-6,16-18,19].

2.2.6 Pine wood fibre

Pine wood fibre belongs to softwood classification biomasses which is found from gymnosperm trees (plants having seeds with no covering). Other softwood fibres are spruce, cedar, fir, larch, douglas-fir, hemlock, cypress, redwood and yew. Pine wood fibres are readily available in large quantities, cheap, biodegradable, non-toxic, and they are widely utilized natural fibres in the development of composite materials. Table 2.2 shows the chemical compositions of some lignocellulosic natural fibres where cellulose is the principal component compared to other components. That makes cellulose to have an influence on the properties of the whole fibre [20].

Table 2.2 Chemical composition of some common lignocellulosic fibres [20]

Fibre	% Cellulose	% Hemicellulose	% Lignin	% Residual ash
Softwood (Pine wood)	40-45	25-30	26-34	-
Hardwood	45-50	21-36	22-30	-
Flax	64	17	2	7
Jute	64	12	12	2
Sisal	66	12	10	2
Husk	35-45	19-25	20	14-17
Whole straw	41-57	33	8-19	8-38
Leaf	37-41	22-25	7-8	26-33
Stem	24-46	24-28	4-6	8-16

2.3 Matrix material

A matrix can be defined as the material in which the reinforcing part of a composite is embedded. The matrix serves as a binder which holds the reinforcing material in place and in a certain orientation. When a composite is subjected to an applied load, the matrix deforms and transfers the external load uniformly to the fibres. The matrix also provides resistance to crack propagation and damage tolerance owing to plastic flow at the crack tips. Their function is also to protect the surface of fibres from adverse environmental effects and abrasion, especially during composite processing. Plastic matrices can generally be classified into two major types: thermoplastics and thermosets. The selection criteria of the matrices depend solely on the composite end use requirements. For example, if chemical resistance together with elevated temperature resistance is needed for a composite material, then thermoset matrices are preferred. If a composite material with high damage tolerance, remoldability and recyclability is needed, then thermoplastics are preferred [1,8,17,20].

2.4 Polyethylenes

Polyethylenes are manufactured by several major processes. These include high-pressure polymerization (free radical polymerization), Ziegler-Natta type catalyzed polymerization, metallocene polymerization, and metal oxide catalyzed polymerization. Their properties depend on their molecular structure, degree of crystallinity and degree of polymerization. Crystalline regions provide rigidity at high temperatures, but the amorphous regions provide flexibility and high impact strength. The polyethylenes are classified according to their densities which is the result of different degrees of crystallinity:

- HDPE or PE-HD (high-density polyethylene)
- MDPE or PE-MD (medium-density polyethylene)
- LDPE or PE-LD (low-density polyethylene)
- LLDPE or PE-LLD (linear low-density polyethylene)
- VLDPE, (very low-density polyethylene)

LDPE is a semi-crystalline polymer and is produced by free radical polymerization at high pressures of 100-300 MPa with oxygen or peroxide catalysts. Under these conditions, PE macromolecules with long chain branching are produced. Crystallinity is from 40-50%,

density 0.915-0.935 g cm^{-3}. There are about 15-25 chain branches per 100 carbon atoms, which makes it be more amorphous and flexible but with a high toughness. It has a good elongation of about 550% due to its flexibility. It also has very good dielectrical and electrical properties, very low water absorption, low water vapour permeability, and a high resistance to chemical attack [21-24].

2.5 Modification of polyethylene/fibre composites

Improved interfacial adhesion between natural fibres and polymer matrices is critically important because the properties of the composite strongly depend on it, as well as on the individual components of the composites. Some modifications were tried to improve the adhesion, i.e. physical treatment, chemical treatment and/or grafting compatibilization [4,16-19,25]. Corona and cold plasma are amongst a number of physical treatment methods. These treatments oxidize the fibre surface, and increase the energy level of the fibre to be the same as that of the matrix for an improved adhesion between the two. Many reactive functional groups like aldehydes are produced on the fibre surface after these treatments, as well as a free radical surface crosslinked network between the fibre and the matrix [4,26]. Mercerization and alkali treatment remove impurities such as waxy layers, oil layers, cuticles and even lignin from the fibre surfaces. It also roughens the cell wall structure on the fibre surface improving mechanical interlocking interaction with the polymer matrix. At higher alkali concentrations, excess removal of lignin occurs resulting in weak cellulose fibres which significantly affect the composite properties [27-28]. Acetylation treatment introduces acetyl groups (CH_3COO^-), decreasing the hydrophilic character of cellulose fibres. Silane treatment forms silanols in the presence of moisture, ultimately forming a crosslink network which improves adhesion between the fibre and the matrix [29-31]. Acrylonitrile treatment, which modifies cellulose fibres through grafting in the presence of initiators, was well explained by Li *et al.* [31]. This method reduces the hydrophilicity of the fibre, improving interfacial adhesion between the fibre and the hydrophobic matrix. Iscocyanate treatment gives rise to isoscyanate functional groups (-NCO) that easily react with cellulose and lignin hydroxyls on the fibre. Strong covalent bonds occur between the hydroxyl and isoscyanate groups. Peroxide treatment uses compounds which decompose at increased temperatures forming two free radicals. The first radical reacts with cellulose while the other one reacts with the polymer matrix. The radicals on the matrix react with the cellulose radicals forming a strong covalent bond (graft) between the two components [32]. Maleated coupling modifies

the polymer matrix. The maleic anhydride groups are grafted to polymers like polypropylene to form maleic anhydride grafted polypropylene (MAPP). MAPP has two functional domains, i.e anhydride carbonyl groups that interact with cellulose hydroxyl groups, and the hydrophobic group which interacts with the matrix. MAPP then forms a sort of a bridge of crosslinks between the polymer matrix and the natural fibre interface [33-35].

Degraded polyolefins also seem to improve the interfacial adhesion between the filler and the polymer matrix due to functional groups on the compatibilizing polymer's backbone. These functional groups will form hydrogen bonds with cellulose hydroxyl groups. However, scientific publications that describe the use of degraded polymers as a compatibilizer are very limited because this idea is quite new. Most former studies are concerned with the methods of degradation of polymers, or the estimation of the life service of polymers under harsh conditions [15,36-43]. Dilara *et al*. [15] investigated the degradation and stabilization of low density polyethylene film used for greenhouse covering material. They noticed that low density polyethylene, when exposed to UV irradiation, heat and/or chemical contact, degrades. Many degradation products, including free radicals, hydroperoxides and carbonyls are incorporated on the polymer main chain.

Favaro *et al.* [41] investigated the effect of $KMnO_4$ oxidation of recycled HDPE on its interfacial adhesion to sisal fibre. To improve the adhesion between sisal fibre-recycled HDPE, the sisal fibre was first treated with NaOH and then acetylated. They noticed that the addition of treated sisal fibre into an oxidized recycled HDPE significantly improved the tensile modulus of the composite. It was believed to be due to strong hydrogen bonding between the incorporated carbon-oxygenated groups on the polymer with hydroxyl groups on the cellulose. The tensile strength, however, deceased, which was attributed to the dewetting effect of the fibres, leading to fibre debonding from the matrix. The same group investigated the effect of the oxidized recycled HDPE on its interfacial adhesion to rice husk fibre [42]. The rice husk flour was treated in the same way as the sisal. Fibre incorporation in the polyethylene matrix increased the tensile modulus and flexural modulus at 10% fibre content, but reduced the tensile strength, similar to their observations on oxidized recycled HDPE mixed with sisal.

2.6 Properties of polyethylene/natural fibre composites

2.6.1 Morphology polyethylene/natural fibre composites

Scanning electron microscopy (SEM) is helpful to detect the fibre dispersion throughout the polymer matrix composites. Good interfacial adhesion between the matrix and natural fibre is essential and favourable to transfer stress across the interface. It is well known that more intimate contact between the matrix and filler will give rise to improvement in the composite properties. Most of the previous researchers [32,44-63] concluded that uncompatibilized polymer-natural fibre composites show (1) fibre pullouts upon fracture, (2) fibre debonding away from the matrix upon fracture, meaning that there is no good interaction between the fibre and the matrix, (3) gaps or voids are seen indicating limited or no adhesion between the hydrophilic fibres and the hydrophobic matrices, and (4) the fibre surfaces are clean without any evidence of matrix still adhering to it. However good adhesion was seen by (1) fibres cracking on the matrix surface without complete pull out, because the fibres are completely stuck into the matrix, (2) fibre surfaces coated with some matrix particles after composite fracture, and (3) little or no gaps or voids between the matrix and the fibres. All these observations depended on the effectiveness of fibre or matrix modification, and on compatibilizers to enhance adhesion between matrices and fibres.

Joseph *et al*. [32] investigated the effect of chemical treatments of sisal fibres with alkali, isocyanate, permanganate, and peroxide on the interfacial adhesion of sisal-LDPE composites. The fracture surfaces of the treated and untreated composites were examined by SEM. All the treated composites showed better adhesion between LDPE and sisal fibres compared to the untreated ones. In untreated composites poor adhesion was seen by pull-out of the fibres from the matrix. Salemane *et al*. [44] investigated the morphology of maleic anhydride modified and unmodified polypropylene-wood powder composites by using SEM. They noted that as MAPP was introduced into composites, smooth and homogeneous composite surfaces were seen, especially when using smaller wood particles.

Thakore *et al*. [45] investigated the morphological effect of converting starch into a hydrophobic derivative by phthalation, giving starch-phthalate (stath) in composites. SEM analysis of unconverted starch showed voids and loose starch fibre due to weak adhesion between the hydrophilic starch and the hydrophobic LDPE. In the stath-LDPE composite

there was intimate contact between the LDPE and the stath. Mohanty *et al* [46] reported on the effect of maleic anhydride grafted polyethylene (MAPE) on the morphology of HDPE-jute composites. For unmodified jute composites they also observed large voids between the fibre and the HDPE matrix due to different surface energies of the two phases, while the MAPE treated fractured composites showed fibres coated with some matrix material with a smaller number of voids. Joseph *et al* [47] reported similar observations in sisal-PP composites that were interface treated with sodium hydroxide, maleic anhydride, a urethane derivative of polypropylene glycol, and permanganate.

Mengeloglu *et al.* [48] analyzed the morphology of HDPE-eucalyptus fibres using MAPE compatibilization. They noted that in the morphology of untreated composites, loose individual fibres were on the HDPE surface meaning poor adhesion. In the MAPE treated composites the fractured surfaces showed fibres totally embedded in the matrix. Sarkhel *et al*. [49] investigated the mechanical, thermal and viscoelastic properties of LDPE-EPDM blends. They used MAPE treated and untreated jute fibres as compatibilizers. For the untreated fibres a large number of voids resulting from fibre pull out was seen, meaning poor interfacial adhesion between the polymer blend and the jute fibres. The jute fibres were smooth without any evidence of polymer adhering to the fibre surface. For the treated composites a smaller number of voids were seen and fibres with broken ends were still embedded in the polymer matrix.

2.6.2 Mechanical properties

The mechanical properties of polyolefins reinforced by wood fibre were found to depend on many factors. The most important of these factors are the interfacial adhesion between fillers and matrices as well as the amount of filler. Tensile strength, modulus of elasticity and elongation at break provide excellent measures of the degree of reinforcement provided by the fibre to a composite. Incorporation of natural fibre into a polymer brings some changes when coming to the composite's final properties. A strong interface is preferred for an effective stress transfer from the matrix to the filler. A number of studies reported on the effect of good interfacial adhesion improving mechanical and viscoelastic properties of polyolefin/natural fibre composites [20,53-56].

Yao *et al.* [20] investigated the effect of five different rice straw fibres in two types of HDPEs (virgin HDPE and recycled HDPE) on the mechanical properties. The fibres were rice husk fibre, rice straw leaf fibre, rice straw stem fibre, rice whole straw fibre, and wood fibre. 30 and 50% of each of these fibres were mixed with either virgin or recycled HDPE. The mechanical properties of the composites were compared to those of neat virgin and recycled HDPE. Not much influence of fibre addition was seen, because of no compatibilizers were used. The storage and loss moduli were enhanced, while the tensile and impact strengths were reduced. It was believed that the increasing moduli was due to the reinforcing effect of wood fibre. The decreasing strength was due the poor adhesion between the filler and polymer matrix leading to ineffective stress transfer at the interface. Jain *et al*. [53] investigated the mechanical behaviour of epoxy resin reinforced with bamboo and bamboo mat. Both these composites showed good strength, even without a compatibilizer.

Sanadi *et al.* [54] examined the mechanical properties of kenaf-PP composites where MAPP was used as a compatibilizer. They noticed that hydrogen bonding might have occurred between the cellulose hydroxyls and anhydride domains of MAPP. They also suggested acid-base interaction instead of hydrogen bonding. The flexural, tensile, and impact properties were improved by the addition of MAPP. Wambua *et al*. [55] compared the mechanical properties of PP reinforced with natural fibres (sisal, kenaf, jute, hemp, and coir) with those containing glass fibre. The tensile strength and modulus increased with increasing fibre content for all the tested fibres due to the reinforcing effect of the fibres. They found that coir gave the worst mechanical properties, which could have been due to its low cellulose content and its high microfibrillar angle.

Marchovich *et al*. [56] investigated the mechanical properties of PE-cellulose (wood flour) composites. They noticed an improvement in mechanical properties between polyethylene and wood fibre after the matrix was modified with maleic anhydride in the presence of a peroxide initiator. The stress at break and modulus increased because of more effective stress transfer between the polymer and the fibre. The elongation at break decreased with increasing wood fibre content due to the restricting effect of wood fibre on the molecular chain deformability. Sreekala *et al*. [57] investigated the effect of different treatments on oil palm empty fruit bunch fibre-phenol formaldehyde composites. They noticed that the surface treatment generally improved the mechanical properties of the composite due to good adhesion between the hydrophilic matrix (in this case) and the hydrophilic wood fibre. Both

phenol formaldehyde and oil palm empty fruit bunch are hydrophilic, so a very strong adhesion was found even before treatment. The impact resistance also improved.

Karmarkar *et al.* [58] investigated natural fibre polypropylene composites, where *m*-isopropenyl-α,α-dimethylbenzyl-isocyanate was used as a compatibilizer. They noticed that the presence of wood in polypropylene (PP) decreased the impact strength, because the presence of wood provided stress concentrations. Compatibilizer addition resulted in greater reinforcement indicated by the improved mechanical properties. Both the tensile strength and flexural properties significantly increased. However the addition of wood fibres resulted in a decrease in elongation at break and impact strength of the composites.

2.6.3 Thermal properties

In thermogravimetric analysis (TGA), wood-polymer composites degrade in more than one step. The first step between 50 and 115 °C is where water evaporation occurs, while hemicelluloses and lignin decomposes around 218 and 260 °C. From about 350 °C cellulose and the C-C polymer backbone start to degrade [64-66]. In most cases treated polymer-wood composites show better thermal stability than both the untreated composites and the pure components [67-73]. It is rare to have untreated composites with a better thermal stability than treated composites [74].

Many researchers found that the addition of natural filler can increase the thermal stability of composites due to the strong interfacial interaction imparted by the compatibilizers. Some of them are Lei *et al*. [39], Kim *et al.* [67], Doan *et al.* [68], Tajeddin *et al*. [69], George *et al*. [74], and Mohanty *et al*. [76]. They all found that strong interaction between the matrix and filler gave composites of higher thermal stability. Lei *et al*. [39] investigated the properties of recycled HDPE filled with natural fibres (wood and bagasse fibres). They found that coupling agents had little influence on the thermal degradation of the composites. However, the addition of the cellulosic fibres increased the thermal stability which was attributed to good adhesion between the esterified cellulose fibres and the PE matrix. Kim *et al.* [67] investigated the thermal properties of PP filled with bio-flour composites and LDPE filled with bio-flour composites where MAPP and MAPE were respectively used as compatibilizers. In both cases they noted that the thermal stability and degradation temperatures slightly increased when MAPP and MAPE were used. This behaviour was

associated with the enhanced adhesion between the cellulose hydroxyl and the anhydride groups in MAPP and MAPE. Doan *et al.* [68] investigated the thermal properties of PP-jute fibre composites using MAPP compatibilization. They found that the 2% MAPP modified jute-PP composites had a good thermal stability. This effect might have been due to the stronger interaction between the fibre and the matrix caused by the formation of covalent bonds at the interface. Tajeddin *et al*. [69] investigated the thermal stability of low-density polyethylene filled with kenaf fibre. A higher thermal stability was found after polyethylene glycol (PEG) was used as a compatibilizer. George *et al*. [74] investigated the effects of fibre loading and surface modification on the thermal stability of LDPE reinforced pineapple leaf fibre (PALF). They found that untreated PALF-LDPE composites containing 20% fibre displayed a minor peak at 410 °C corresponding to the degradation of PE and a major peak at 510 °C corresponding to the degradation of dehydrocellulose. The treated composites with the same fibre content showed small increases in thermal stability. Mohanty *et al*. [76] investigated the influence of MAPP as a compatibilizer for sisal-polypropylene composites. They found that the addition of fibre enhanced the thermal stability of polypropylene. The MAPP treated composite showed even higher thermal stability, which means that the interfacial adhesion was improved between the fibre and the matrix.

Other researchers found a decreased thermal stability due to poor interfacial adhesion between fillers and matrices as well as ineffectiveness of compatibilizers. Tajvidi *et al.* [70] investigated the thermal degradation characteristics of natural fibre reinforced polypropylene composites using MAPP as a compatibilizer. Even though they expected an increase in the thermal stability as the natural fibre content was increased, a decrease in thermal stability was found. This was due to the lower thermal stability of the compatibilizers. Luyt *et al*. [75] investigated the influence of sisal fibre content, peroxide crosslinking, and wax addition on the thermal properties of low-density polyethylene-sisal composites. Both wax and sisal seemed to have reduced the thermal stability of LDPE in the absence of crosslinking.

Generally the crystallization behaviour and crystallinity of polymers in natural fibre-polymer composites were influenced by the presence of the fibre. In this case the fibres act as heterogeneous nucleating sites that increases the polymer crystallinity [56, 73,77,78,70,80,81]. Marcovich *et al.* [56] investigated linear low-density polyethylene (LLDPE) modified with an organic peroxide and by maleic anhydride. The composites were extruded in the presence of untreated wood flour. The degree of crystallinity decreased in the

modified LLDPE, but increased with the addition of wood flour, and this was attributed to the nucleating effect of the wood flour. The fibres acted as sites for heterogeneous nucleation that induced the crystallization of the matrix. That was shown by all the composites, and so it was independent of the degree of compatibility between the matrix and the filler. Bouafif *et al.* [73] investigated HDPE filled with different types of softwoods. MAPE was used as a compatibilizer to improve the compatibility. Addition of wood particles to HDPE increased the crystallization temperature as well as the crystallinity of all the composites. Lee *et al.* [77] investigated the coupling effect of lysine-based diisocyanate (LDI) as a coupling agent of bamboo fibre (BF) with poly(lactic acid) (PLA) and poly(butylene succinate) (PBS) respectively. In both the PLA/BF and PBS/BF composites the crystallization temperature increased by adding either BF or LDI. That was considered to be due to the nucleation effect of BF and LDI. The strong urethane linkages between the polymer matrix and the BF, produced by the addition of LDI, further enhanced the nucleation of the polymer matrix, even though the crystallization enthalpy was decreased by increasing LDI content. The molecular motion of the polymer matrix could have been restricted by the addition of LDI, resulting in a decrease in the crystallization chain packing enthalpy. Similar results were found by Amash *et al.* [78], Pracella *et al.* [79], Sailaja *et al.* [80] and Nayak *et al.* [81]. They all confirmed that natural filler can act as a nucleating agent. Amash *et al.* [78] used PP filled with cellulose fibre and MAPP as a compatibilizer. They found that small amounts of fibre increased the crystallization temperature and the crystallinity. Pracella *et al.* [79] used isotactic polypropylene (PP) with hemp fibres. Either the fibre or the PP was modified by treatment withj glycidyl methacrylate giving hemp-GMA or PP-GMA. Various compatibilizers (PP-g-GMA, SEBS, SEBS-g-GMA) were used to improve the fibre–matrix interactions. They found that addition of fibres to PP resulted in an increase crystallinity of the PP matrix. After adding modified fibres the crystallisation temperature and crystallinity further increased, and the same was observed when PP-GMA was used. Sailaja *et al.* [80] found that when wood pulp was grafted with polymethyl methacrylate (PMMA), there was not much of a difference between the melting temperatures of the composites. However, the presence of poly(ethylene-co-glycidyl methacrylate) (PEGMA) as compatibilizer showed a remarkable increase in the crystallinity of the matrix. In the absence of a compatibilizer, the crystallinity of the matrix decreased as the filler loading increased. The reason given was that the presence of the fibres inhibited the close packing of the LDPE chains and that there was poor adhesion at the interface. The DSC results by Nayak *et al.* [81] showed that the addition of bamboo fibre, glass fibre and MAPP did not significantly influence the T_m of a PP matrix. However,

the introduction of these fibres and MAPP interrupted the linear crystallizable sequence of the PP phase and reduced the degree of crystallinity. The degree of crystallinity was increased by the incorporation of fibres.

Some studies also showed that there can be a reduction in the polymer crystallinity due to inhibited molecular chain mobility, preventing chain close packing [47,82,83,84,85-91]. Both these observations were attributed to strong interaction between the different components in natural fibre-polymer composites. Malunka *et al*. [82] and Dikobe and Luyt [83] reported on the properties of EVA-natural fibre composites. The expected enthalpies for EVA/sisal fibre composites were higher than the measured enthalpies. This was attributed to a decrease in the mobility of the EVA chains as a result of grafting. This also gave rise to the formation of thinner crystal lamellae, confirmed by the steady decrease in the melting temperatures, and a lower crystallinity. They also observed that wood fibre (WF) influenced the melting temperatures and crystallization behaviour of EVA in EVA/WF composites. The EVA crystallized fairly normally, even though the crystals were not as perfect as expected. The formation of perfect crystals was hindered by the presence of WF particles, which probably led to epitaxial crystallization on the surfaces of the WF particles that were well dispersed in the EVA matrix.

2.6.4 Viscoelastic properties

Dynamic mechanical analysis (DMA) is a technique which determines the viscoelastic behaviour of pure polymers and polymer-wood composites. It provides valuable information about the relationship between structure, morphology and properties of composite materials. The storage modulus, E′, is associated with the elastic response of the composite and indicates the stiffness of the material. The loss modulus, E″, is proportional to the amount of energy that has been dissipated as heat by the sample and represents its viscous response. Tan δ is the ratio of the loss modulus (E″) to the storage modulus (E′) [67,86]. Branched and linear PE, for example, displays three well known transitions. It is common to label these observed transitions with decreasing transition temperatures as α-, β- and γ-transitions.

Kim *et al.* [67] observed that the storage modulus of LDPE substantially increased at higher temperatures due to the incorporation of rice husk flour (RHF). With increasing coupling agent content, the E' values of the composites slightly increased compared to those of the untreated composites. The enhanced stiffness of the composites was mainly attributed to the improved compatibility between the RHF and LDPE. The T_g of the treated composites slightly increased due to the existence of interfacial bonding between the components at the interface. The loss modulus peak temperatures of LDPE and the treated composites were in the range of -23 to -19 °C, which was attributed to the β-relaxation. The tan δ values of the treated composites were lower than those of the untreated composites over the complete temperature range, indicating that the energy dissipation of the modified composites was less than that of the uncoupled composites.

Pedroso *et al.* [86] compared the viscoelastic behaviour of recycled and virgin LDPE where both were reinforced with corn starch. They noticed that recycled LDPE had a higher storage modulus than the virgin LDPE, which was due to better adhesion in recycled LDPE. This behaviour was attributed to higher rigidity, crosslinking, or increased crystallinity. Virgin LDPE had a higher loss modulus than recycled LDPE, as a result of increased rigidity or crosslinking of recycled LDPE during degradation. The peaks where tan δ was a maximum broadened and shifted to higher temperatures as starch was added to LDPE. For blends with recycled LDPE, it was not possible to determine the temperature where tan δ was a maximum, since only a shoulder in the range 80–85 C was observed.

Hong *et al*. [11] investigated the influence of organofunctionalised silane on the dynamic mechanical properties and interfacial adhesion in jute-polypropylene composites. They noticed an improved storage modulus for the silane treated composites. This was due to improved interfacial adhesion between the jute fibres and the polypropylene. The polypropylene glass transition temperature also shifted from 11 to 15 °C after the addition of natural fibres, which was attributed to the reinforcing effect imparted by the jute fibres. Mohanty *et al*. [76] investigated the influence of MAPP as a compatibilizer for sisal-polypropylene composites on the dynamic mechanical properties. They found that regardless of whether the fibre was treated or untreated, the modulus of the composites increased. They attributed this behaviour to the reinforcing effect of the fibre which allowed even distribution of stress throughout the interface. The presence of MAPP gave even higher moduli while also shifting the glass transition slightly to higher temperatures.

2.7 References

1. M.A. Munawar, S. Khan. Natural fiber-reinforced polymer composites. Proceedings of the Pakistan Academy of Science 2007; 44:129-144.
2. H. Hargitai, I. Racz, and R.D. Anandjiwala. Development of hemp fiber reinforced polypropylene composites. Journal of Thermoplastic Composite Materials 2008; 21:165-174.
   DOI: 10.1177/0892705707083949
3. A.K. Mohanty, M. Misra, L.T. Drzal. Sustainable bio-composites from renewable resources: Opportunities and challenges in the green materials world. Journal of Polymers and the Environment 2002; 10:19-26.
   DOI: 10.1023/A:102101391916
4. A.K. Bledzi, J. Gassan. Composites reinforced with cellulose based fibres. Progress in Polymer Science 1999; 24:221-274.
   DOI: 10.1016/S0079-6700(98)00018-5
5. A.K. Mohanty, M.A. Khan, G. Hinrichsen. Surface modification of jute and its influence on performance of biodegradable jute-fabric/biopolymer composites. Composites Science and Technology 2000; 60:1115-1124.
   DOI: 10.1016/S0266-3538(00)00012-9
6. A. Habrant, C. Gaillard, M.C. Ralet, D. Lairez, B. Cathala. Relation between chemical structure and supramolecular organization of synthetic lignin-pectin particles. Biomacromolecules 2009; 10:3151-3156.
   DOI: 10.1021/bm900950r
7. A. Ashori**.** Wood–plastic composites as promising green-composites for automotive industries! Bioresource Technology 2008; 99:4661-4667.
   DOI: 10.1016/j.biortech.2007.09.043
8. J. Holbery, D. Houston. Natural-fiber-reinforced polymer composites in automotive applications. JOM Journal of the Minerals, Metals and Materials Society 2006; 58:80-86.
   DOI: 10.1007/s11837-006-0234-2
9. M. Liu, R. Horrocks, M.E. Hall. Correlation of physicochemical changes in UV-exposed low density polyethylene films containing various UV stabilizers. Polymer Degradation and Stability 1995; 49:151-161.
   DOI: 10.1016/0141-3910(95)00036-L

10. D.N. Saheb and J.P. Jog. Natural fibre polymer composites: A review. Advances in Polymer Technology 1999; 18:351-363.
DOI: 10.1002/(SICI)1098-2329(199924)
11. C.K. Hong, I. Hwang, N. Kim, D.H. Park, B.S. Hwang, C. Nah. Mechanical properties of silanized jute-polypropylene composites. Journal of Industrial and Engineering Chemistry 2008; 14:71-76.
DOI: 10.1016/j.jiec.2007.07.002
12. U. Hujuri, S.K. Chattopadhay, R. Uppaluri, A.K. Ghoshal. Effect of maleic anhydride grafted polypropylene on the mechanical and morphological properties of chemically modified short-pineapple-leaf-fibre-reinforced polypropylene composites. Journal of Applied Polymer Science 2008; 107:1507-1516.
DOI: 10.1002/app.27156
13. S. Dabin. Surface modification of LDPE by CO_2 pulsed laser irradiation. Europian Polymer Journal 2002; 38:2489-2495.
DOI: 10.1016/S0014-3057(02)00134-9
14. D.H. Mueller, A. Krobjilowski. New discovery in the properties of composites reinforced with natural fibres. Journal of Industrial Textiles 2003; 33:111-130.
DOI: 10.1177/152808303039248
15. P.A. Dilara, D. Briassoulis. Degradation and stabilization of low-density polyethylene films used as greenhouse covering materials. Journal of Agricultural Engineering Research 2000; 76:309-321.
DOI: 10.1006/jaer.1999.0513
16. J.C.M. De-Bruijn. Natural fibre mat thermoplastic products from a processor's point of view. Applied Composite Materials 2000; 7:415–420.
DOI: 10.1023/A:1026554610834
17. P. Franco, A. González. A study of the mechanical properties of short natural fiber-reinforced composites. Composites: Part B 2005; 36:597-608.
DOI: 10.1016/j.compositesb.2005.04.001
18. J.L. Ren, R.C. Sun, C.F. Liu, Z.Y. Chao, W. Luo. Two-step preparation and thermal characterization of cationic 2-hydroxypropyltrimethylammonium chloride hemicellulose polymers from sugarcane bagasse. Polymer Degradation and Stability 2006; 91:2579-2587.
DOI: 10.1016/j.polymdegradstab.2006.05.008

19. M. Micic, K. Radotic, M. Jeremic, D. Djikanovic, S.B. Kämmer. Study of the lignin model compound supramolecular structure by combination of near-field scanning optical microscopy and atomic force microscopy. Colloids and Surfaces B: Biointerfaces 2004; 34:33-40.
DOI: 10.1016/j.colsurfb.2003.10.018

20. F. Yao, Q. Wu, Y. Lei, Y. Xu. Rice straw fibre-reinforced high-density polyethylene composites: Effect of fibre type and loading. Industrial Crops and Products 2008; 28:63-72.
DOI:10.1016/j.indcrop.2008.01.007

21. H.S. Cho, J.S. Chung, W.Y. Lee. Control of molecular weight distribution for polyethylene catalyzed over Ziegler–Natta metallocene hybrid and mixed catalysts. Journal of Molecular Catalysis A: Chemical 2000; 159:203-213.
DOI: 10.1016/S1381-1169(00)00222-3

22. H.S. Cho, J.S. Chung, W.Y. Lee. Characteristics of ethylene polymerization over Ziegler–Natta/metallocene catalysts. Comparison between hybrid and mixed catalysts. Catalysis Today 2000; 63:523-530.
DOI: 10.1016/S0920-5861(00)00499-5

23. W. Kaminsky, A. Laban. Metallocene catalysis. Applied Catalysis A: General 2001; 222:47-61.
DOI: 10.1016/S0926-860X(01)00829-8

24. M.J. John, R.D. Anandjiwala. Recent developments in chemical modification and characterization of natural fiber-reinforced composites. Polymer Composites 2008; 29:187-207.
DOI: 10.1002/pc.20461

25. P.S. Razi, R. Portier, A. Raman. Studies on polymer-wood interface bonding: Effect of coupling agents and surface modification. Journal of Composite Materials 1999; 33:1064-1079.
DOI: 10.1177/002199839903301201

26. K.M.M. Rao, A.V.R. Prasad, M.N.V.R. Babu, K.M. Rao, A.V.S.S.K.S. Gupta. Tensile properties of elephant grass fiber reinforced polyester composites. Journal of Materials Science 2007; 42:3266-3272.
DOI: 10.1007/s10853-006-0657-8

27. M. Soleimani, L. Tabil, S. Panigrahi, A. Opoku. The effect of fiber pretreatment and compatibilizer on mechanical and physical properties of flax fiber-polypropylene composites. Journal of Polymers and the Environment 2008; 16:74–82.
DOI: 10.1007/s10924-008-0102-y

28. M. Jacob, K.T. Varughese, S. Thomas. Dielectric characteristics of sisal–oil palm hybrid biofibre reinforced natural rubber biocomposites. Journal of Materials Science 2006; 41:5538-5547.
DOI: 10.1007/s10853-006-0298-y

29. J.I. Moran, V.A. Alvarez, V.P. Cyras, A. Vazquez. Extraction of cellulose and preparation of nanocellulose from sisal fibers. Chemistry and Materials Science 2008; 15:149-159.
DOI: 10.1007/s10570-007-9145-9

30. K. Joseph, S. Varghese, G. Kalaprasad, S. Thomas, L. Prasannakumari, P. Koshy, C. Pavithran. Influence of interfacial adhesion on mechanical properties and fracture behavior of short sisal fibre reinforced polymer composites. European Polymer Journal 1996; 32:1243-1250.
DOI: 10.1016/s0014-3057(96)00051-1

31. X. Li, L.G. Tabil, S. Panigrahi. Chemical treatments of natural fibre for use in natural fibre-reinforced composites. Journal of Polymers and the Environment 2007; 15:25-33.
DOI: 10.1007/s10924-006-0042-3

32. K. Joseph, S. Thomas, C. Pavithran. Effect of chemical treatment on the tensile properties of short sisal fibre-reinforced polyethylene composites. Polymer 1996; 37:5139-5149.
DOI: 10.1016/0032-3861(96)00144-9

33. M.T.B. Pimenta, A.J.F. Carvalho, F. Vilaseca, J. Girones, J.P. Lopez, P. Mutje, A.A.S. Curvelo. Soda-treated sisal/polypropylene composites. Journal of Polymers and the Environment 2008; 16:35-39.
DOI: 10.1007/s10924-008-0080-0

34. M. Scoponi, S. Cimmino, M. Kaci. Photo-stabilisation mechanism under natural weathering and accelerated photo-oxidative conditions of LDPE films for agricultural applications. Polymer 2000; 41:7969-7980.
DOI: 10.1016/S0032-3861(00)00160-9

35. P.K. Roy, P. Surekha, C. Rajagopal, S.N. Chatterjee, V. Choudhary. Studies on the photo-oxidative degradation of LDPE films in the presence of oxidised polyethylene. Polymer Degradation and Stability 2007; 92:1151-1160.
DOI: 10.1016/j.polymdegradstab.2007.01.010

36. N. Lucas, C. Bienaime, C. Belloy, M. Queneudec, F. Silvestre, J. Nava-Saucedo. Polymer biodegradation: Mechanisms and estimation techniques. Chemosphere 2008; 73:429-442.
DOI: 10.1016/j.chemosphere.2008.06.064

37. M.A. Esmeraldo, A.C.H. Barreto, J.E.B. Freitas, P.B.A. Fechine, A.S.B. Sombra, E. Corradini, G. Mele, A. Maffezzoli, S.E. Mazzetto. Dwarf-green coconut fibres: A versatile natural renewable raw bioresource. Treatment, morphology, and physicochemical properties. Bioresources 2010; 5:2478-2501.

38. A.K. Mishra, A.S. Luyt. Effect of sol-gel derived nano-silica and organic peroxide on the thermal and mechanical properties of low density polyethylene/wood flour composites. Polymer Degradation and Stability 2008; 93:1-8.
DOI: 10.1016/j.polymdegradstab.2007.11.006

39. Y. Lei, Q. Wu, F. Yao, Y. Xu. Preparation and properties of recycled HDPE/natural fibre composites. Composites: Part A 2007; 38:1664-1674.
DOI: 10.1016/j.compositesa.2007.02.001

40. H.Jiang, D.P. Kamdem. Thermal and dynamic mechanical behavior of poly(vinyl chloride)/wood flour composites. Journal of Applied Polymer Science 2008; 107:951-957.
DOI: 10.1002/app.26370

41. S.L. Favaro, T.A. Ganzerli, A.G.V. de Carvalho Neto, O.R.R.F. da Silva, E. Radovanovic. Chemical, morphological and mechanical analysis of sisal fibre-reinforced recycled high-density polyethylene composites. eXPRESS Polymer Letters 2010; 4:465-473.
DOI: 10.3144/expresspolymerlett.2010.59

42. S.L. Favaro, M.S. Lopes, A.G.V. de Carvalho Neto, .R.R. de Santana, E. Radovanovic. Chemical, morphological and mechanical analysis of rice husk/post-consumer polyethylene composites. Composites: Part A 2010; 41:154-160.
DOI: 10.1016/j.compositea.2009.09.021

43. O. Motta, A. Proto, F. De Carlo, F. De Caro, E. Santoro, L. Brunetti, M. Capunzo. Utilization of chemically oxidized polystyrene as co-substrate by filamentous fungi. International Journal of Hygiene and Environmental Health 2009; 212:61-66.
DOI: 10.1016/j.ijheh.2007.09.014

44. M.G. Salemane, A.S. Luyt. Thermal and mechanical properties of polypropylene-wood powder composites. Journal of Applied Polymer Science, 2006; 100:4173-4180.
DOI: 10.1002/app.23521

45. I.M. Thakore, S. Desai, B.D. Sarawade, S. Devi. Studies on biodegradability, morphology and thermo-mechanical properties of LDPE/modified starch blends. European Polymer Journal 2007; 37:151-160.
DOI: 10.1016/S0014-3057(00)00086-0

46. S. Mohanty, S.K. Verma, S.K. Nayak. Dynamic mechanical and thermal properties of MAPE treated jute/HDPE composites. Composites Science and Technology 2006; 66:538-547.
DOI: 10.1016/j.compscitech.2005.06.014

47. P.V. Joseph, K. Joseph, S. Thomas. Effect of processing variables on the mechanical properties of sisal-fibre-reinforced polypropylene composites. Composites Science and Technology 1999; 59:1625-1640.
DOI: 10.1016/S0266-3538(99)00024-X

48. F. Mengeloglu, A. Kabakci. Determination of thermal properties and morphology of eucalyptus wood residue filled high density polyethylene composites. International Journal of Molecular Sciences 2008; 9:107-119.
DOI: 10.3390/ijms9020107

49. G. Sarkhel, A. Choudhury. Dynamic mechanical and thermal properties of PE-EPDM based jute fibre composites. Journal of Applied Polymer Science 2008; 108:3442-3453.
DOI: 10.1002/app.28024

50. A. Viksne, L. Rence, M. Kalnins, A.K. Bledzki. The effect of paraffin on fibre dispersion and mechanical properties of polyolefin-sawdust composites. Journal of Applied Polymer Science 2004; 93:2385-2393.
DOI: 10.1002/app.20664

51. S.L. Fávaro, T.A. Ganzerli, A.G.V. de Carvalho Neto, O.R.R.F. da Silva, E. Radovanovic. Chemical, morphological, and mechanical analysis of sisal fibre-reinforced high-density polyethylene composites. eXPRESS Polymer Letters 2010; 4:465-473.

DOI: 10.3144/expresspolymlett.2010.59

52. S. Mohanty, S.K. Nayak. Interfacial, dynamic mechanical, and thermal fibre reinforced behavior of MAPE treated sisal fibre reinforced HDPE composites. Journal of Applied Polymer Science 2006; 102:3306-3315.
DOI: 10.1002/app.24799

53. S. Jain, R. Kumar, U.C. Jindal. Mechanical behaviour of bamboo and bamboo composites. Journal of Materials Science 1992; 27:4598-4604.
DOI: 10.1007/BF01165993

54. A.R. Sanadi, D.F. Caulfield, R.E. Jacobson: and R.M. Rowell. Renewable agricultural fibers as reinforcing fillers in plastics: Mechanical properties of kenaf fiber-polypropylene composites. Industrial and Engineering Chemistry Research 1995; 34:1889-1896.
DOI: 10.1021/ie00044a041

55. P. Wambua, J. Ivens, I. Verpoest. Natural fibres: Can they replace glass in fibre reinforced plastics? Composites Science and Technology 2003; 63:1259-1264.
DOI: 10.1016/S0266-3538(03)00096-4

56. N.E. Marcovich, M.A. Villar. Thermal and mechanical characterization of linear low density polyethylene/wood flour composites. Journal of Applied Polymer Science, 2003; 90:2775-2784.
DOI: 10.1002/app.12934

57. M.S. Sreekala, M.G. Kumaran, S. Joseph, M. Jacob, S. Thomas. Oil palm fibre reinforced phenol formaldehyde composites: Influence of fibre surface modifications on the mechanical performance. Applied Composite Materials 2000; 7:295-329.
DOI: 10.1023/A:1026534006291

58. A. Karmarkar, S.S. Chauhan, J.M. Modak, M. Chanda. Mechanical properties of wood–fiber reinforced polypropylene composites: Effect of a novel compatibilizer with isocyanate functional group. Composites: Part A 2007; 38:227–233.
DOI: 10.1016/j.compositesa.2006.05.005

59. A. Akinci, E. Ercenk, S. Yilmaz, U. Sen. Slurry erosion behaviors of basalt filled low density polyethylene composites. Materials and Design 2011; 32:3106–3111.
DOI: 10.1016/j.matdes.2010.12.029

60. D. Oldak, H. Kaczmarek, T. Buffeteau, C. Sourisseau. Photo and biodegradation processes in polyethylene, cellulose and their blends studied by ATR-FTIR and Raman spectroscopies. Journal of Materials Science 2005; 40:4189-4198.

DOI: 10.1007/s10853-005-2821-y

61. Y. Habibi, W.K. El-Zawawy, M.M. Ibrahim, A. Dufresne. Processing and characterization of reinforced polyethylene composites made with lignocellulosic fibre from egyptian agro-industrial residues. Composites Science and Technology 2008; 68:1877-1885.
DOI: 10.1016/j.compscitech.2008.01.008
62. V. Nair, N. Sandhyarani. Studies on the photodegradation of TiO_2 incorporated polyethylene-film under visible white light and UV radiation. International Conference on Advances in Polymer Technology 2010; 26-27:338-341.
63. M. Koutny, J. Lemaire, A. Delort. Biodegradation of polyethylene films with prooxidant additives. Chemosphere 2006; 64:1243-1252.
DOI: 10.1016/j.chemosphere.2005.12.060
64. J. Weon. Effect of thermal ageing on the mechanical and thermal behaviors of linear low density polyethylene pipe. Polymer Degradation and Stability 2010; 95:14-20.
DOI: 10.1016/j.polymdegradstab.2009.10.016
65. Y.-T. Zheng, D.-R. Cao, D.-S. Wang, J.-J. Chen. Study on the interface modification of bagasse fibre and the mechanical properties of its composite with PVC. Composites: Part A 2007; 38:20-25.
DOI: 10.1016/j.compositesa.2006.01.023
66. A.N. Shebani, A.J. van Reenen, M. Meincken. The effect of wood extractives on the thermal stability of different wood species. Thermochimica Acta 2008; 471:43-50.
DOI: 10.1016/j.tca.2008.02.020
67. H.S. Kim, S. Kim, H.J. Kim, H.S. Yang. Thermal properties of bio-flour-filled polyolefin composites with different compatibilizing agent type and content. Thermochimica Acta 2006; 451:181-188.
DOI: 10.1016/j.tca.2006.09.013
68. T.T.L. Doan, H. Brodowsky, E. Mader. Jute fibre/polypropylene composites II. Thermal, hydrothermal and dynamic mechanical behavior. Composites Science and Technology 2007; 67:2707-2714.
DOI: 10.1016/j.compscitech.2007.02.011
69. B. Tajeddin, R.A. Rahman, L.C. Abdulah, N.A. Ibrahim, Y.A. Yusof. Thermal properties of low density polyethylene-filled kenaf cellulose composites. European Journal of Scientific Research 2009; 32:223-230.
DOI: 10.1016/j.ijbiomac.2010.04.004

70. M. Tajvidi, A. Takemura. Thermal degradation of natural fiber-reinforced polypropylene composites. Journal of Thermoplastic Composite Materials 2010; 23:281-298.
DOI: 10.1177/0892705709347063

71. J.R. Araujo, W.R. Waldman, M.A. De Paoli. Thermal properties of high density polyethylene composites with natural fibres: Coupling agent effect. Polymer Degradation and Stability 2008; 93:1770-1775.
DOI: 10.1016/j.polymdegradstab.2008.07.021

72. C.F. Kuan, H.C. Kuan, C.C.M. Ma, C.M. Huang. Mechanical, thermal and morphological properties of water-crosslinked wood flour reinforced linear low-density polyethylene composites. Composites: Part A 2006; 37:1696-1707.
DOI: 10.1016/j.compositesa.2005.09.020

73. H. Bouafif, A. Koubaa, P. Perre, A. Cloutier, B. Riedl. Wood particle/high-density polyethylene composites: Thermal sensitivity and nucleating ability of wood particles. Journal of Applied Polymer Science 2009; 113:593-600.
DOI: 10.1002/app.30129

74. J. George, S.S. Bhagawan, S. Thomas. Thermogravimetric and dynamic mechanical thermal analysis of pineapple fibre reinforced polyethylene composites. Journal of Thermal Analysis 1996; 47:1121-1140.
DOI: 10.1007/BF01979452

75. A.S. Luyt, M.E. Malunka. Composites of low-density polyethylene and short sisal fibres: The effect of wax addition and peroxide treatment on thermal properties. Thermochimica Acta 2005; 426:101-107.
DOI: 10.1016/j.tca.2004.07.010

76. S. Mohanty, S.K. Verma, S.K. Nayak, S.S. Tripathy. Influence of fiber treatment on the perfomance of sisal-polypropylene composites. Journal of Applied Polymer Science 2004; 94:1336-1345.
DOI: 10.1002/app.21161

77. S.H. Lee, S. Wang. Biodegradable polymers/bamboo fiber biocomposite with bio-based coupling agent. Composites: Part A 2006; 37:80-91.
DOI: 10.1016/j.compositesa.2005.04.015

78. A. Amash, P. Zugenmaier. Morphology and properties of isotropic and oriented samples of cellulose fibre–polypropylene composites. Polymer 2000; 41:1589–1596.
DOI: 10.1016/S0032-3861(99)00273-6

79. M. Pracella, D. Chionna, I. Anguillesi, Z. Kulinski, E. Piorkowska. Functionalization, compatibilization and properties of polypropylene composites with hemp fibres. Composites Science and Technology 2006; 66:2218–2230.
DOI: 10.1016/j.compscitech.2005.12.006

80. R.R.N. Sailaja. Mechanical and thermal properties of bleached kraft pulp–LDPE composites: Effect of epoxy functionalized compatibilizers. Composites Science and Technology 2006; 66:2039–2048.
DOI: 10.1016/j.compscitech.2006.01.029

81. S.K. Nayak, S. Mohanty, S.K. Samal. Influence of short bamboo/glass fibre on the thermal, dynamic mechanical and rheological properties of polypropylene hybrid composites. Materials Science and Engineering A 2009; 523:32-38.
DOI: 10.1016/j.msea.2009.06.020

82. M.E. Malunka, A.S. Luyt, H. Krump. Preparation and characterization of EVA-sisal fibre composites. Journal of Applied Polymer Science 2006; 100:1607-1617.
DOI: 10.1002/app.23650

83. D.G. Dikobe, A.S. Luyt. Effect of filler content and size on the properties of ethylene vinyl acetate copolymer-wood fibre composites. Journal of Applied Polymer Science 2007; 103:3645-3654.
DOI: 10.1002/app.25513

84. S.M.B. Nachtigall, G.S. Cerveira, S.M.L. Rosa. New polymeric-coupling agent for polypropylene/wood-flour composites. Polymer Testing 2007; 26:619-628.
DOI: 10.1016/j.polymertesting.2007.03.007

85. X.C. Ge, X.H. Li, Y.Z. Meng. Tensile properties, morphology, and thermal behavior of PVC composites containing pine flour and bamboo flour. Journal of Applied Polymer Science 2004; 93:1804-1811.
DOI: 10.1002/app.20644

86. A.G. Pedroso, D.S. Rosa. Mechanical, thermal and morphological characterization of recycled LDPE/corn starch blends. Carbohydrate Polymers 2005; 59:1-9.
DOI: 10.1016/j.carbpol.2004.08.018

87. M.A. Mokoena, V. Djokovic, A.S. Luyt. Composites of linear low density polyethylene and short sisal fibres: The effects of peroxide treatment. Journal of Materials Science 2004; 39:3403-3412.
DOI: 10.1023/B:JMSC.0000026943.47803.0b

88. D.G. Dikobe, A.S. Luyt. Morphology and properties of polypropylene/ethylene vinyl acetate copolymer/wood powder blend composite. eXPRESS Polymer Letters 2009; 3:190-199.
DOI: 10.3144/expresspolymerlett.2009.24

89. G. Kalaprasad, B. Francis, S. Thomas, C.R. Kumar, C. Pavithran, G. Groeninckx, S. Thomas. Effect of fibre length and chemical modifications on the tensile properties of intimately mixed short sisal/glass hybrid fibre reinforced low density polyethylene composites. Polymer International 2004; 53:1624-1638.
DOI: 10.1002/pi.1453

90. S. Shinoj, R. Visvanathan, S. Panigrahi, M. Kochubabu. Oil palm fibre (OPF) and its composites: A review. Industrial Crops and Products 2011; 33:7-22.
DOI: 10.1016/j.indcrop.2010.09.009

91. S. Zahra**,** S.S. Abbas, M.T. Mahsa**,** N. Mohsen**.** Biodegradation of low-density polyethylene (LDPE) by isolated fungi in solid waste medium. Waste Management 2010; 30:396-401.
DOI: 10.1016/j.wasman.2009.09.027

Chapter 3

Experimental

3.1 Materials

3.1.1 Low-density polyethylene (LDPE)

Unstabilized LDPE was supplied in pellet form by Sasol Polymers, Johannesburg, South Africa. It has M_n = 29417 g mol^{-1}, M_w = 142584 g mol^{-1} and a melting point of 108 °C.

3.1.2 Wood flour (WF)

Pine wood flour was a cream-white powder supplied by Taurus furniture manufacturers, Phuthaditjhaba, South Africa. It was sieved to < 150 μm sizes, and it has a density of 1.5 g cm^{-3}.

3.2 Methods

3.2.1 Wood flour treatment

The WF was dried at 80 ºC for 24 hours to obtain the lowest moisture level possible in the wood particles.

3.2.2 Preparation of degraded LDPE (dLDPE)

Unstabilized LDPE was degraded in an oven at 80 °C for 2, 3, 4, 5, 7, and 9 weeks to functionalize the LDPE. The formation of functional groups was monitored by FTIR spectroscopy.

3.2.3 Blends and composites preparation

The mass ratios used for the blends and composites are shown in Table 3.1. All the samples were prepared by a melt mixing process using a Brabender Plastograph 50 mL internal mixer at 120 ºC and 30 r.p.m. for 10 min. The samples were then melt-pressed at 120 ºC for 5 min under 50 bar pressure using a hydraulic melt-press to form 15 x 15 cm^2 square sheets. Test samples were then cut from the sheets for the various analyses.

Table 3.1 Sample ratios used for the preparation of the different blends and composites

LDPE/ dLDPE (w/w)	LDPE/WF (w/w)	LDPE/WF/ dLDPE (w/w)	LDPE/WF/ dLDPE (w/w)	LDPE/WF/ dLDPE (w/w)
100/0	-	-	-	-
98/2	90/10	88/10/2	78/20/2	68/30/2
95/5	80/20	85/10/5	75/20/5	65/30/5
93/7	70/30	83/10/7	73/20/7	63/30/7

3.3 Characterization techniques

3.3.1 Fourier transform infrared spectroscopy (FTIR)

FTIR is a technique that provides information about the structure of a certain molecular compound. It can be used as a unique collection of absorption bands to easily identify how a certain compound bonds. It uses infrared radiation where a monochromatic beam of light at different frequencies is passed through sample. A fraction of the incident irradiation is absorbed by the sample giving absorption signals at different wavenumbers [1].

A Perkin Elmer Spectrum 100 FTIR spectrometer was used for this analysis. FTIR spectra were recorded for 8 scans in the 400 to 4000 cm^{-1} wavenumber region using a 4 cm^{-1} resolution.

3.3.2 Scanning electron microscopy (SEM)

SEM gives the microscopic images of the sample structure, morphology, and homogeneity of the sample compositions. An electron beam is scanned across the sample surface generating a variety of electron signals from the surface. These signals can be secondary electron signals, Auger electron signals or backscattered electron signals. These signals are then detected by detectors and collected to finally produce microscopic images of the samples. Before SEM analysis is done on the samples, the sample surface must be conductive to avoid accumulation of charges during surface irradiation. The surfaces are mostly coated with gold, platinum, tungsten, or iridium [2].

After the samples were fastened onto SEM pegs, they were sputtered-coated with gold before analysis. A Leo® 1430VP scanning electron microscope, fitted with backscatter, cathodoluminescence, variable pressure, and energy dispersive detectors was used to analyze the samples at an accelerating voltage of 7 kV.

3.3.3 Differential scanning calorimetry (DSC)

Power compensated DSC, which is the technique used for this project, analyzes thermal transitions in substances by individually heating or cooling two pans, containing respectively the sample and an inert solid. The DSC measures the difference in electrical power (ΔQ) supplied to the two pans as function of time or temperature, and ultimately gives information about the sample's thermal transitions. For polymers DSC is frequently applied to determine transitions such as the glass transition temperature, the melting and crystallization temperatures, as well as the melting and crystallization enthalpies [3,4].

A Perkin-Elmer DSC7 differential scanning calorimeter was used for the analyses. The samples were analysed under nitrogen flow (20 mL min^{-1}). The instrument was calibrated using the onset temperatures of melting of indium and zinc standards, as well as the melting enthalpy of indium. Samples (5-10 mg) were sealed in aluminium pans. The samples were heated from 25 to 125 °C at a heating rate of 10 °C min^{-1}, and cooled to 25 °C at the same rate. For the second scan, the samples were heated and cooled under the same conditions. The peak temperatures of melting and crystallization, as well as melting and crystallization enthalpies, were determined from the second scans to eliminate any thermal history effects.

All the DSC measurements were repeated on three different samples for each composition. The results are reported as average values with standard deviations.

3.3.4 Thermogravimetric analysis (TGA)

TGA is a characterization technique which monitors sample mass loss as function of time or temperature in a specified atmosphere. This technique is used mainly to investigate the decomposition and thermal stability of materials under a variety of conditions [3,4].

The TGA used was a Perkin-Elmer TGA7 thermogravimetric analyzer. Samples of masses between 5 and 10 mg were heated from ambient to 600 °C at a heating rate of 10 ºC min^{-1} under flowing nitrogen (20 mL min^{-1}).

3.3.5 Dynamic mechanical analysis (DMA)

This method of analysis determines the viscoelastic properties such as the storage modulus, loss modulus and damping factor of substances against either temperature, time, or frequency. In DMA an oscillating sinusoidal stress force is applied on the sample which ultimately generates sinusoidal strain waves with a phase lag. By measuring the amplitude differences in these two sinusoidal waves, the storage modulus, loss modulus and damping factors of the sample are calculated as function of temperature or frequency [4].

The dynamic mechanical properties of the blends and composites were investigated using a Perkin Elmer Diamond DMA from Waltham, Massachusetts, U.S.A. The analysis settings were as follows:

Frequency	1 Hz
Amplitude	20 μm
Temperature range	-80 to 110 ºC
Heating rate	3 ºC min^{-1}
Preload force	0.02 N
Sample length	20 mm
Sample width	12.0-12.5 mm
Sample thickness	1.0-1.3 mm

3.3.6 Tensile testing

Tensile testing is where the mechanical properties of a sample are analyzed as force is applied by pulling the sample [5-7]. Tensile testing was done on a Hounsfield H5KS universal tester at a cross-head speed of 20 mm min^{-1}. At least five dumbbell samples of 20 mm gauge length, 2 mm thickness, and 5 mm width were tested for each composition. The tensile modulus, stress at break and elongation at break were calculated from the stress strain curves, and average values with standard deviations are reported.

3.3.7 Surface hardness testing

A hardness test determines how hard a sample is from an indentation made with a load or force penetrating the sample surface [6]. A UHL VMHT MOT micro-hardness tester with a test load of 25 g, dwell time of 15 s and an indentation speed of 50 μm s^{-1} was used. The samples were round disks of 21 mm diameter and 3.5 mm thickness, and the indenter shape was a diamond pyramid. Ten samples of each composition were analysed.

3.3.8 Impact properties

Impact testing of samples measures the fracture resistance of the samples. Different methods are used to measure impact strength. The Izod impact strength test method is divided into notched or unnotched Izod impact methods. For the notched Izod impact test, a V- or U-shaped cut-notch is done on the sample and it is then mounted vertically in the tester while broken by a swinging pendulum. For the unnotched test method, no cut is done on the sample before testing. The Charpy impact strength is measured by fracturing the sample on the side opposite to the notch. [5,7].

The impact properties were determined with unnotched Izod impact testing using a Ceast Torino 6546/000 impact pendulum tester. The specimens were tested using 15 J pendulum energy and a 150º release angle. The samples (5 mm x 50 mm x 1.5 mm) were injection moulded. At least three samples were tested for each composition.

3.4 References

1. B. Stuart. Infrared Spectroscopy: Fundamentals and Applications. John Willey and Sons Ltd., Chichester (2004) p.2-10.
2. J. Liu. High resolution scanning electron microscopy. In: N. Yao, Z.L. Wang (Editors). Handbook of Microscopy for Nanotechnology. Kluwer Academic Publishers, New York (2005) p.325-330.
3. P.J. Haines, M. Reading, F.W. Wilburn. Differential thermal analysis and differential scanning calorimetry. In: M.E Brown (Editor). Handbook of Thermal Analysis and Calorimetry, Volume 1. Elsevier Science, Amsterdam (1998) p. 279-286, 225-228.
4. T. Hatakeyama, F.X. Quinn. Thermal Analysis. Fundamentals and Applications to Polymer Science. 2nd Edition. John Willey and Sons, Chichester (1999) p.1-9, 45-50, 125-134.
5. A. Rudin. The Elements of Polymer Science and Engineering. 2nd Edition. Academic Press, San Diego (1999) p.419-426, 429-431.
6. http://www.walteruhl.com (accessed 27 June 2011).
7. L.H. Sperling. Introduction to Physical Polymer Science. 4th Edition. John Wiley and Sons, Hoboken (2006) p.557-561, 573-576.

Chapter 4

Results and discussion

4.1 Attenuated total reflectance Fourier-transform infrared spectroscopy (ATR-FTIR) and gel permeation chromatography (GPC)

Figures 4.1 to 4.3 show the FTIR spectra of LDPE, dLDPE (degraded for different periods of time), WF, as well as uncompatibilized and compatibilized composites, while Tables 4.1 and 4.3 summarize the main vibrations observed in these spectra. The formation of several functional groups like hydroxyls, carbonyls, vinyls, aldehydes and esters are expected when LDPE is degraded in air. All the composite spectra are dominated by peaks around 2850-3000 cm^{-1} and 1000-1100 cm^{-1} due to the C-H and C-O-C stretching vibrations.

Figure 4.1 shows the effect of degradation times and the development of functional groups on the LDPE chains. The carbonyl stretching vibration appears around 1735 cm^{-1} for all the dLDPEs. However, for LDPE degraded for five weeks it was weak and small. Beyond five weeks this peak intensity increases significantly and continuously until sixth week; then thereafter the increase is inconsistent. Asymmetric and symmetric C-H stretching vibrations around 2916 and 2848 cm^{-1} were also noticed for LDPE and dLDPE. With increasing degradation time there was an inconsistent increase in the C-O-C stretching vibrations around 1300-1000 cm^{-1}. There were no obvious peak shifts as a result of degradation.

Table 4.1 Summary of FTIR vibrational peaks for LDPE and dLDPE

Wavenumber / cm^{-1}	Assigned vibrations	Vibration	Appears in
2916	CH_2	Assymetric stretch	LDPE and dLDPE
2848	CH_2	Symmetric stretch	LDPE and dLDPE
1715	C=O	Carbonyl stretch	dLDPE only
1470-1450	CH_2	C-H bending	dLDPE
1376	CH_3	Methyl rocking	dLDPE
1300-1000	C-O	Esters and acetate	LDPE and dLDPE
730	C-H(in long chains)	Methyl rocking	LDPE and dLDPE

Figure 4.2 shows the differences between the LDPE spectra before degradation and after 5, 5.5 and 7 weeks degradation. All the spectra show equally intense absorption peaks around 2840 and 2920 cm^{-1} that correspond to the C–H symmetric and asymmetric stretching of methylene groups [1-4]. Additional peaks are seen in the dLDPE spectra confirming the oxidative degradation of LDPE. The peaks around 1714-1780 and 1000-1100 cm^{-1} are respectively related to the carbonyl and C-O-C stretching vibrations. The 5 weeks degraded sample has a relatively weak carbonyl peak, and the intensity significantly increases for the 5.5 weeks degraded sample and even further for the 7 weeks degraded sample. The respective carbonyl indices for these dLDPE samples are shown on Table 4.2. A hydroxyl stretching vibration around 3300-3700 cm^{-1} is visible, but very weak. A number of research scientists observed that the oxidative degradation of polyolefins gave rise to the formation of carbonyls or ketones, C-O-C, and hydroxyls. Mendes *et al*. [1] investigated the effect of weathering of unstabilized and stabilized HDPE. They found that upon oxidative weathering of these polymers, carbonyl, vinyl, and hydroxyl groups appeared on the polymer backbone. Huang *et al*. [2] obtained similar results when investigating the thermal oxidation of polyethylene. Motta *et al*. [3] oxidized atactic polystyrene by chemical treatment in order to introduce functional groups, and they confirmed the formation of carbonyl and hydroxyl groups.

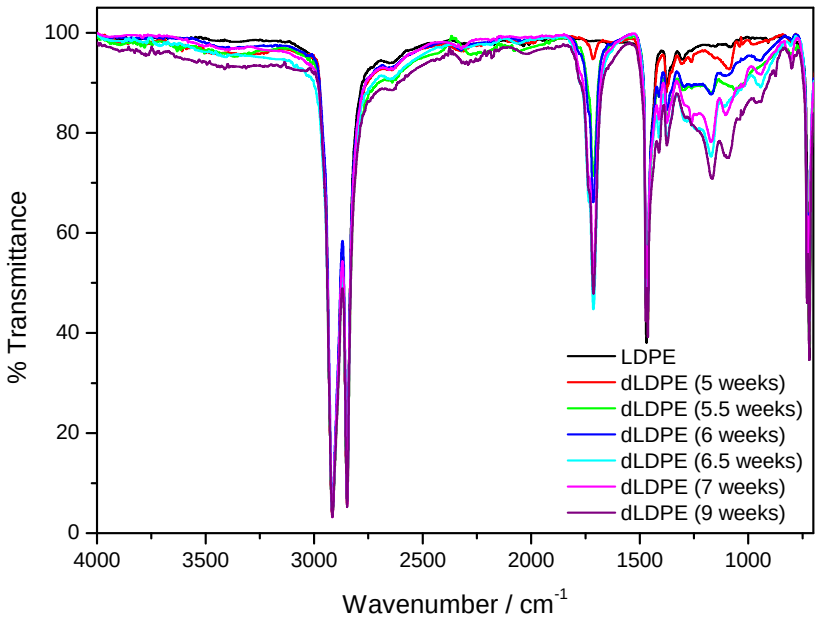

Figure 4.1 FTIR spectra of LDPE and the different dLDPEs

Figure 4.3 shows the FTIR spectra of WF and the uncompatibilized and compatibilized composites, while Table 4.3 summarizes the main vibrations observed in these spectra. The spectrum of WF shows the characteristic O-H stretching vibration around 3430-3300 cm^{-1}, which is also visible in the composites' spectra (Figure 4.4). Around 1730 cm^{-1} and 1245 cm^{-1} there are peaks related to the C=O and C-O-C vibrations of cellulose and hemicelluloses. The bands observed around 2920, 2850 and 1496 cm^{-1} are due to the C−H stretching vibration of methyl or methylene and C−H bending or scissoring. The spectrum of the 80/20 w/w LDPE/WF composite also shows vibrational peaks around 1740 and 3430-3300 cm^{-1} due to the presence of carbonyl and hydroxyl groups in cellulose and hemicelluloses. To summarize, this spectrum shows all the characteristic peaks for LDPE and WF.

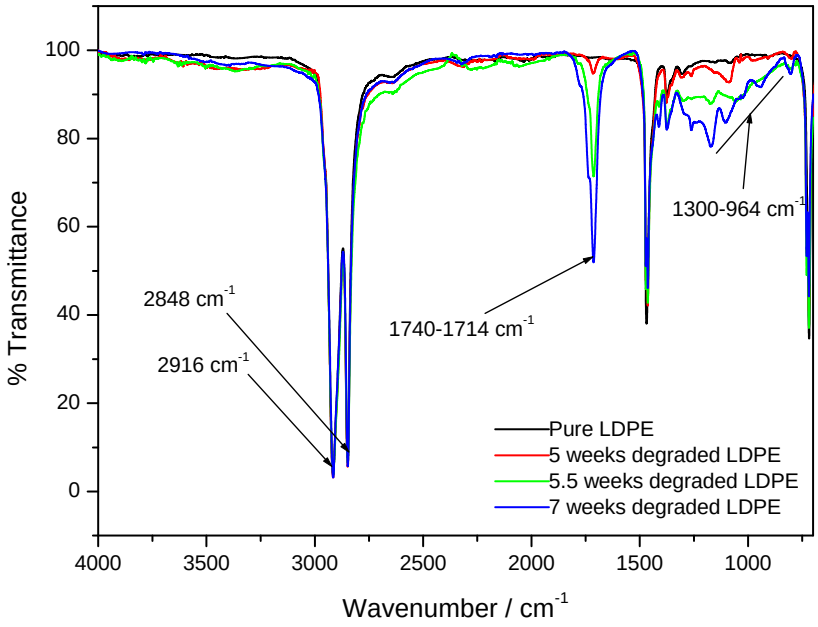

Figure 4.2 FTIR spectra of LDPE and dLDPE (5, 5.5 and 7 weeks degradation)

Table 4.2 Carbonyl indices of dLDPEs

	Absorbance / %		
Degradation time / weeks	CO stretching vibration (1720 cm^{-1})	Methylene bending vibration (1463 cm^{-1})	Carbonyl index
5	6.2	58.2	0.11
5.5	28.9	57.4	0.50
7	48.5	54.0	0.90

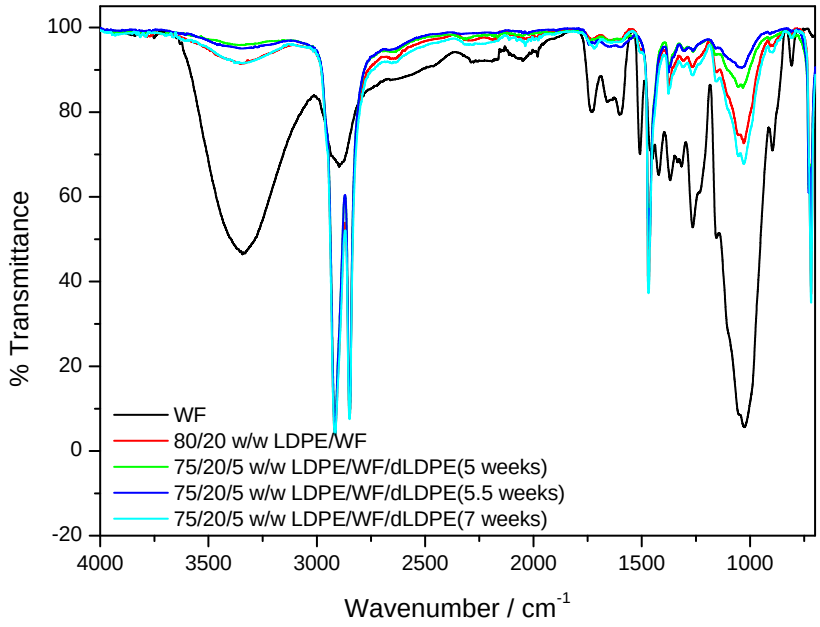

Figure 4.3 FTIR spectra of WF, as well as the uncompatibilized and compatibilized composites containing 5, 5.5 and 7 weeks degraded LDPE

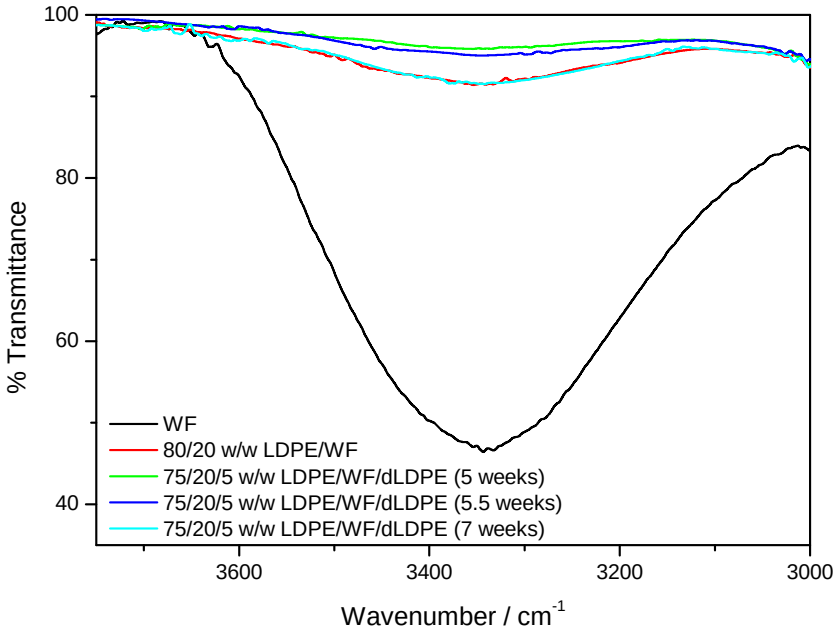

Figure 4.4 High-wavenumber region of the FTIR spectra of WF, as well as the uncompatibilized and compatibilized composites containing 5, 5.5 and 7 weeks degraded LDPE

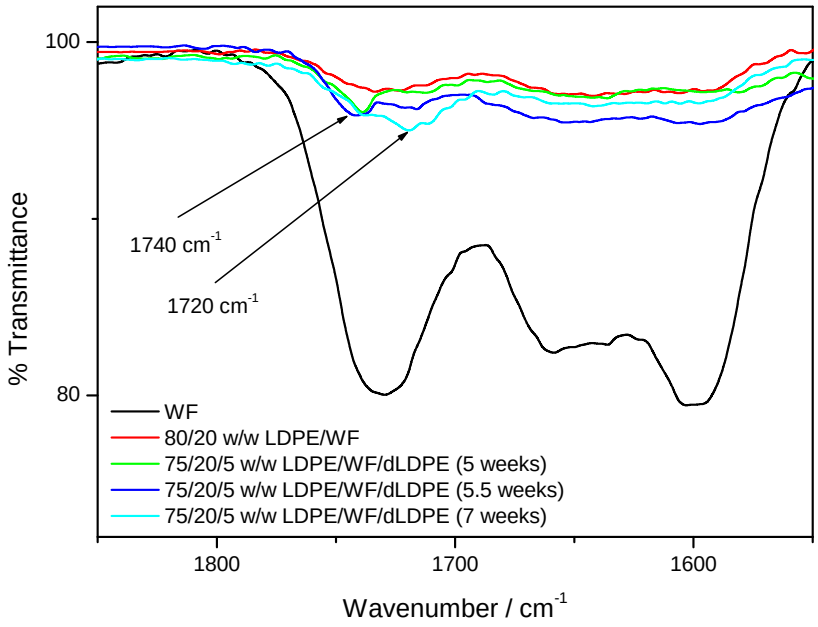

Figure 4.5 Intermediate wavenumber region of the FTIR spectra of WF, as well as the uncompatibilized and compatibilized composites containing 5, 5.5 and 7 weeks degraded LDPE

Table 4.3 Summary of FTIR vibrational peaks for WF, as well as the uncompatibilized and compatibilized 20% WF containing composites

Wavenumber / cm^{-1}	Assigned vibrations	Vibration	Appears in
3500-3250	H-O	Hydroxyl stretch	All samples
2916	CH_2	Assymetric stretch	All samples
2848	CH_2	Symmetric stretch	All samples
1780-1690	C=O	Carbonyl stretch	All samples
1470-1450	CH_2	C-H bending	All samples
1376	CH_3	Methyl rocking	All samples
1300-1000	C-O-C	Esters and acetate	All samples

From the spectra of the compatibilized composites it can be seen that C-H asymmetric and symmetric (2916 and 2848 cm^{-1}) stretching peak intensities were not influenced by the presence of dLDPE. The uncompatibilized composite shows a very weak carbonyl stretching vibration at about 1730 cm^{-1} (Figure 4.5). In the compatibilized composites the carbonyl band

clearly splits into peaks at 1720 and 1740 cm^{-1}. The reason for this is the formation of hydrogen bonds between the OH groups on WF and the carbonyl groups on dLDPE. The hydrogen bonding carbonyl band at 1720 cm^{-1} also increases in intensity as the dLDPE carbonyl index increases.

Table 4.4 Summary of molecular weight and polydispersity data for dLDPE obtained after different degradation times

	M_n / g mol^{-1}	M_w / g mol^{-1}	PD
LDPE	29417	142584	4.8
dLDPE (5 weeks)	22605	115627	5.1
dLDPE (5.5 weeks)	15573	42003	2.7
dLDPE (6 weeks)	8380	25463	3.0
dLDPE (6.5 weeks)	5911	19740	3.3
dLDPE (7 weeks)	6262	20854	3.3
dLDPE (9 weeks)	5622	17348	3.1

M_n, M_w, and PD are respectively the number average molecular weight, weight average molecular weight, and polydispersity

From Table 4.4 it is clear that chain scission already started before 5 weeks degradation, and that there is a progressive decrease in number average molecular weight with increasing degradation time. The weight average molecular weight decreased significantly after 5 weeks degradation. A number of research scientists, amongst them Liu *et al*. [5] and Khan *et al*. [6], confirmed that a polymer can withstand thermal heat degradation until a certain limit. During prolonged heat exposure the polymer can also degrade through free radical crosslinking, decreasing the molecular weight through random chain scission. The dLDPE (5 weeks) has not yet degraded too much, and it contains a fairly small number of carbonyl groups, while the dLDPE (7 weeks) has a high carbonyl index, but it is significantly degraded. The 5.5 weeks sample seems to be the optimum sample in terms of carbonyl index (Figure 4.1) and extent of degradation (Table 4.4). Based on this knowledge, it was decided to concentrate the discussion of the other analysis results on the 80/20 w/w LDPE/WF, 75/20/5 LDPE/WF/dLDPE (5 weeks), 75/20/5 LDPE/WF/dLDPE (5.5 weeks) and 75/20/5 LDPE/WF/dLDPE (7 weeks) composites.

4.2 Scanning electron microscopy (SEM)

Figure 4.6 shows SEM photos of the untreated 80/20 w/w LDPE/WF composite. Both photos show a very lose structure with lots of voids, and it is difficult to distinguish between the LDPE phase and the WF. Joseph *et al*. [7], who investigated LDPE/sisal composites, found that in their untreated composites there were large fibre pull-out, voids and holes in the matrix. In our case, however, it was not possible to distinguish these specific features in Figure 4.6.

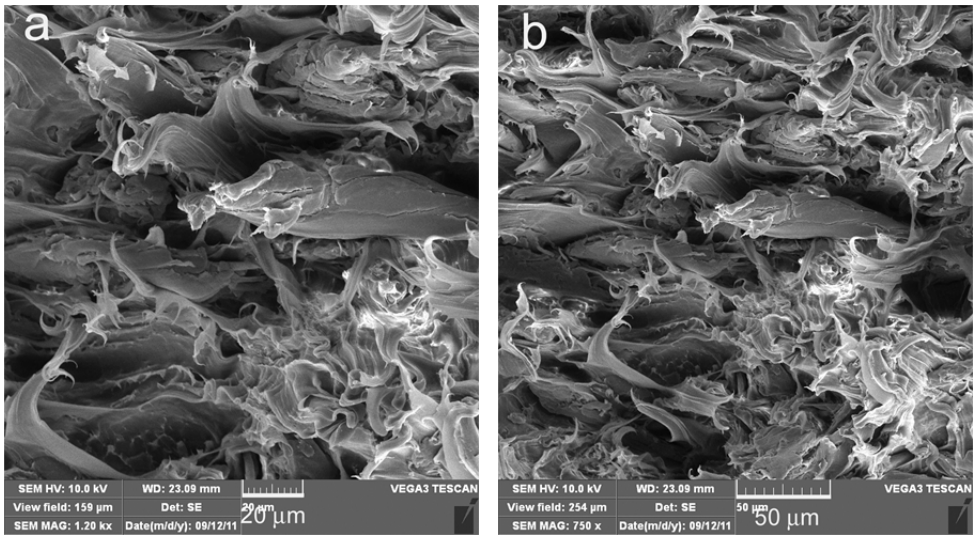

Figure 4.6 SEM images of 80/20 w/w LDPE/WF at (a) 1200x and (b) 750x magnification

Figure 4.7 shows the effect of using 5 weeks degraded LDPE as a compatibilizer in LDPE/WF composites containing 20% WF. The images show a much finer morphology with the WF particles (arrows A) fairly well dispersed and embedded in the matrix. There is, however, also evidence of narrow voids around some of the WF particles (arrow B), but mostly there seems to be more intimate contact between the matrix and the WF particles. These features indicate an improved interfacial adhesion and better wetting of the fibres by the matrix.

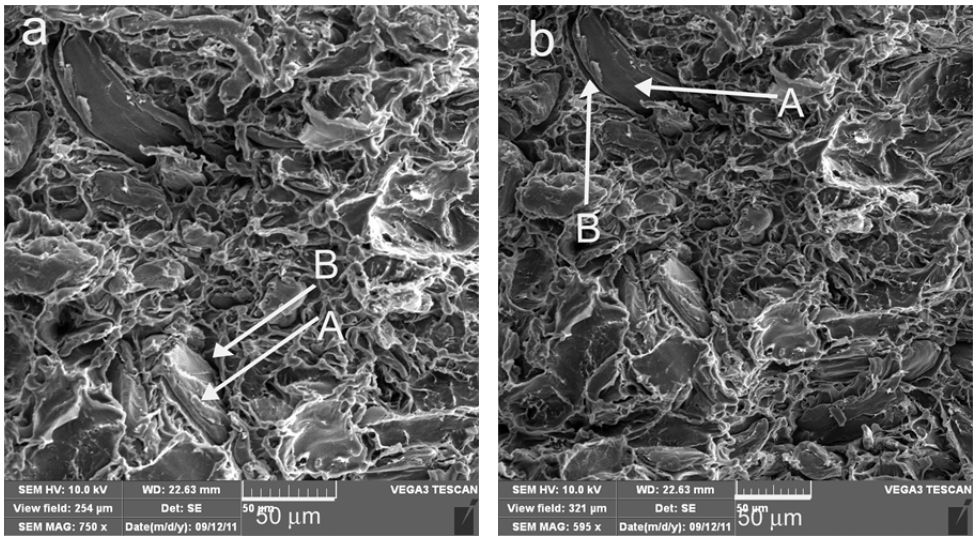

Figure 4.7 SEM images of 75/20/5 w/w LDPE/WF/dLDPE (5 weeks degraded) at magnifications of (a) 750x and (b) 595x

The images in Figure 4.8 show an even finer surface morphology with fewer voids. The WF particles (arrows A) are fairly well dispersed and embedded in the matrix. This can be attributed to the higher carbonyl index of the 5.5 weeks dLDPE, which gave rise to more hydrogen bonding and improved interfacial interaction.

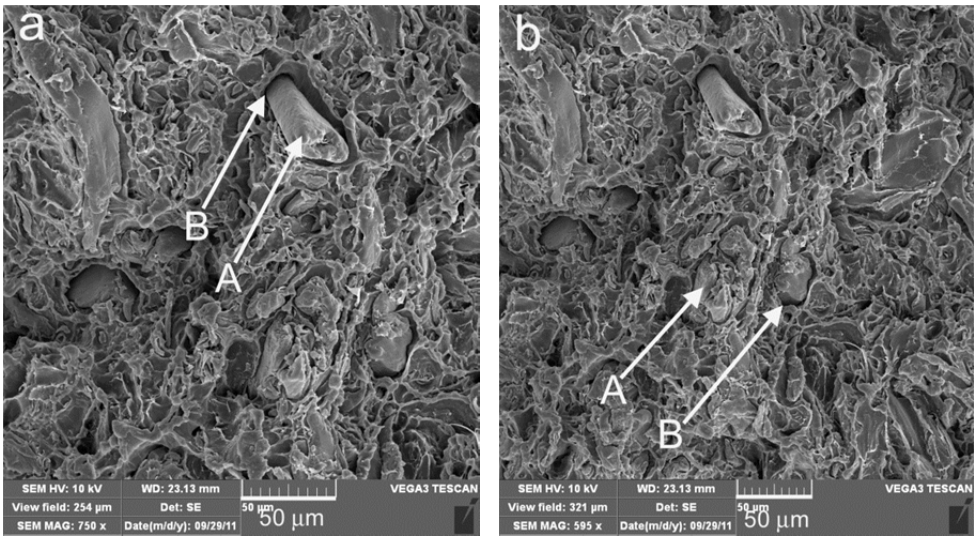

Figure 4.8 SEM images of 75/20/5 w/w LDPE/WF/dLDPE (5.5 weeks degraded) at magnifications of (a) 750x and (b) 595x

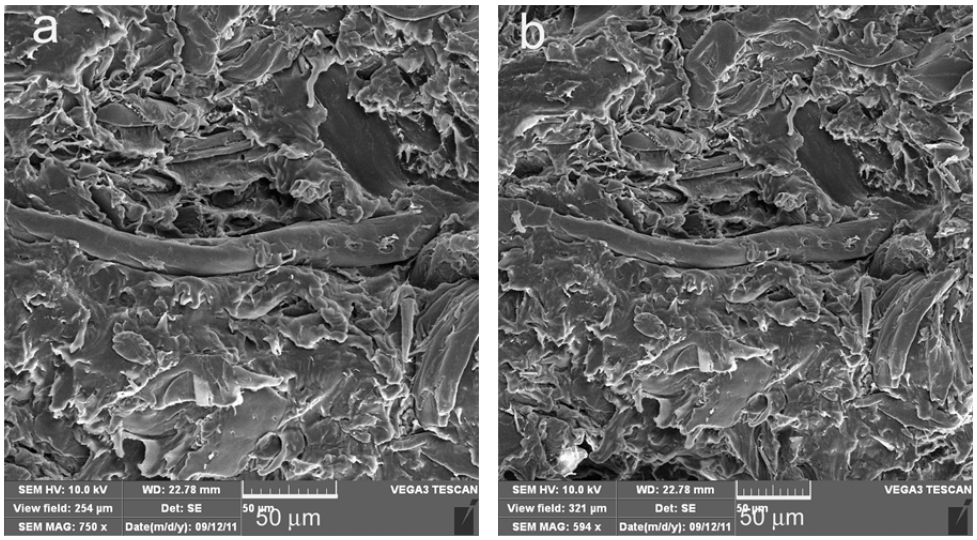

Figure 4.9 SEM images of 75/20/5 w/w LDPE/WF/dLDPE (7 weeks degraded) at magnifications of (a) 750x and (b) 594x

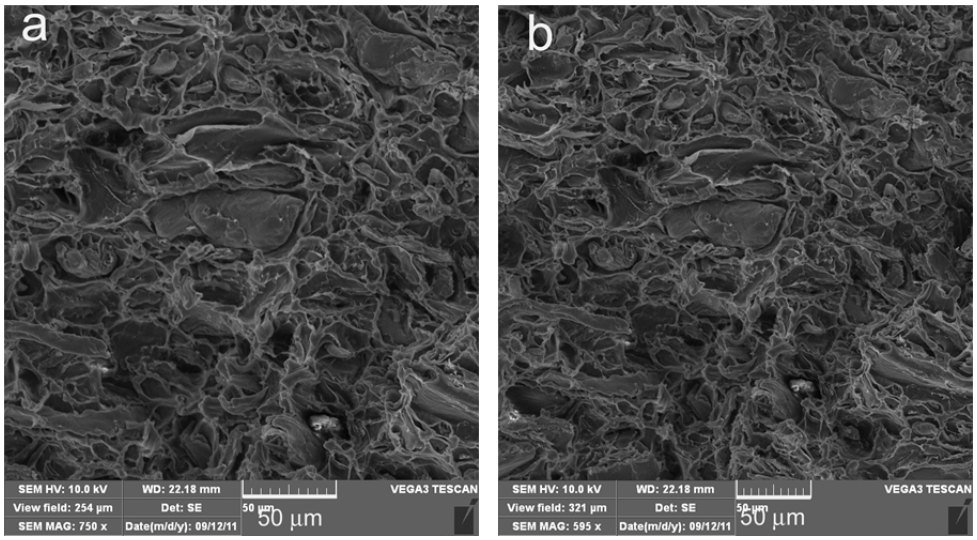

Figure 4.10 SEM images of 75/20/5 w/w LDPE/WF/dLDPE (9 weeks degraded) at magnifications of (a) 750x and (b) 595x

Figure 4.9 shows that for the sample containing 7 weeks degraded LDPE the fractured surface is much smoother and there seems to be much better adhesion between the WF and the matrix. This is probably due to the higher concentration of carbonyl groups in the 7 weeks degraded LDPE which significantly improved the interaction between the WF and the matrix. The sample containing the 9 weeks degraded LDPE, however, a more uneven morphology and more obvious voids between the fibre and the matrix (Figure 4.10). The GPC results showed that this dLDPE was already highly degraded and it is possible that the smaller

dLDPE molecules penetrated the WF pores and had very little contact with LDPE at the LDPE/WF interface.

Mengeloglu *et al.* [8] analysed the morphology of HDPE-eucalyptus fibres using MAPE compatibilization. They noted that in the morphology of untreated composites, loose individual fibres were on the HDPE surface meaning poor adhesion. In the MAPE treated composites the fractured surfaces showed fibres totally embedded in the matrix. Kuruvilla *et al.* [9] investigated the adhesion between sisal and polyethylene as a result of different sisal treatments. They noticed the existence of some matrix adhering to the fibre surface, meaning enhanced adhesion. For untreated sisal, they observed smooth voids, agglomeration, and no matrix adhering to the fibre surface, which is also in agreement with observations made by other authors [10-11].

4.3 Differential scanning calorimetry (DSC)

The DSC heating and cooling curves of LDPE, dLDPE (5, 5.5 and 7 weeks degradation), as well as the uncompatibilized and degraded LDPE compatibilized composites are shown in Figures 4.11 to 4.16. Tables 4.5 and 4.6 summarize the melting peak temperatures, crystallization peak temperatures, experimental and calculated melting enthalpies, and crystallization enthalpies. The calculated enthalpy values (ΔH_m^{calc}) were calculated from the melting enthalpies of pure LDPE, the respective dLDPEs, and the weight fractions of LDPE and dLDPE in the composites using Equation 4.1, assuming that wood flour had no effect on the LDPE and the dLDPE melting and crystallization behaviour.

$$\Delta H_m^{calc} = w_{LDPE}\,\Delta H_{m,LDPE} + w_{dLDPE}\Delta H_{m,dLDPE} \qquad (4.1)$$

where $\Delta H_{m,LDPE}$ and $\Delta H_{m,dLDPE}$ are the specific melting enthalpies of pure LDPE and degraded LDPE, while w_{LDPE} and w_{dLDPE} are the weight fractions of LDPE and degraded LDPE in the composites.

Figure 4.11 shows the DSC heating curves for pure LDPE and the LDPE/WF composites with different WF contents. Only one endothermic melting peak was observed around 108 ºC, which is the melting point of LDPE. Table 4.5 shows that the presence of WF and increasing WF content had very little influence on the melting and crystallization behaviour of the composites. There was almost no change in the melting peak temperature, and the experimental melting enthalpies were the same as the calculated ones within experimental error. This indicates that in the uncompatibilized composites neither the degree of crystallinity nor the lamellar thickness changed in the presence of and with increasing amount of WF. This is probably because there was no real interaction between the polymer matrix and the WF in these composites, as was evidenced by the large voids around the WF particles observed in the SEM images of these composites (Figure 4.4).

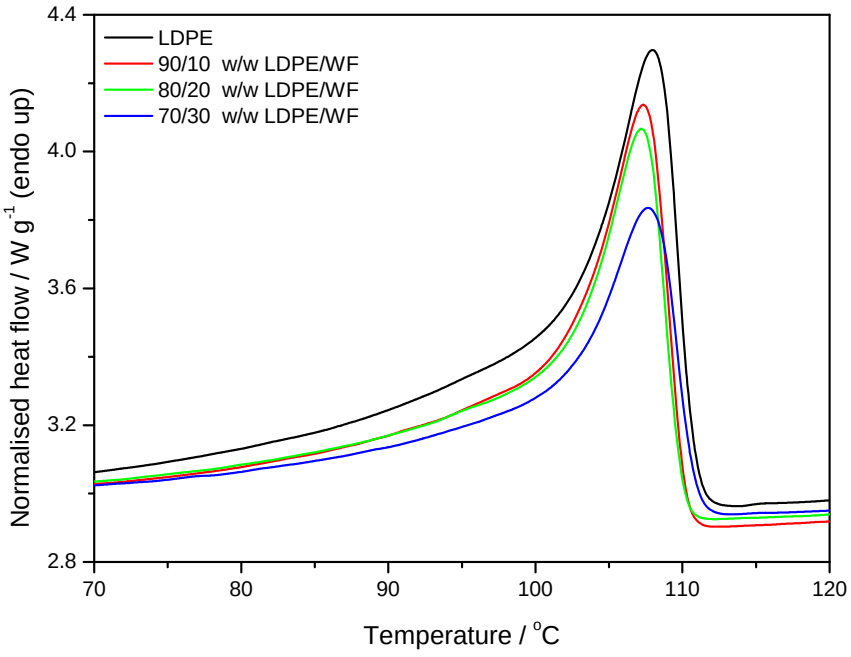

Figure 4.11 DSC heating curves of pure LDPE and the uncompatibilized LDPE/WF composites

Table 4.5 Summary of DSC data for LDPE, dLDPE (5, 5.5 and 7 weeks degradation), and the uncompatibilized LDPE/WF composites

LDPE/WF (w/w)	$T_{p,m}$ / °C	ΔH_m^{obs} / J g^{-1}	ΔH_m^{calc} / J g^{-1}	$T_{p,c}$ / °C	ΔH_c^{obs} / J g^{-1}
100/0	108.0 ± 4.2	54.1 ± 1.8	-	91.6 ± 0.3	-58.3 ± 1.8
90/10	107.5 ± 4.3	48.9 ± 0.4	48.7	90.6 ± 1.3	-54.6 ± 1.9
80/20	107.3 ± 4.2	43.9 ± 1.8	43.3	91.6 ± 1.3	-46.5 ± 2.4
70/30	107.9 ± 3.4	38.0 ± 1.4	37.9	91.6 ± 1.6	-40.4 ± 2.9
dLDPE					
5 weeks	107.4 ± 0.6	52.4 ± 1.4	-	88.2 ± 0.1	-57.3 ± 3.2
5.5 weeks	108.0 ± 0.1	57.1 ± 2.0	-	87.4 ± 0.2	-60.7 ± 0.7
7 weeks	107.3 ± 0.6	61.8 ± 3.7	-	87.3 ± 0.8	-66.1 ± 2.1

$T_{p,m}$ and $T_{p,c}$ are the melting and crystallization peak temperatures; ΔH_m^{obs} and ΔH_c^{obs} are the observed melting and crystallization enthalpies; ΔH_m^{calc} is the theoretically calculated melting enthalpy

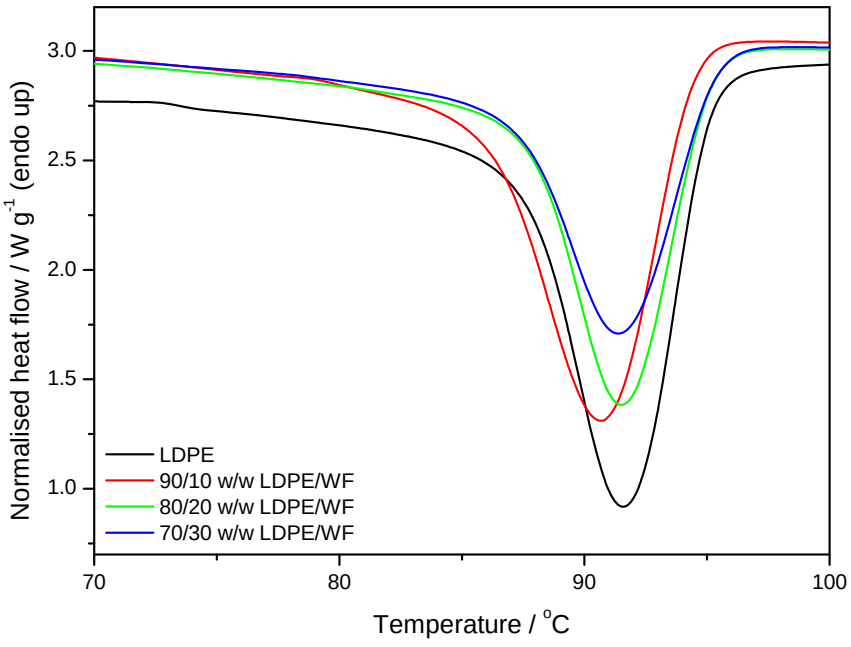

Figure 4.12 DSC cooling curves of pure LDPE and uncompatibilized LDPE/WF composites

Figure 4.12 shows exothermic crystallization peaks of LDPE with peak temperatures around 91 ºC. Again the presence and amount of WF had very little influence on these temperatures (Table 4.5). There is very little difference, within experimental error, between the melting peak temperatures of LDPE and the different dLDPEs (Figure 4.13 and Table 4.5). The melting and crystallization enthalpies clearly increased with increasing extent of degradation. Amongst many scientists who noticed similar behaviour are Khan *et al*. [6], Krupa *et al.* [12], and Lui *et al.* [5]. They all attributed this behaviour to the re-crystallization of the freed molecular segments, after chain scission, of semi-crystalline polymers like LDPE. The increase in functionality of the dLDPE probably also contributed to the higher crystallinity, because of improved inter- and intramolecular interaction.

Figure 4.14 shows that the dLDPEs crystallized at much lower temperatures, and that the crystallization temperature decreased with increasing extent of degradation. This may be attributed to their shorter chains (after chain scission – see GPC results in section 4.1) that are more mobile and therefore crystallize at lower temperatures, according to the kinetic theories of polymer crystallization [5,12-15].

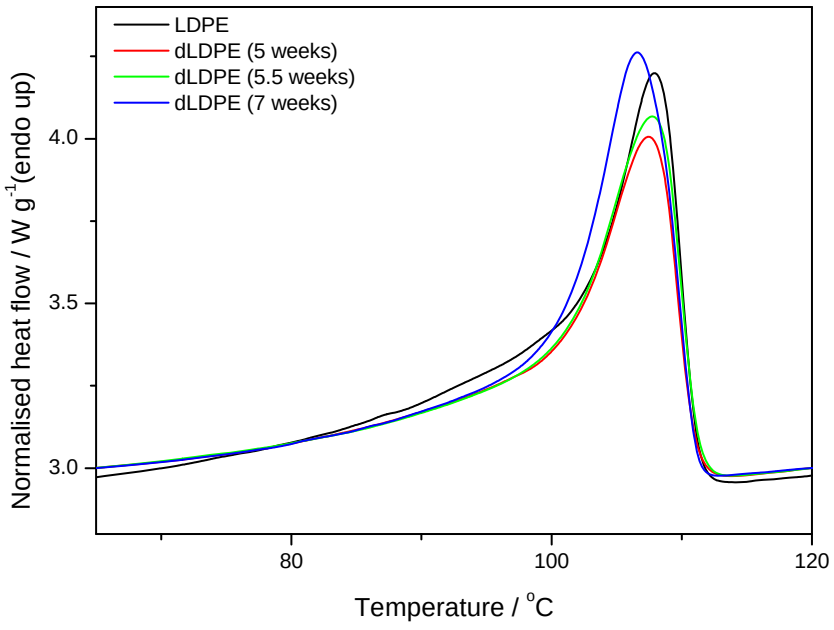

Figure 4.13 DSC heating curves of pure LDPE and the 5, 5.5 and 7 weeks dLDPEs

Table 4.6, as well as Figures 4.15 4.16, show the DSC results of LDPE and the 20% WF containing composites (uncompatibilized and compatibilized with different different dLDPEs). For the compatibilized composites, the observed melting and crystallization enthalpies are higher than the calculated ones. From the GPC and FTIR results discussed earlier, it was seen that the dLDPEs had carbonyl groups that interacted with the cellulose hydroxyl groups, which improved the contact between the matrix and WF. Because of this improved contact the WF particles seemed to have been more effective as nucleation centres for the crystallization of LDPE. The higher crystallinity of the dLDPEs probably also contributed to the overall higher crystallinity of the matrices. All the composites had almost the same melting peak temperatures, indicating that the lamellar thickness was not significantly affected.

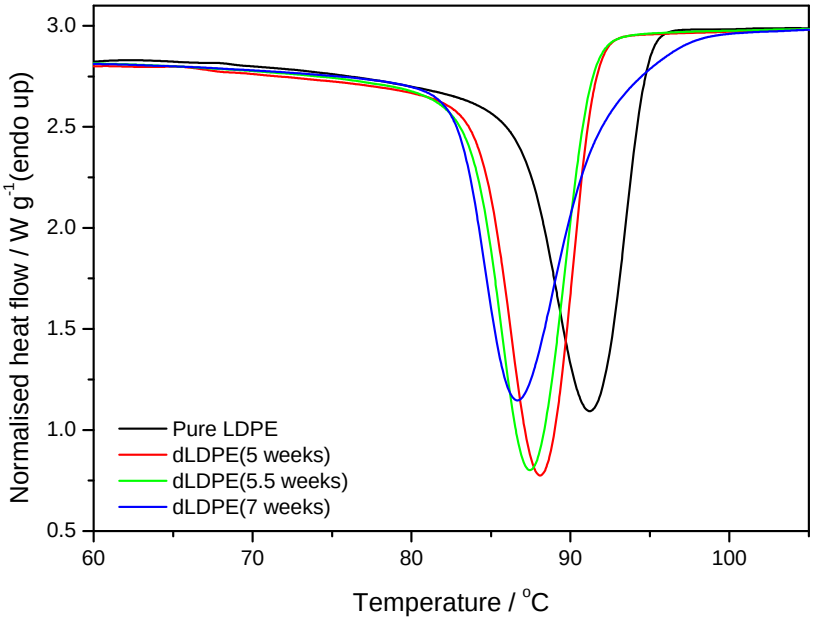

Figure 4.14 DSC cooling curves of pure LDPE and the 5, 5.5 and 7 weeks dLDPEs

Table 4.6 Summary of DSC data showing the effect of different dLDPE on the melting and crystallization behaviour of LDPE/WF composites

LDPE/WF/dLDPE (w/w)	$T_{p,m}$ / °C	ΔH_m^{obs} / J g^{-1}	ΔH_m^{calc} / J g^{-1}	$T_{p,c}$ / °C	ΔH_c^{obs} / J g^{-1}
100/0/0	108.0 ± 0.6	54.1 ± 1.8	54.1	91.6 ± 0.3	-58.3 ± 1.8
80/20/0	107.3 ± 4.2	43.9 ± 1.8	43.3	91.6 ± 1.3	-46.5 ± 2.4
75/20/5 (5 weeks)	107.6 ± 4.1	49.3 ± 2.1	43.9	91.6 ± 0.3	-50.3 ± 0.8
75/20/5 (5.5 weeks)	109.7 ± 3.6	48.7 ± 2.3	44.6	91.2 ± 1.5	-47.0 ± 3.9
75/20/5 (7 weeks)	107.4 ± 4.5	47.5 ± 2.5	43.7	91.8 ± 1.3	-46.3 ± 1.1

$T_{p,m}$ and $T_{p,c}$ are the melting and crystallization peak temperatures; ΔH_m^{obs} and ΔH_c^{obs} are the observed melting and crystallization enthalpies; ΔH_m^{calc} is the theoretically calculated melting enthalpy

Similar observations were made by a number of scientists such as Mishra *et al.* [16], Malunka *et al*. [17], Bouafif *et al.* [18] and Lee *et al.* [19]. Bouafif *et al.* [18] investigated HDPE filled with different types of softwoods. MAPE was used as a compatibilizer to improve the compatibility between wood and HDPE in the composites. The presence of wood particles increased the crystallization temperature as well as the crystallinity of all the composites. It was assumed that the WF particles effectively acted as nucleating agents. Lee *et al.* [19] investigated the effect of lysine-based diisocyanate (LDI) as a coupling agent of bamboo fibre (BF) in poly(lactic acid) (PLA) and poly(butylene succinate) (PBS). In both the PLA/BF and PBS/BF composites, the crystallization temperature increased by adding the LDI, but the crystallization enthalpy decreased. That was considered to be due to the nucleation effect of BF in the presence of LDI. The strong urethane linkages (produced by the addition of LDI) between the polymer matrix and the BF enhanced the nucleation of the polymer chains so that crystallization started at higher temperatures. However, the molecular chain mobility was reduced by the same interfacial interaction resulting in a reduced overall crystallinity.

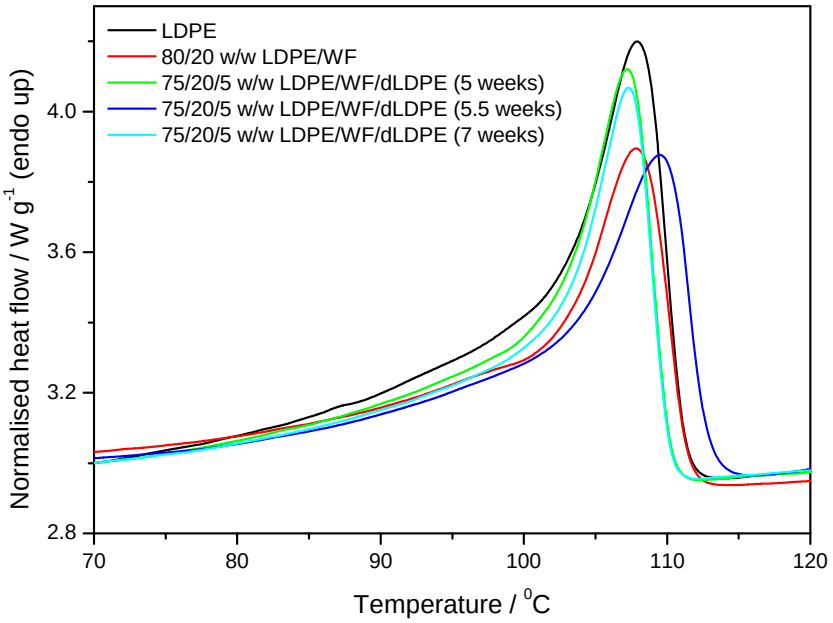

Figure 4.15 DSC heating curves of pure LDPE and the uncompatibilized and compatibilized composites

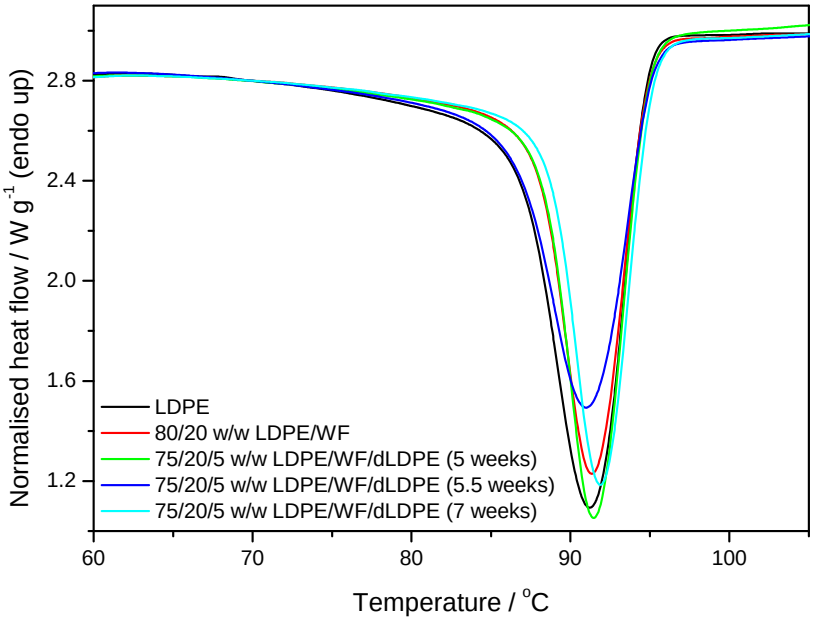

Figure 4.16 DSC cooling curves of pure LDPE and the uncompatibilized and compatibilized composites

4.4 Thermogravimetric analysis (TGA)

The TGA curves of LDPE, as well as the uncompatibilized and compatibilized composites, are shown in Figures 4.17 to 4.19. One degradation step was seen for LDPE, while the composites showed more than one degradation step. The WF curve shows three steps. Water evaporation occurred below 200 ºC. The second step, which is related to the degradation of WF, occurs between 270 and 350 ºC and can be attributed to the decomposition of wood components such as extractives, hemicelluloses, and glycosidic cellulose linkages. The third degradation step between 350 and 570 ºC is due to the degradation of α-cellulose and lignin, which ultimately forms a char around 550 ºC [20]. For the composites the first degradation step could be attributed to the decomposition of WF, while the second step is attributed to LDPE decomposition. The separate degradation of WF is not well resolved for the composite containing 10% WF, probably because all the WF particles were well protected by the thermally more stable LDPE. For the 80/20 LDPE/WF sample, the percentage mass loss of the first step corresponds well with the amount of WF initially mixed into the composite. However, the mass loss after the first step of the 70/30 w/w LDPE/WF sample was only 25%, and this result is reproducible. The reason for this is not very clear, but it is possible that some of the WF may have degraded together with LDPE in the second step, because there is an overlap between the third mass loss step of the WF and the LDPE mass loss.

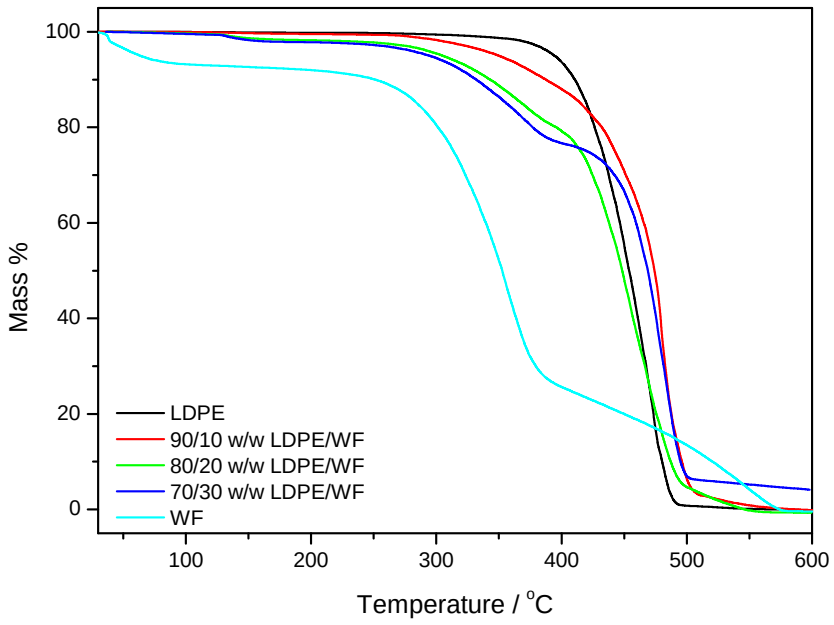

Figure 4.17 TGA curves of LDPE, and the uncompatibilized LDPE/WF composites

The degradation mechanism of polyethylene is complex and not yet well understood [21-24]. It is assumed that degradation of polyethylene occurs *via* free radical chain scission of its chains, resulting in shorter chains. Hydroperoxides are the major products formed in the oxidative degradation of polyethylenes and they initiate further degradation. Thermal degradation also leads to the formation of oxygen containing functional groups such as C=O, O-H, and C-O-C, as was also observed in our own FTIR spectra. From Figure 4.18 it can be seen that the thermal stability of LDPE in nitrogen decreases with increasing extent of degradation. There are two possible reasons for this observation: (i) The lower molecular weights of the dLDPEs as observed from the GPC results. The shorter chains formed after chain scission require less energy to degrade; (ii) The oxidative degradation products such as hydroperoxides further initiate degradation, as was also explained by Roy *et al.* [23]. Krupa *et al.* [12] pointed out that degrading a polyolefin may influence its thermal stability in two ways. When degradation occurs through oxidative decomposition (like in this study), weak points and defects may be incorporated into the polymer, resulting in easy further degradation and deterioration. However, three-dimensional crosslinked network structures may also be formed that will increase the thermal stability of the polymer.

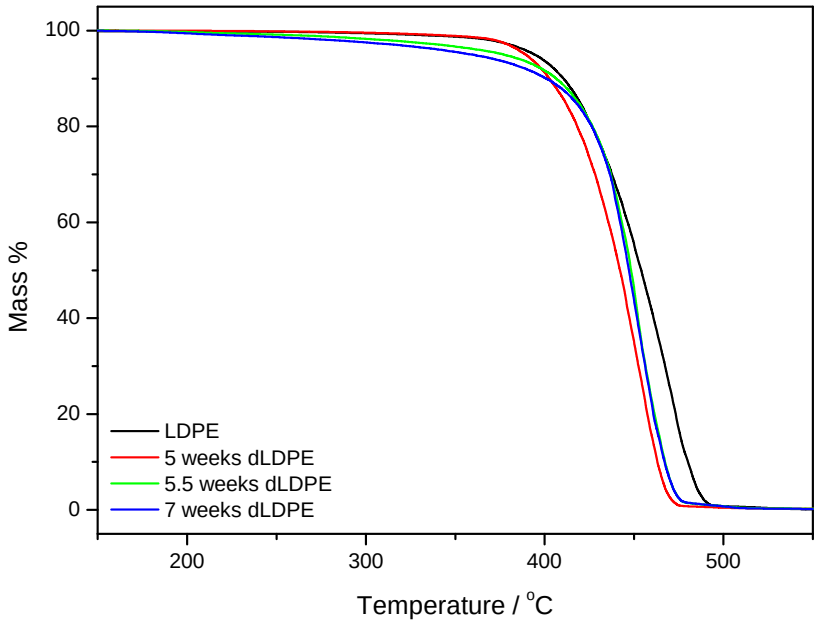

Figure 4.18 TGA curves of LDPE and 5, 5.5 and 7 weeks dLDPE

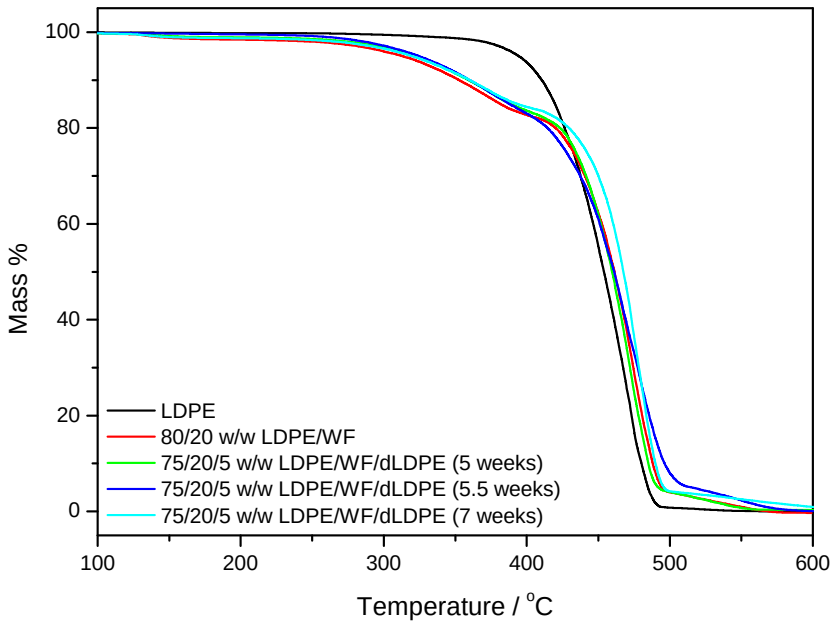

Figure 4.19 TGA curves of LDPE, as well as some uncompatibilized and compatibilized composites

Figure 4.19 shows the effect of different dLDPE compatibilizers in the 20% fibre containing composites on the thermal degradation of these composites. The presence of dLDPE did not seem to significantly influence the thermal stability of these composites. However, the 7 weeks dLDPE treated composite has a higher thermal stability than the uncompatibilized and the 5 and 5.5 weeks compatibilized composites. This may be due to the improved interfacial adhesion between WF and the polymer matrix. From the FTIR results it was seen that the 7 weeks dLDPE had the highest carbonyl index. Strong interaction between the cellulose hydroxyl and dLDPE carbonyl groups in some way influenced the degradation mechanism, and inhibited the evaporation of degradation products from the degrading sample. Shebani *et al*. [25] investigated the thermal properties of LLDPE mixed with four different extractive free fibres using EVOH as a compatibilizer. They observed that the EVOH compatibilized composites had the highest thermal stability due to the strong interfacial hydrogen bonding between the fibre and the polymer matrix. Kim *et al.* [26] investigated the thermal properties of PP and LDPE filled with bio-flour composites, where MAPP and MAPE were respectively used as compatibilizers. In both cases they noted that the thermal stability and degradation temperatures slightly increased when MAPP and MAPE were used. This behaviour was associated with the enhanced adhesion between the cellulose hydroxyl and the reactive

anhydride functional groups of MAPP and MAPE. These observations and explanation are in line with our own.

4.5 Dynamic mechanical analysis (DMA)

Generally, DMA analyses the viscoelastic properties of materials such as stiffness and elastic response (from the storage modulus), viscous response (from the loss modulus) and energy dissipated as heat (from the damping factor, tan δ). The storage modulus (E') is related to the stiffness of the material. Normally the storage modulus decreases with increasing temperature due to softening of the material and relaxation processes. Figure 4.20 shows the storage modulus as a function of temperature for the LDPE and its uncompatibilized composites. It is evident from the figure that addition of WF increases the storage modulus in the region of and above the glass transition. This is the result of the additive effect of the respective moduli of the LDPE matrix and WF, where WF has a much higher modulus than LDPE [27,28].

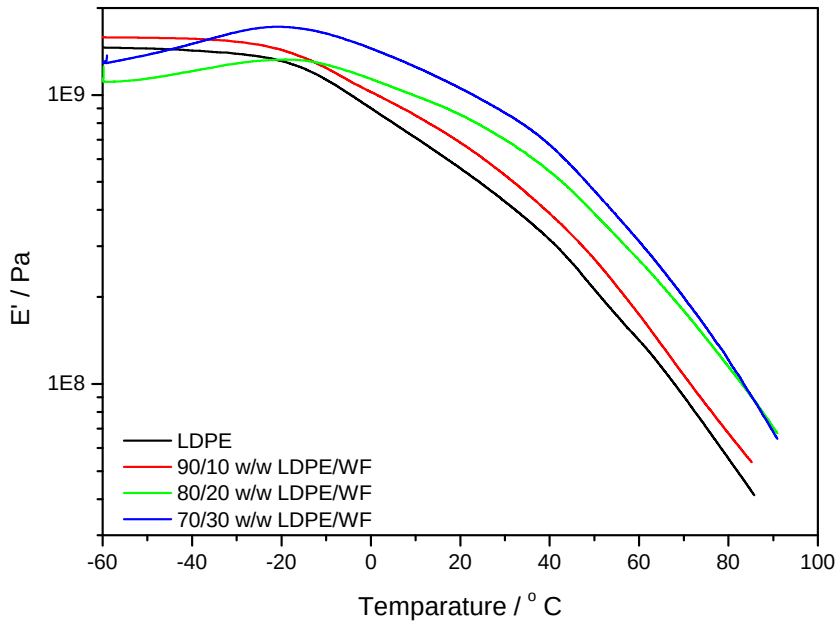

Figure 4.20 DMA storage modulus curves for the untreated LDPE/WF composites

Figure 4.21 shows the loss modulus as a function of temperature for the pure LDPE and the uncompatibilized composites. From the figure it is noticed that the glass transition temperature around -9 ºC increases as WF loading increases. This shows that there was some

sort of polymer chain immobilization interaction between the natural fibres and the matrix, even without any treatment. More energy was needed to mobilize the polymer chains, thus the glass transition shifted to higher temperatures.

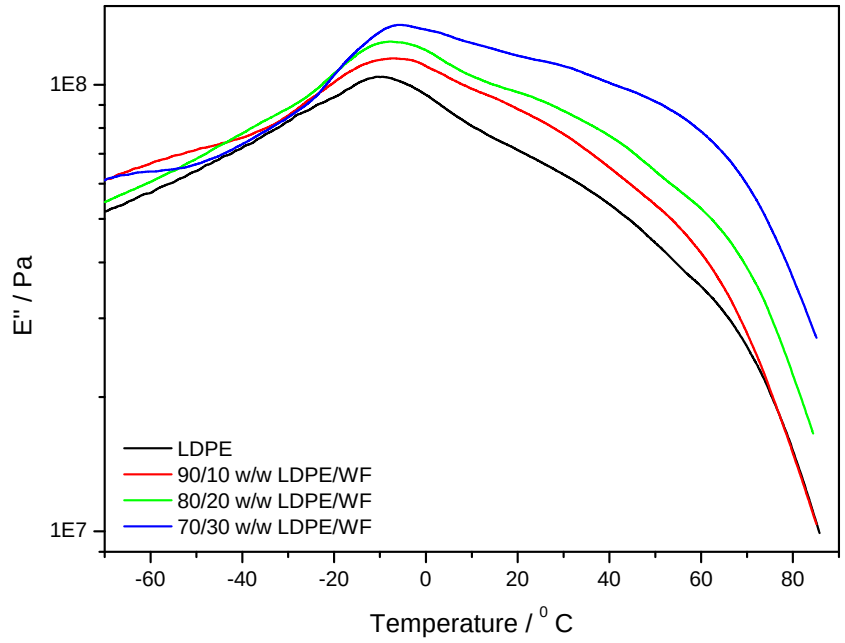

Figure 4.21 DMA loss modulus curves for the untreated LDPE/WF composites

The damping factor (tan δ) as a function of temperature for the pure LDPE and the uncompatibilized composites is shown on Figure 4.22. A weak peak is seen around -5 ºC which can be attributed to the β-relaxation (glass transition) of the LDPE. The peak is not well resolved, and it is difficult to indicate any changes in peak position or intensity with respect to the presence and amount of fibre in LDPE. The α-transition around 70 ºC is normally associated with the molecular motion within the crystalline phase in the samples, and to lamellar slip in the crystalline phase [29]. There was no obvious shift in this transition peak, which means that there was no obvious influence on the chain motion within the crystalline phase in the presence of WF. This is in agreement with the DSC results (Table 4.5), where the melting peak temperatures were not influenced by the presence of fibre in the untreated composites. However, the α- transition temperature for the composite with 10% WF is slightly lower than those of the other composites. This might have been due to less agglomeration and better dispersion of the fibre in the LDPE matrix, but the possibility of experimental error due to imperfect sample geometry cannot be ruled out.

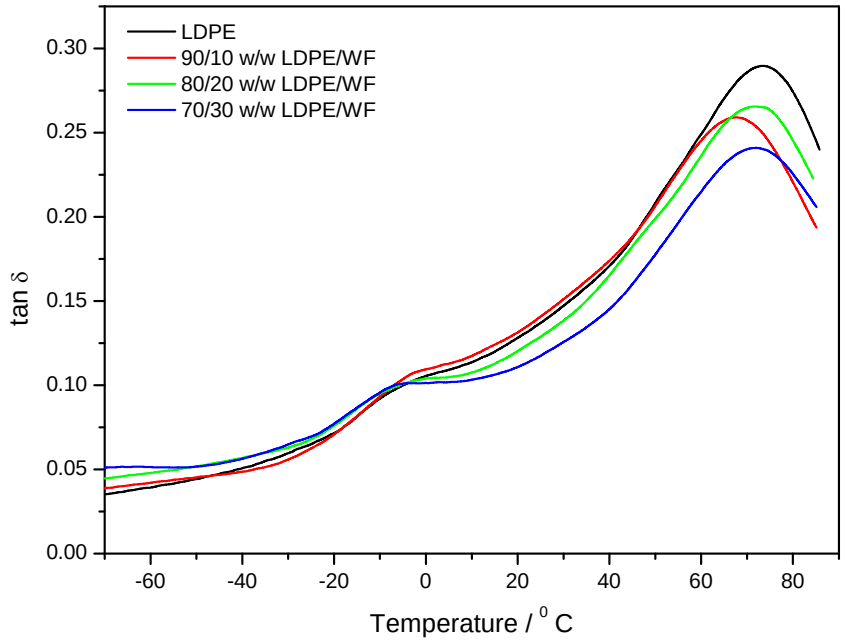

Figure 4.22 Damping factor curves for the untreated LDPE/WF composites

Figures 4.23 and 4.24 show the effect of degradation time on the storage and loss modulus of the dLDPEs as a function of temperature. From Figure 4.23 it is noticed that below the glass transition temperature, the storage modulus slightly increases with increasing degradation time. Since the polymer chains are frozen in within this temperature region, the increased modulus should not be the result of the higher crystallinity. There is also no trend in the change in modulus values as function of extent of degradation, and the modulus values in this temperature range have the same order of magnitude. However, above the glass transition temperature, higher crystallinities should give rise to higher storage modulus values. However, there were no appreciable differences between the storage modulus values in this temperature range, and no trend. Although the DSC results show higher crystallinity values for the dLDPEs, this is for some reason not reflected in the DMA storage modulus results.

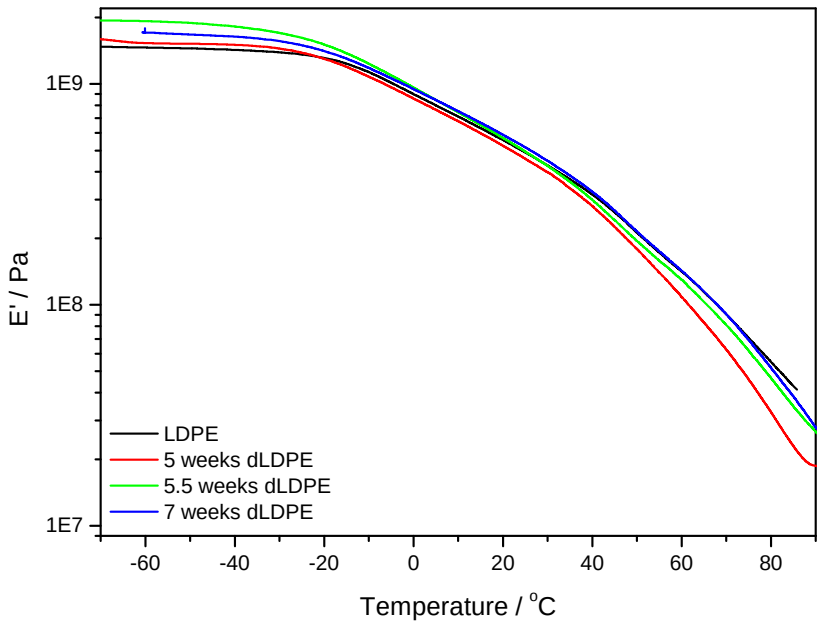

Figure 4.23 DMA storage modulus curves for LDPE and the different dLDPEs

Figure 4.24 does not show any trend in loss modulus change with increased extent of degradation over the whole temperature range. However, the glass transition slightly shifted to lower temperatures. This is probably the result of the shorter polymer chains. It is known that polymer chain ends are more mobile than the bulk of the chain [30], the degradation that resulted in shorter chains with more chain ends increased the chain mobility and decreased the glass transition temperature of the dLDPEs. Sethi *et al*. [31] said that a decrease in glass transition temperature might be due to a reduction in crystalliniy as well as a plasticization effect which enhances molecular motion in the amorphous phase. However, in their work they noticed an increase in glass transition temperature with increasing exposure of an LDPE-EVA blend to electron beam irradiation. They attributed this observation to a combined effect of increased crystallinity and crosslinking in the amorphous regions. The degradation in our case was obviously not accompanied by crosslinking, therefore the reduced glass transition.

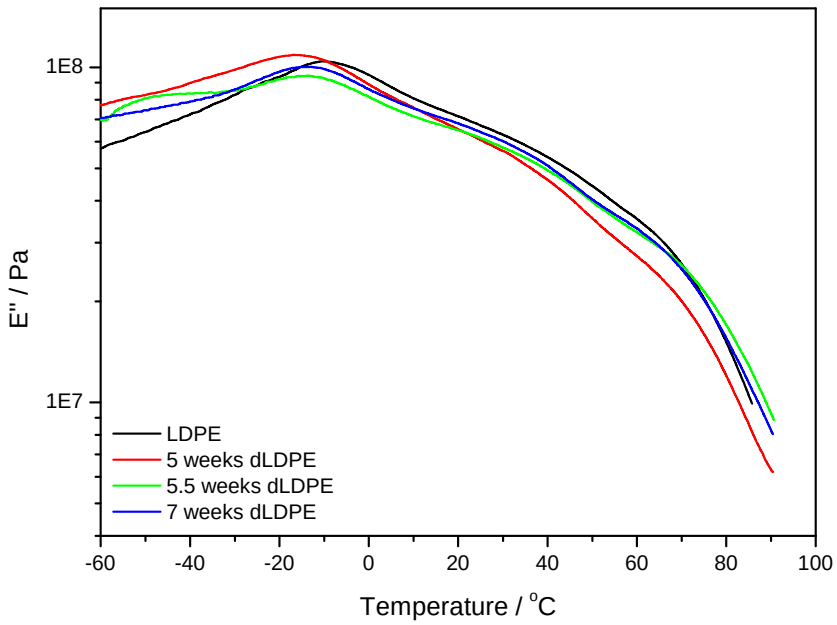

Figure 4.24 DMA loss modulus curves for LDPE and the different dLDPEs

Figure 4.25 shows that the temperature of the β-transition around -5 ºC decreased with increasing extent of degradation. This observation is the same as that for the loss modulus, and can be explained in the same way. The α-transition of the dLDPEs at about 75 °C shifted to higher temperatures compared to that of pure LDPE. This behaviour can be either as a result of the higher crystallinity of the dLDPEs observed in the DSC, or because of the presence of functional groups in the dLDPEs which resulted in stronger interactions between the polymer chains, giving rise to reduced mobility of the interlamellar amorphous parts of the polymer chains. Sethi *et al.* [31] noticed an increase in the α-transition temperature with increasing exposure of an LDPE-EVA blend to electron beam irradiation. They attributed this behaviour to some crosslinks that hindered chain mobility. Hristov *et al.* [32] stated that the higher α-transition temperature in PP-wood composites treated by MAPP compatibilizer indicated rigid immobilized chains in the crystalline phase, either as a result of the higher degree of composite crystallinity, or better interfacial adhesion.

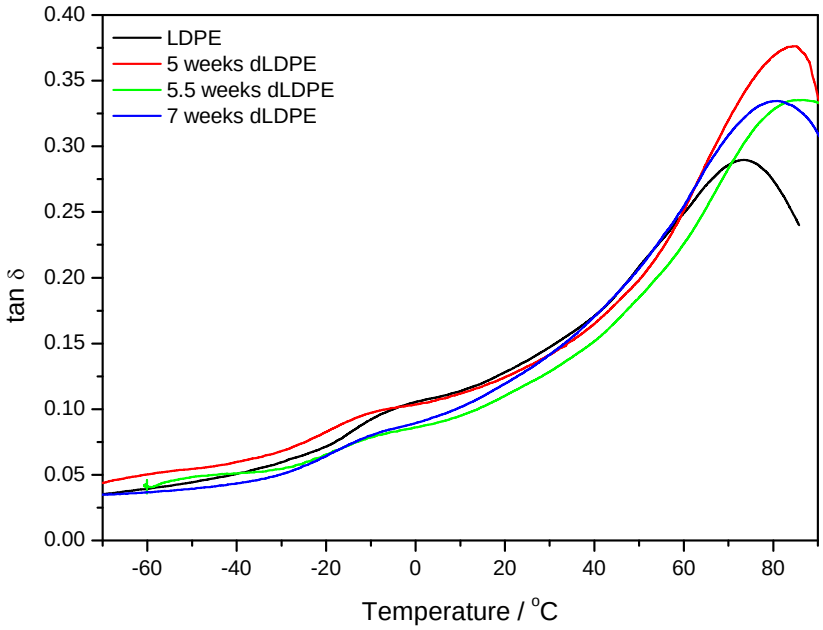

Figure 4.25 Damping factor curves for LDPE and the different dLDPEs

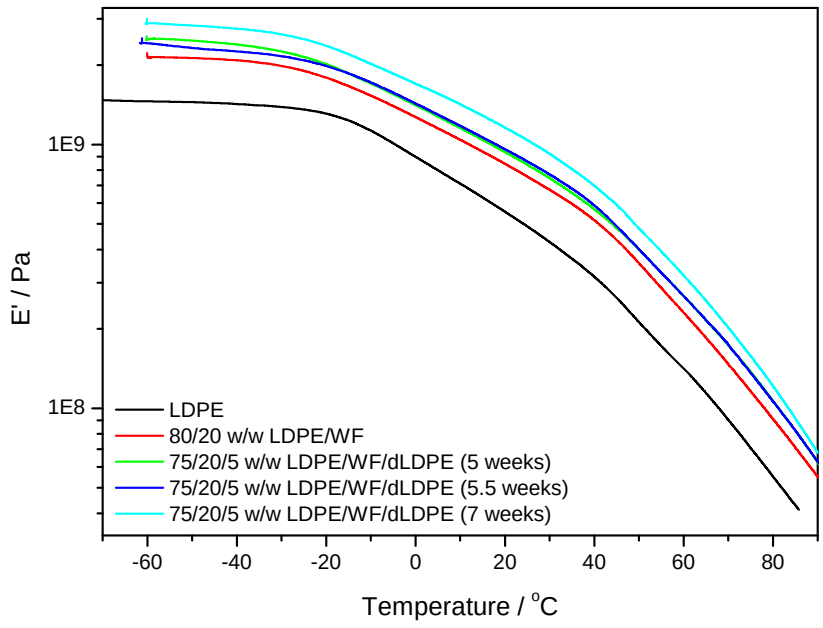

Figure 4.26 DMA storage modulus curves for LDPE and the different uncompatibilized and compatibilized composites

Figure 4.26 shows the storage modulus of LDPE, as well as the uncompatibilized and compatibilized composites, as function of temperature. These values observably increase with the addition of WF, and increase even further in the presence of dLDPE compatibilizer and with increasing dLDPE carbonyl index. As already mentioned earlier in this section, WF has a higher storage modulus than LDPE, and therefore an increase in storage modulus is expected for the LDPE/WF composites. The increased storage modulus for the dLDPE compatibilized composites is the result of the improved interfacial adhesion imparted by the dLDPEs.

Pedroso *et al.* [33] compared the viscoelastic behaviour of recycled and virgin LDPE where both were reinforced with corn starch. They noticed that the recycled LDPE composites had a higher storage modulus than the virgin LDPE composites, which was due to better interfacial adhesion between the recycled LDPE and the corn starch. Hong *et al*. [34], who investigated the influence of organofunctionalised silane on the dynamic mechanical properties and interfacial adhesion in jute-polypropylene composites, also noticed an improved storage modulus for the silane treated composites, and they also related it to the improved interfacial adhesion between the jute fibres and the polypropylene.

Figure 4.27 shows the loss modulus of LDPE, as well as the uncompatibilized and compatibilized composites. These results show the same trend as the storage modulus results, and can be explained in the same way. The presence of dLDPE improved the interaction between the fibres and the matrix, which is seen from the increasing loss modulus values. However, for the treated composites the glass transition peak around -9 ºC slightly shifted to lower temperatures. This may have been the result of the more mobile dLDPE chains at the polymer-WF interface which gave rise to a slightly higher observed chain mobility.

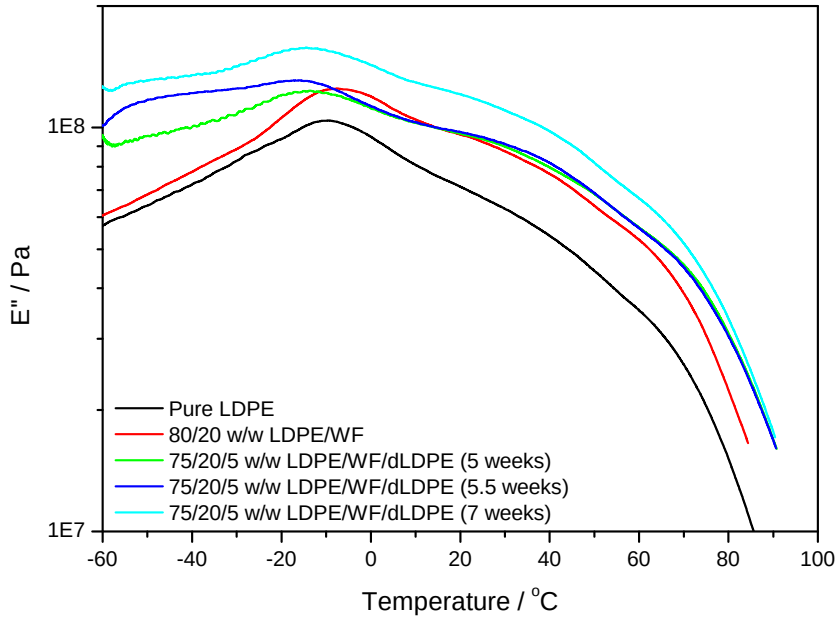

Figure 4.27 DMA loss modulus curves for LDPE and the different uncompatibilized and compatibilized composites

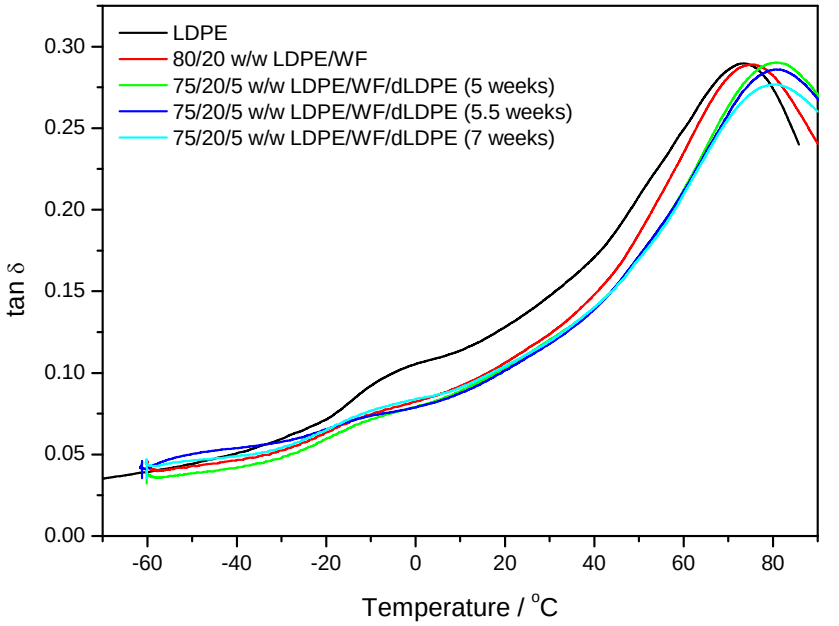

Figure 4.28 Damping factor curves for LDPE and the different uncompatibilized and compatibilized composites

Figure 4.28 shows the damping factor as function of temperature of LDPE, as well as the uncompatibilized and compatibilized composites. These values indicate molecular motions at a composite's interface. It is noticed that the presence of WF lowers the tan δ values in the rubbery region due to improved interfacial interaction imparted by compatibilizers resulting in a hindered chain mobility at the interface. Lai *et al.* [35] also noticed a decrease in tan δ after the addition of four different compatibilizers (LLDPE-g-MA, HDPE-g-MA, SEBS-g-MA and PP-g-MA) respectively in HDPE-wood composites. According to them the decrease in tan δ is expected, and is the result of a decreased number of mobile segments at the interface due to the improved interfacial adhesion.

The dLDPE compatibilizers had very little influence on the T_g values and on the tan δ values around the glass transition. On the other hand, the compatibilized composites show an α-transition at higher temperatures than LDPE and the uncompatibilized LDPE/WF composite. This is a consequence of the restricted molecular motion within the crystalline phase in the samples. It was noticed from the DSC results that the dLDPE compatibilized composites have higher crystallinities than LDPE and the uncompatibilized composite due to the nucleating effect of WF because of stronger interfacial interaction. This is in agreement with the work done by Hristov *et al.* [32], who noticed an increase in the α-transition temperature for polypropylene/wood composites prepared in the presence of maleic grafted polypropylene as compatibilizer and polybutadiene-styrene rubber as impact modifier. They associated this behaviour with the higher degree of crystallinity in these composites resulting in restricted chain mobility in the crystalline phase.

4.6.1 Tensile properties

The tensile properties of LDPE, the dLDPEs, and the compatibilized and uncompatibilized composites are summarized in Figures 4.29 to 4.37 and in Table 4.7. Young's modulus increases with decreasing molecular weight and increasing carbonyl index (Figures 4.29 and 4.30). This is probably a consequence of the increased crystallinity which is seen by the increasing melting enthalpies of the degraded LDPEs (Table 4.1). Krupa *et al.* [12] also noticed an increasing Young's modulus with increasing gamma irradiation of LLDPE. They associated this behaviour with increasing crystallinity, since the modulus of the crystalline phase is higher than that of the amorphous phase. Luyt *et al.* [36] observed a higher Young's modulus for LLDPE compared to LDPE, because LLDPE has a higher crystallinity than LDPE. In our case the higher crystallinity can be linked to the shorter polymer chains (lower

average molecular weight) and the stronger interaction between the functional groups on the chains (higher carbonyl index).

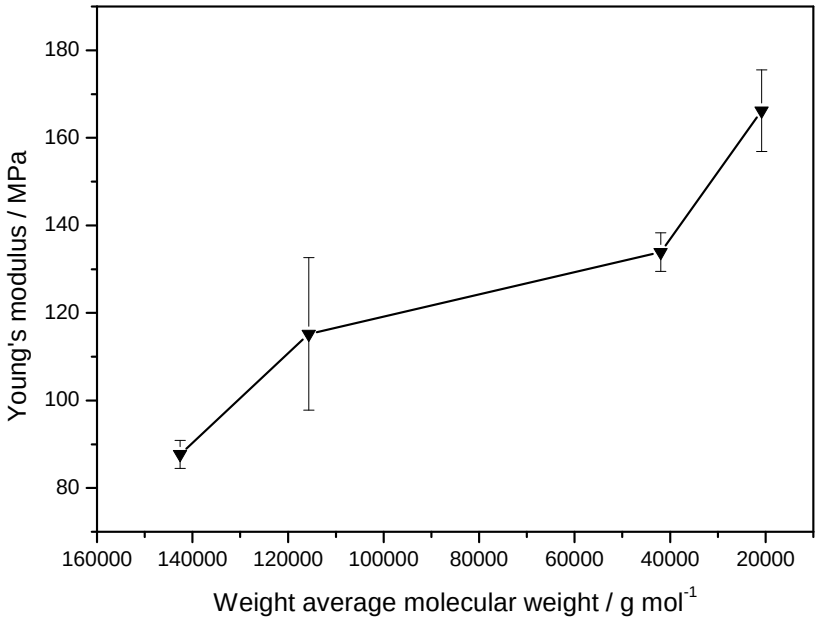

Figure 4.29 Young's modulus against weight average molecular weight of pure LDPE and of LDPE degraded for 5, 5.5 and for 7 weeks

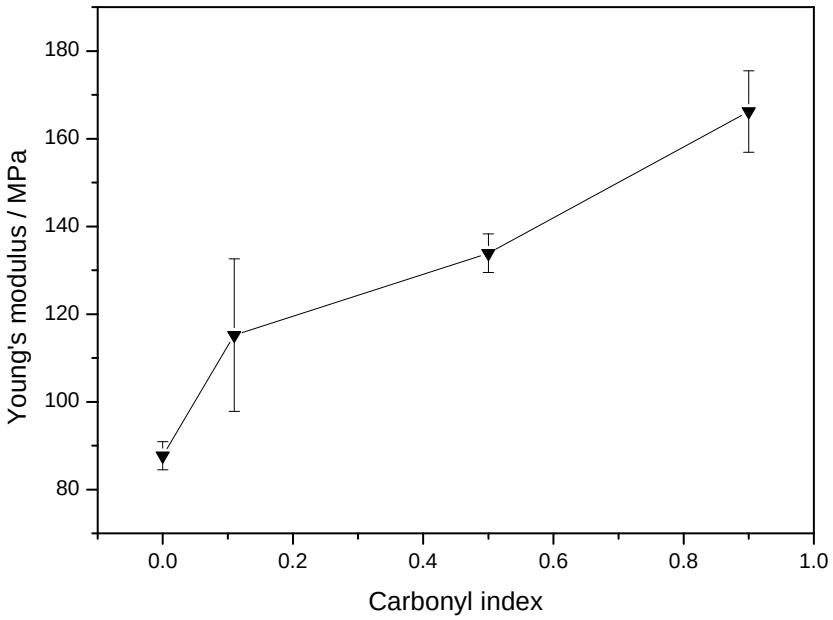

Figure 4.30 Young's modulus against carbonyl index of pure LDPE and of LDPE degraded for 5, 5.5 and for 7 weeks

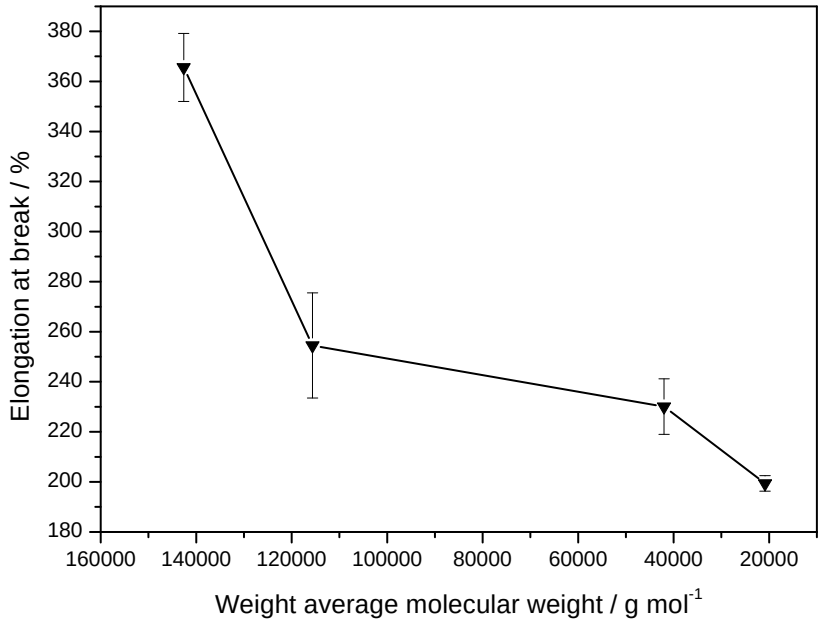

Figure 4.31 Elongation at break against weight average molecular weight of pure LDPE and of LDPE degraded for 5, 5.5 and for 7 weeks

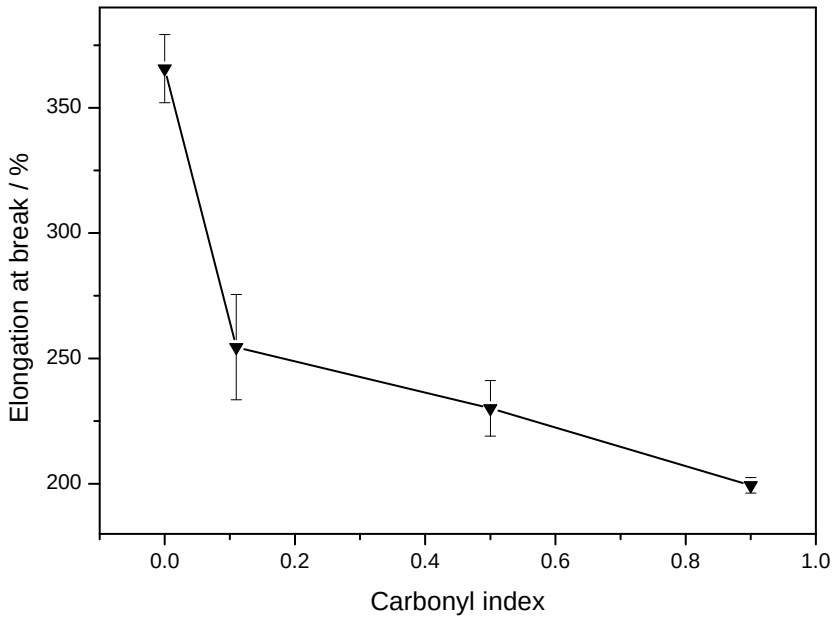

Figure 4.32 Elongation at break against carbonyl index of pure LDPE and of LDPE degraded for 5, 5.5 and for 7 weeks

Figures 4.31 and 4.32 show that as the molecular weight decreases and the carbonyl index increases due to thermooxidative degradation, the elongation at break decreases. Non-degraded LDPE has the largest elongation at break, because of its larger amorphous fractions and longer chains that enable chain flexibility so that the polymer chains can slip and tilt more easily to orientate in the direction of the applied stress. It can therefore be expected that the elongation at break will decrease with decreasing chain dimensions (decreasing average molecular weight). Weon *et al.* [37] also observed a reduction in elongation at break with increasing thermal degradation of LLDPE. They concluded that the behaviour is either because of a reduction in the dimensions of chain segments by molecular scission, or because of a reduction in the density of chain entanglements leading to deleterious effects in all the mechanical properties.

Figures 4.33 and 4.34 clearly show an increase in stress at break with decreasing average molecular weight and increasing carbonyl index. This is most probably due to strong interactions between the functional groups on the chains of the degraded LDPE, similar to the hydrogen bonding between polyamide chains which gives these polymers their exceptional strength.

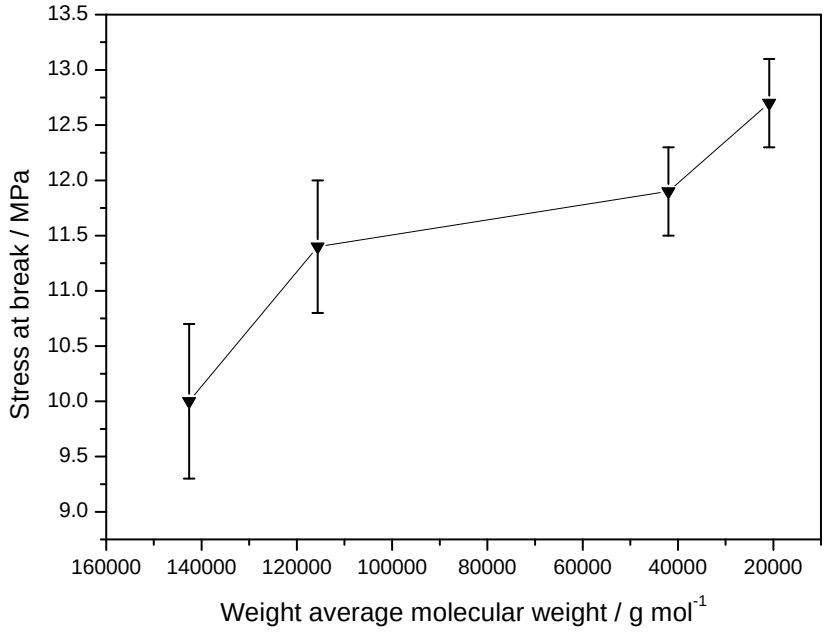

Figure 4.33 Stress at break against weight average molecular weight of pure LDPE and of LDPE degraded for 5, 5.5 and for 7 weeks

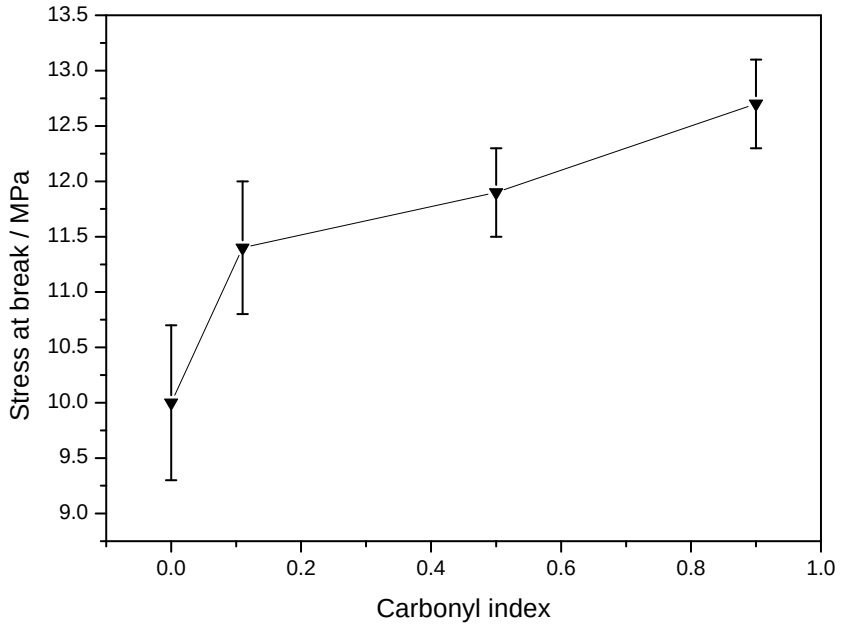

Figure 4.34 Stress at break against carbonyl index of pure LDPE and of LDPE degraded for 5, 5.5 and for 7 weeks

For the untreated composites, Young's modulus increases as fibre loading is increased (Figure 4.35) due to the stiffness imparted by the fibres. This behaviour is expected because fillers are normally stiffer than polymers. Dikobe *et al.* [38] also saw an increase in modulus for untreated EVA/WF composites. They explained it as a fibre reinforcing effect, even in untreated composites. Both the 5 and 5.5 weeks dLDPEs did not improve the Young's modulus as compared to the untreated composites, but the 7 weeks dLDPE compatibilized samples clearly show higher Young's modulus values than the uncompatibilized composites. From the GPC and FTIR results discussed earlier, it was seen that dLDPEs had carbonyl groups that might have interacted with the cellulose hydroxyl groups, improving the interfacial interaction between the matrix and WF. In the case of the 5 and 5.5 weeks dLDPEs this interaction does not seem to be effective enough to improve the modulus of the compatibilized composites above that of the uncompatibilized composites, but the very high carbonyl index of the 7 weeks dLDPE seems to have provided enough interaction for effective stress transfer between the matrix and the WF particles, leading to observably higher Young's modulus values.

Table 4.7 Tensile properties of pure LDPE, dLDPEs, as well as uncompatibilized and compatibilized LDPE/WF composites

Sample (w/w)	ε_b / %	σ_b / MPa	E / MPa
Pure LDPE	366 ± 14	10.0 ± 0.7	87.7 ± 3.2
dLDPE (5 weeks)	255 ± 21	11.4 ± 0.6	115 ± 17
dLDPE (5.5 weeks)	230 ± 11	11.9 ± 0.4	133 ± 4
dLDPE (7 weeks)	199 ± 3	12.7 ± 0.4	166 ± 9
LDPE/WF			
90/10	43.0 ± 3.8	9.6 ± 0.1	270 ± 20
80/20	15.9 ± 1.5	9.6 ± 0.5	379 ± 14
70/30	8.1 ± 0.6	8.5 ± 0.2	431 ± 9
LDPE/WF/dLDPE (5 weeks dLDPE)			
85/10/5	24.1 ± 4.1	10.2 ± 0.4	275 ± 5
75/20/5	10.0 ± 0.5	9.9 ± 0.6	334 ± 12
65/30/5	5.8 ± 0.5	9.7 ± 0.6	374 ± 30
LDPE/WF/dLDPE (5.5 weeks dLDPE)			
85/10/5	21.6 ± 9.0	9.0 ± 0.8	229 ± 15
75/20/5	10.3 ± 1.2	8.9 ± 0.1	350 ± 17
65/30/5	5.9 ± 1.1	7.6 ± 0.2	303 ± 15
LDPE/WF/dLDPE (7 weeks dLDPE)			
85/10/5	22.4 ± 6.1	10.3 ± 0.3	321 ± 6
75/20/5	8.9 ± 1.8	10.4 ± 0.3	426 ± 16
65/30/5	5.9 ± 1.1	11.5 ± 0.6	560 ± 28

ε_b is the elongation at break; σ_b is the stress at break and E is Young's modulus

The elongation at break significantly decreased, even with small amounts of WF and in the presence of compatibilizers (Figure 4.36). This is the result of WF particles acting as defect centres for crack formation and propagation, and the presence of compatibilizer does not seem to improve this behaviour. Figure 4.36 further shows lower elongation at break values for the composites treated with the different dLDPEs. This behaviour can either be associated with restricted amorphous fractions formed in the presence of the compatibilizers, or because of the strong reinforcement making the whole composite brittle, and hence reducing elongation.

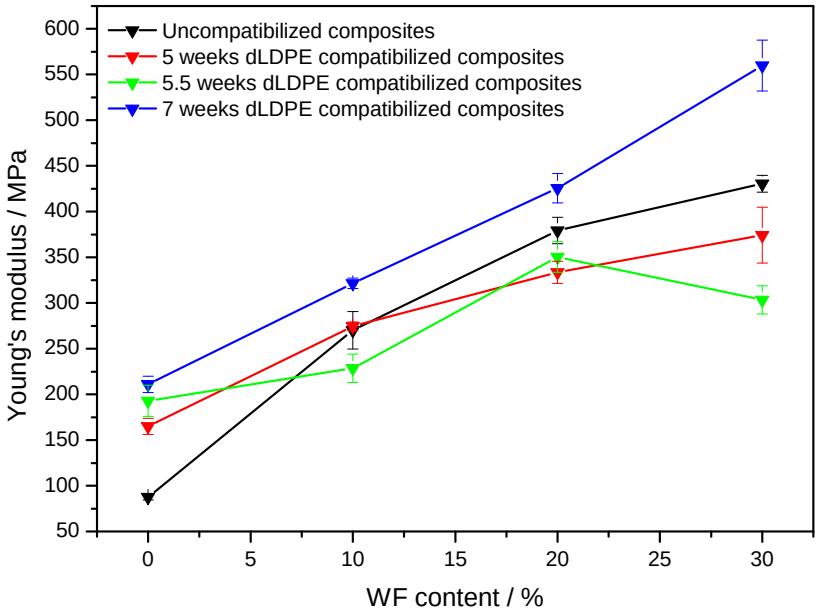

Figure 4.35 Young's modulus of treated and untreated LDPE/WF composites as function of WF content

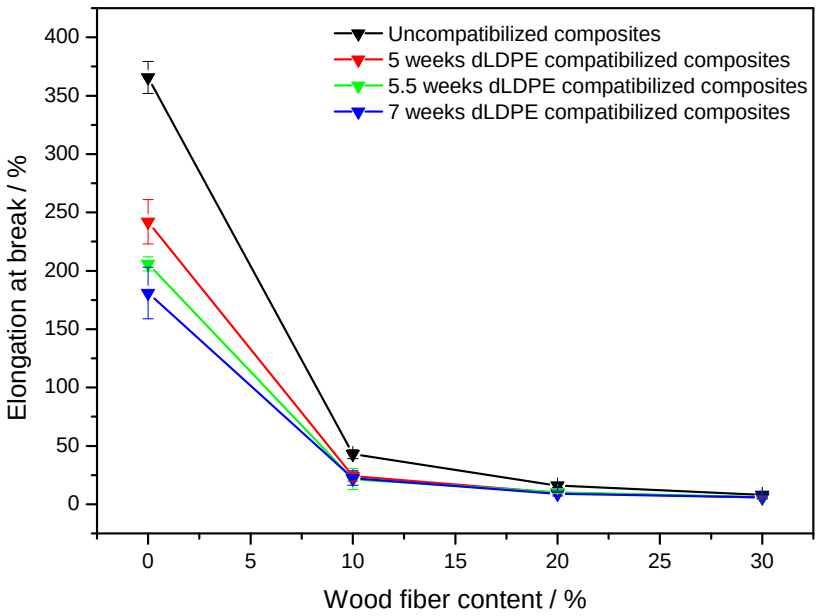

Figure 4.36 Elongation at break of treated and untreated LDPE/WF composites as function of WF content

The stress at break of the uncompatibilized composites slightly decreases with increasing WF content (Figure 4.37). This is due to the weak interaction between the hydrophilic fibres and the hydrophobic matrix, giving rise to weaker stress transfer and easier crack formation and propagation. As with the Young's modulus results, there are no clear trends with increasing extent of degradation of the dLDPEs, but the 7 weeks dLDPE compatibilized composites show obviously higher stress at break values than those of the uncompatibilized composites, and the stress at break continuously increases with increasing WF content. The reason for this is the strong interfacial adhesion between the LDPE matrix and WF induced by the high carbonyl index dLDPE. This gives rise to effective stress transfer between the matrix and the fibre, and a lower tendency for crack formation and propagation. Rahman *et al.* [28] also observed a decreasing tensile strength in both oxidized and raw jute fibres-PP composites up to 35% jute fibre content. However, when they post-treated the oxidized jute by urea, the tensile strength increased due to the interaction between the aldehyde groups of the oxidized jute fibres and the urea molecules at the interface.

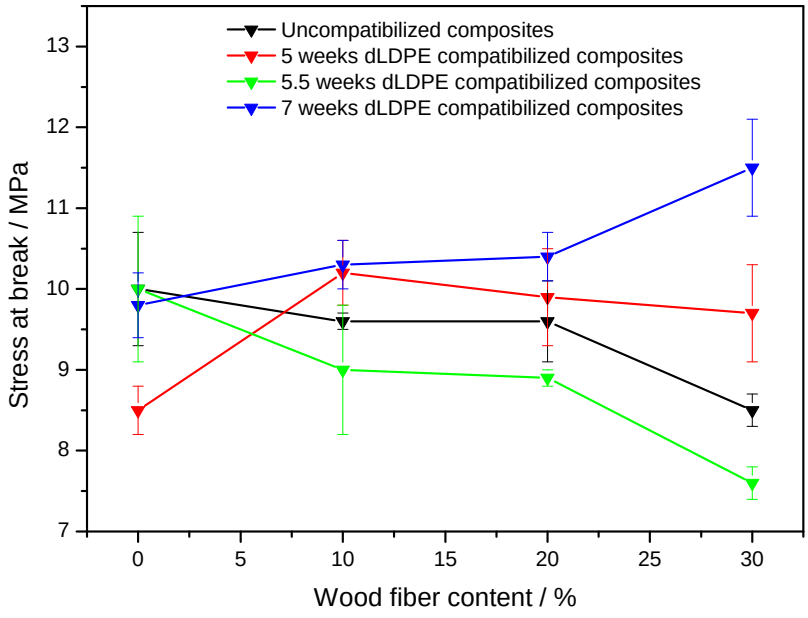

Figure 4.37 Stress at break of treated and untreated LDPE/WF composites as function of WF content

4.6.2 Impact strength

The impact strength of LDPE, as well as the uncompatibilized and compatibilized composites, is shown on Figure 4.38 and Table 4.8. Generally the impact strength refers to the ability of any material to absorb the applied impact energy and deform without any immediate fracturing. Flexible amorphous materials usually have higher impact resistance than crystalline brittle ones. In Figure 4.38 it is seen that pure LDPE is a tough plastic (an amorphous flexible polymer) having the highest impact strength of about 571.1 J m^{-1}. A substantial decrease in impact strength is seen with increasing fibre content due to the fibres acting as stress concentration points providing sites for crack initiation in the composites. The dLDPEs also have much lower impact strengths, probably because of their shorter chains and higher crystallinities.

Karmarkar *et al.* [39] noticed that the presence of wood fibres in PP provided stress concentrations, stiffened chain molecules not to deform easily, and acted as crack initiators when force was applied. According to them a slightly weaker adhesion is desirable for improvement of impact strength. Kuan *et al.* [40] also observed a decreasing impact strength in LLDPE-wood flour composites as more wood flour was added. They attributed this behaviour to the stiffness imparted by the wood flour. They further stated that crosslinking can also strengthen the interface between matrix and filler helping impact strength transfer across the interface, thus improving the impact strength. In our case the impact strengths of the 7 weeks dLDPE compatibilized composites are lower than that of the uncompatibilized composite, probably because of the much stronger interaction between the WF and the matrix. Although there may have been better stress transfer because of this interaction, there may also have been more inflexibility at the interface.

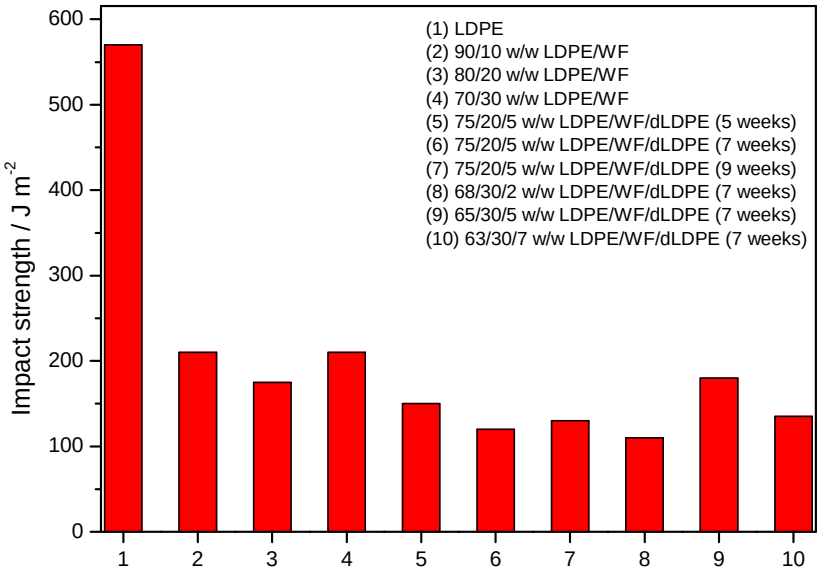

Figure 4.38 Impact strength of LDPE and its uncompatibilized and compatibilized composites

Table 4.8 Impact and hardness strengths of LDPE and its uncompatibilized and compatibilized composites

Sample (w/w)	Impact strength / J m^{-1}	Hardness / MPa
LDPE	571	1.9 ± 0.6
LDPE/WF/dLDPE		
90/10/0	210	1.9 ± 0.3
80/20/0	174	2.2 ± 0.4
70/30/0	209	3.2 ± 0.6
75/20/5 w/w LDPE/WF/dLDPE		
5 weeks dLDPE	150	1.5 ± 0.7
7 weeks dLDPE	120	1.6 ± 0.5
9 weeks dLDPE	130	2.0 ± 0.7
LDPE/WF/dLDPE		
68/30/2 dLDPE (7 weeks)	110	1.6 ± 0.7
65/30/5 dLDPE (7 weeks)	181	1.8 ± 0.4
63/30/7 dLDPE (7 weeks)	135	2.1 ± 0.3

4.6.3 Hardness

Figure 4.39 and Table 4.8 show the hardness of pure LDPE as well as the uncompatibilized and compatibilized LDPE/WF/dLDPE composites. It can be seen that pure LDPE is not hard but flexible due to its more amorphous character. Even when 10% wood fibres were added, there was no clear increase in the composite hardness. At higher fibre loadings, however, there is an obvious increase in hardness. This behaviour can be attributed to the reinforcing effect of the fibres in the matrix. Akinci *et al.* [41] noticed an increasing hardness as more basalt were added in basalt particles filled LDPE. They also attributed this behaviour as to the stiffness imparted by the fibres.

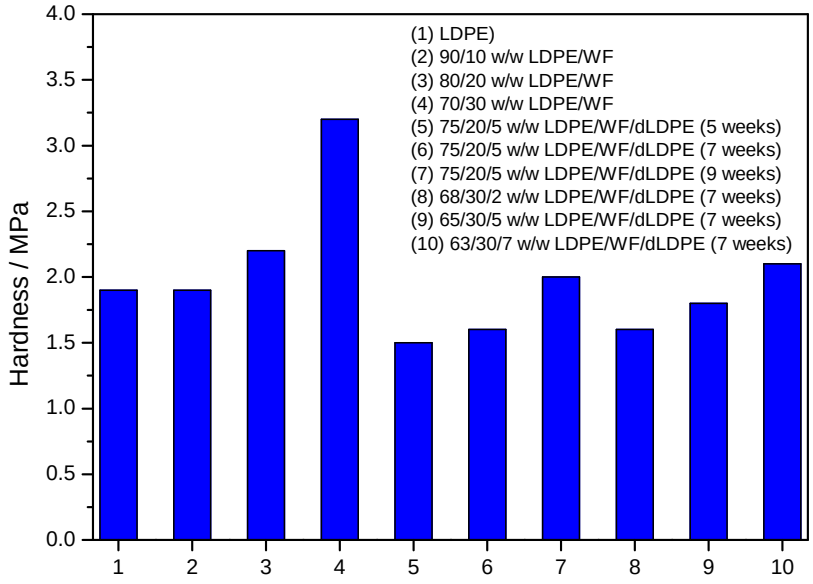

Figure 4.39 Hardness of LDPE and its uncompatibilized and compatibilized composites

Generally the hardness values of the dLDPE compatibilized composites were lower than the 70/30 w/w LDPE/WF composite. These values, however, increased with increasing extent of degradation of the LDPE, and with increasing amount of 7 weeks dLDPE in the composites. It seems as if there is a competition between increased interfacial interaction between the WF and the matrix, and increased flexibility in the interface because of the shorter dLDPE chains. Rahman *et al.* [28] observed an enhancement in hardness for both oxidized jute fibres and oxidized-urea treated jute fibres-PP composites. They ultimately associated this behaviour with the increased stiffness imparted by the fibres. They further noticed that oxidized and urea post treated fibres showed the largest hardness values.

4.7 References

1. L.C. Mendes, E.S. Rufino, F.O.C. de Paula, A.C. Torres Jr. Mechanical, thermal and microstructure evaluation of HDPE after weathering in Rio de Janeiro City. Polymer Degradation and Stability 2003; 79:371-383.
   DOI: 10.1016/S0141-3910(02)00337-3
2. H.J. Huang, Q.B. Wang, B.H. Xie, W. Yang, M.B. Yang. Thermal oxidation and structural changes of degraded polyethylene in an oxygen atmosphere. Journal of Macromolecular Science: Part B 2011; 50:1376-1387.
   DOI: 10.1080/00222348.2010.516687
3. O. Motta, A. Proto, F. De Carlo, F De Caro, E. Santoro, L. Brunetti, M. Capunzo. Utilization of chemically oxidized polystyrene as co-substrate by filamentous fungi. International Journal of Hygiene and Environmental Health 2009; 212:61-66.
   DOI: 10.1016/j.ijheh.2007.09.014
4. S.L. Favaro, T.A. Ganzerli, A.G.V. de Carvalho Neto, O.R.R.F. da Silva, E. Radovanovic. Chemical, morphological and mechanical analysis of sisal fibre-reinforced recycled high-density polyethylene composites. eXPRESS Polymer Letters 2010; 4:465-473.
   DOI: 10.3144/expresspolymerlett.2010.59
5. M. Liu, A.R. Horrocks, M.E. Hall. Correlation of physicochemical changes in UV-exposed low density polyethylene films containing various UV stabilizers. Polymer Degradation and Stability 1995; 49:151-161.
   DOI: 10.1016/0141-3910(95)00008-A
6. J.H. Khan, S.H. Hamid. Durability of HALS-stabilized polyethylene film in a greenhouse environment. Polymer Degradation and Stability 1995; 48:137-142.
   DOI: 10.1016/0141-3910(95)00015-E
7. K. Joseph, S. Thomas, C. Pavithran. Effect of chemical treatment on the tensile properties of short sisal fibre-reinforced polyethylene composites. Polymer 1996; 37:5139-5149.
   DOI: 10.1016/0032-3861(96)00144-9
8. F. Mengeloglu, A. Kabakci. Determination of thermal properties and morphology of eucalyptus wood residue filled high density polyethylene composites. International Journal of Molecular Sciences 2008; 9:107-119.
   DOI: 10.3390/ijms9020107

9. Paul, J. Kuruvilla, S. Thomas. Effect of surface treatments on the electrical properties of low-density polyethylene composites reinforced with short sisal fibers. Composites Science and Technology 1997; 57:67-79.
DOI: 10.1016/S0266-3538(96)00109-1
10. I.M. Thakore, S. Desai, B.D. Sarawade, S. Devi. Studies on biodegradability, morphology and thermo-mechanical properties of LDPE/modified starch blends. European Polymer Journal 2007; 37:151-160.
DOI: 10.1016/S0014-3057(00)00086-0
11. S. Mohanty, S.K. Verma, S.K. Nayak. Dynamic mechanical and thermal properties of MAPE treated jute/HDPE composites. Composites Science and Technology 2006; 66:538-547.
DOI: 10.1016/j.compscitech.2005.06.014
12. I. Krupa, A.S. Luyt. Thermal and mechanical properties of LLDPE cross-linked with gamma radiation. Polymer Degradation and Stability 2001; 71:361-366.
DOI: 10.1016/S0141-3910(00)00186-5
13. M. Liu, A.R. Horrocks. Effect of carbon black on UV stability of LLDPE films under artificial weathering conditions. Polymer Degradation and Stability 2002; 75:485-499.
DOI: 10.1016/S0141-3910(01)00252-X
14. H.I. Craig, J.R. White. Crystallization and chemi-crystallization of recycled photodegraded polyethylenes. Polymer Engineering and Science 2005; 45:588-595.
DOI: 10.1002/pen.20314
15. H.I. Craig, J.R. White. Mechanical properties of photo-degraded recycled photo-degraded polyolefins. Journal of Materials Science 2006; 41:993-1006.
DOI: 10.1007/s10853-006-6596-6
16. A.K. Mishra, A.S. Luyt. Effect of sol-gel derived nano-silica and organic peroxide on the thermal and mechanical properties of low density polyethylene/wood flour composites. Polymer Degradation and Stability 2008; 93:1-8.
DOI: 10.1016/j.polymdegradstab.2007.11.006
17. A.S. Luyt, M.E. Malunka. Composites of low density polyethylene and short sisal fibres: the effect of wax addition and peroxide treatment on the thermal properties. Thermochimica Acta 2005; 426:101-107.
DOI: 10.1016/j.tca.2004.07.101

18. H. Bouafif, A. Koubaa, P. Perre, A. Cloutier, B. Riedl. Wood particle/high-density polyethylene composites: Thermal sensitivity and nucleating ability of wood particles. Journal of Applied Polymer Science 2009; 113:593-600.
DOI: 10.1002/app.30129
19. S.H. Lee, S. Wang. Biodegradable polymers/bamboo fiber biocomposite with bio-based coupling agent. Composites: Part A 2006; 37:80-91.
DOI: 10.1016/j.compositesa.2005.04.015
20. N.E. Marcovich, M.A. Villar. Thermal and mechanical characterization of linear low density polyethylene/wood flour composites. Journal of Applied Polymer Science, 2003; 90:2775-2784.
DOI: 10.1002/app.12934
21. B. Saha, A.K. Ghashal. Model-free kinetics analysis of ZSM-5 catalyzed pyrolysis of waste LDPE. Thermochimica Acta 2007; 453:120-127.
DOI: 10.1016/j.tca.2006.11.012
22. J.D. Peterson, S. Vyazovkin, C.A. Wight. Kinetics of the thermal and thermo-oxidative degradation of polystyrene, polyethylene and poly(propylene). Macromolecular Chemistry and Physics 2001; 202:775-784.
DOI: 10.1002/1521-3935(20010301) 202:6<775::AID-MACP775>3.0.CO;2-G
23. P.K. Roy, P. Surekha, C. Rajagopal, S.N. Chatterjee, V. Choudhary. Studies on the photo-oxidative degradation of LDPE films in the presence of oxidised polyethylene. Polymer Degradation and Stability 2007; 92:1151-1160.
DOI: 10.1016/j.polymdegradstab.2007.01.010
24. P.K. Roy, P. Surekha, C. Rajagopal, S.N. Chatterjee, V. Choudhary. Thermal degradation studies of LDPE containing cobalt stearate as pro-oxidant. eXPRESS Polymer Letters 2007;1:208-216.
DOI: 10.3144/expresspolymlett.2007.32
25. A.N. Shebani, A.J. van Reenen, M. Meincken. The effect of wood extractives on the thermal stability of different wood-LLDPE composites. Thermochimica Acta 2009; 48:52-56.
DOI: 10.1016/j.tca.2008.10.008
26. H.S. Kim, S. Kim, H.J. Kim, H.S. Yang. Thermal properties of bio-flour-filled polyolefin composites with different compatibilizing agent type and content. Thermochimica Acta 2006; 451:181-188.
DOI: 10.1016/j.tca.2006.09.013

27. J. George, S.S. Bhagawan, S. Thomas. Thermogravimetric and dynamic mechanical thermal analysis of pineapple fibre reinforced polyethylene composites. Journal of Thermal Analysis 1996; 47:1121-1140.
28. M.R. Rahman, M. Hasan. Physico-mechanical properties of jute fibre reinforced composites. Journal of Reinforced Plastics and Composites 2010; 29:445-455. DOI: 10.1177/0731684408098008
29. M. Bengtsson, P. Gatenholm, K. Oksman. The effect of crosslinking on the properties of polyethylene/wood flour composites. Composites Science and Technology 2005;65:1468-1479. DOI: 10.1016/j.compscitech.2004.12.050
30. R. Bouza, A. Lasagabaster, M.J. Abad, L. Barral. Effects of vinyltrimethoxy silane on thermal properties and dynamic mechanical properties of polypropylene-wood flour composites. Journal of Applied Polymer Science 2008; 109:1197-1204. DOI: 10.1002/app.28159
31. M. Sethi, N.K. Gupta, A.K. Srivastava. Dynamic mechanical analysis of polyethylene and ethylene vinylacetate copolymer blends irradiated by electron beam. Journal of Applied Polymer Science 2002; 86:2429-2434. DOI: 10.1002/app.10940
32. A.G. Pedroso, D.S. Rosa. Mechanical, thermal and morphological characterization of recycled LDPE/corn starch blends. Carbohydrate Polymers 2005; 59:1-9. DOI: 10.1016/j.carbpol.2004.08.018
33. C.K. Hong, I. Hwang, N. Kim, D.H. Park, B.S. Hwang, C. Nah. Mechanical properties of silanized jute-polypropylene composites. Journal of Industrial and Engineering Chemistry 2008; 14:71-76. DOI: 10.1016/j.jiec.2007.07.002
34. S.M. Lai, F.C. Yeh, Y. Wang, H.C. Chan, H.F. Shen. Comparative study of maleated polyolefins as compatibilizers for polyethylene/wood flour composites. Journal of Applied Polymer Science 2003; 87:487-496. DOI: 10.1002/app.11419
35. V. Hristov, S. Vasileva. Dynamic mechanical and thermal properties of modified polypropylene wood fibre composites. Macromolecular Material and Engineering 2003; 288:798-806. DOI:10.1002/mame.200300110

36. A.S. Luyt, J.A. Molefi, H. Krump. Thermal, mechanical and electrical properties of copper powder filled low-density and linear low density polyethylene composites. Polymer Degradation and Stability 2006; 91:1629-1636.
DOI: 10.1016/j.polymdegradstab.2005.09.014

37. J.I. Weon. Effect of thermal ageing on mechanical and thermal behaviours of linear low density polyethylene pipe. Polymer Degradation and Stability 2010; 95:14-20.
DOI: 10.1016/j.polymdegradstab.2009.10.016

38. D.G. Dikobe, A.S. Luyt. Morphology and properties of polypropylene/ethylene vinyl acetate copolymer/wood powder blend composite. eXPRESS Polymer Letters 2009; 3:190-199.
DOI: 10.3144/expresspolymerlett.2009.24

39. A Karmarkar, S.S. Chauhan, J.M. Modak, M. Chanda. Mechanical properties of wood–fiber reinforced polypropylene composites: Effect of a novel compatibilizer with isocyanate functional group. Composites: Part A 2007; 38:227-233.
DOI:10.1016/j.compositesa.2006.05.005

40. C.F. Kuan**,** H.C. Kuan**,** C.C.M. M**a,** C.M. Huang**.** Mechanical, thermal and morphological properties of water-crosslinked wood flour reinforced linear low-density polyethylene composites. Composites Part A 2006; 37:1696-1707.
DOI: 10.1016/j.compositesa.2005.09.020

41. A. Akinci, E. Ercenk, S. Yilmaz, U. Sen. Slurry erosion behaviors of basalt filled low density polyethylene composites. Materials and Design 2011; 32:3106–3111.
DOI: 10.1016/j.matdes.2010.12.029

CHAPTER 5

Conclusions

The objective of this study was to investigate the effect of degraded LDPEs (dLDPEs) in LDPE/WF composites. The LDPE was degraded at 80 ºC for different periods of time from 5 to 9 weeks and used as compatibilizers in LDPE/WF composites. Part of the investigation was to see which degradation period gave the best balance between functionalization of the polymer and reduced molecular weight. The composites (with and without dLDPE as compatibilizer) were characterized using FTIR spectroscopy, GPC, SEM, DSC, TGA, and DMA, as well as tensile, impact and hardness testing.

FTIR spectroscopy showed that thermal degradation of LDPE resulted in the formation of several functional groups including hydroxyls and carbonyls, on the LDPE chains, with the carbonyl index increasing to 0.90 for the 7 weeks dLDPE. Strong interaction was expected to occur between these groups and the cellulose hydroxyl groups, influencing the composites properties. GPC analysis showed a decreasing molecular weight with increasing degradation time.

For the uncompatibilized composites, there was no improvement in composite properties due to poor interfacial adhesion between hydrophilic fibres and hydrophobic LDPE polymer. Loose structure with lot of voids and holes as a result of poor adhesion between hydrophilic fibres and hydrophobic LDPE matrix were noticed. However, extent of interfacial adhesion of dLDPE compatibilized composites can be seen by less voids and finer morphology with fibres embedded in matrix. On the otherhand, combined influence of WF addition and dLDPEs treatment resulted in both higher melting and crystallization enthalpies, while for untreated composites enthalpies were not influenced but were just in experimental error. Although the increased melting and crystallization enthalpies of the dLDPE compatibilized composites was noticed, thermal stability did not increase which might either be due to low short molecular weight which require less energy to degrade or products such as hydroperoxides further prolonged degradation process. Viscoelastic and mechanical properties respectively showed observably increase in the presence of dLDPE compatibilizers and with increasing dLDPE carbonyl index as a result of the improved interfacial adhesion

imparted by the dLDPEs between fibres and matrix. The effect of higher carbonyl index of 7 weeks observably increased most properties as compare to other two dLDPE compatibilizers (5 and 5.5 weeks dLDPEs). Addition of the dLDPEs (5, 5.5 and 7 weeks degraded) improved most of the composites' properties due to the strong hydrogen bonding assumed to occur between the cellulose hydroxyl groups and the functional groups on the dLDPE. The 7 weeks dLDPE had the most significant influence despite its significantly lower molecular weight. This indicates that the effectiveness of dLDPE depends more on the carbonyl index than the molecular weight.

ACKNOWLEDGEMENTS

- My deepest gratitudes goes to **Almighty God** for His strength, courage and the wisdom He gave to me to be brave enough for this research study. This is all possible because of His grace and mercy which is upon me throughout the days of my life.

- My most sincere gratitudes also goes to my supervisor **Prof. Adriaan Stephanus Luyt**, not only for his guidance and support but also for his consistent supervision, encouragement and patience during all stages of this project. I thank him for the chance he gave it to me for this study. I am also grateful to my co-supervisor **Prof. Albert van Reenen**, for following the progress and providing technical guidance and valuable contributions throughout the whole research program. I acknowledge the financial support from NRF and the University of the Free State. All the partners in the project are thanked for sharing their expertise with me in the project meetings as well as for their enthusiasm, willingness, kindness and good mood every time. I am grateful to the faculty, staff and colleagues in the Department of Natural and Agricultural Sciences for their assistance in every aspect of my project. I am grateful also to the entire polymer research team PhDs, MScs and Honours students, including the staff and colleagues of polyolefins group under the supervision of **Prof. Albert van Reenen** from Stellenbosch University for their warm welcoming hearts.

- **To my entire Family**: Siphiwe Samson Ndlovu (Father), Zodwa Samaria Ndlovu (Mother), Thandeka Nomusa Lebohang Ndlovu (Daughter), Palisa Mofokeng, Mphikeleli Jabulani Ndlovu (Brother), Lindiwe Doris Ndlovu (Sister), Thulani Ernest Ndlovu (Brother), Sipho Ndlovu (Brother), Sizakele Elizabeth Ndlovu (Sister), Sibongiseni Amos Ndlovu, Lucky Samuel Ndlovu, Sifiso, Khanyisile, Simangaliso, Thembelihle, Nosihle, Wandile, Nothile, Thalente, Thandokuhle, Khethiwe, Nhlakanipho, Njabulo.

- Lastly, my gratitude goes to my wife Nokuphiwa Ashley Mofokeng-Ndlovu for the patience and support she gave me while busy studying towards my MSc degree.

-

"DUE TO THE FACT THAT WE ARE THE IMAGES OF GOD"

"TO GOD BE THE GLORY"

APPENDIX A

SEM analysis

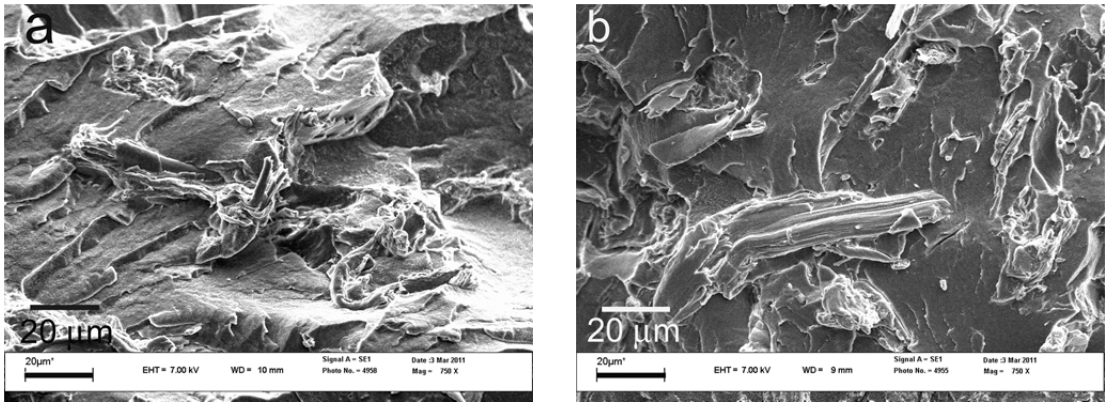

Figure A.1 SEM images of LDPE/WF at 750x magnifications (a) 90/10 w/w and (b) 80/20 w/w

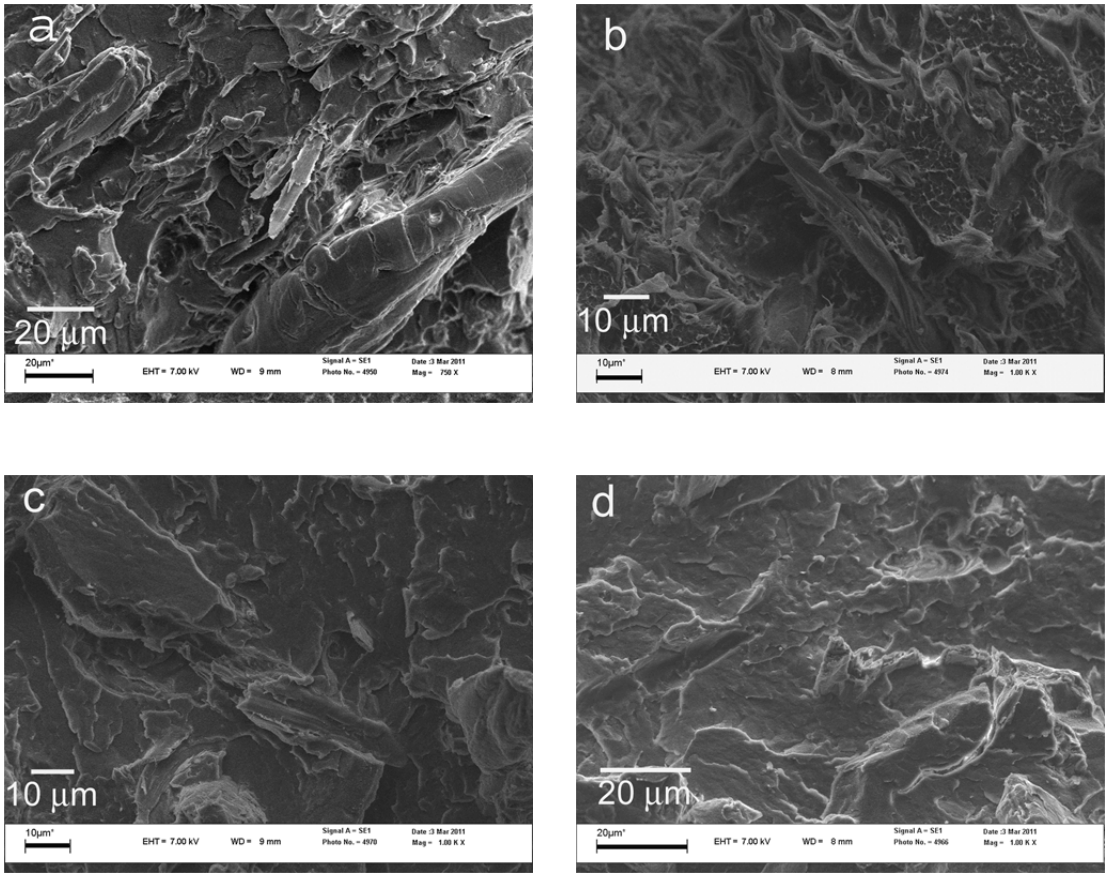

Figure A.2 SEM images showing the influence of increasing 7 weeks dLDPE compatibilizer in LDPE/WF/dLDPE (a) 70/30/0 w/w at 750x magnification, (b) 68/30/2 w/w at 1000x magnification, (c) 65/30/5 w/w at 1000x magnification and (d) 63/30/7 w/w at 1000x magnification

APPENDIX B

DSC analysis

Table B.1 DSC summary table of the effect of different types of degraded LDPE on LDPE pine wood fibre composites

Sample	HEATING			COOLING	
LDPE/WF/dLDPE (w/w)	**$T_{p,m}$ / °C**	**ΔH_m^{obs} / J g^{-1}**	**ΔH_m^{calc} / J g^{-1}**	**$T_{p,c}$ / °C**	**ΔH_c^{obs} / J g^{-1}**
100/0/0	108.0 ± 4.2	54.1 ± 1.8	-	91.6 ± 0.3	-58.3 ± 1.8
90/10/0	108.0 ±0.6	45.4 ± 2.0	48.7	91.0 ± 0.3	-52.9 ± 2.9
80/20/0	107.3 ± 4.2	43.9 ± 1.8	43.3	91.6 ± 1.3	-46.5 ± 2.4
70/30/0	108.4 ±0.4	36.1 ± 2.9	37.9	91.4 ± 0.1	-38.8 ± 3.1
LDPE/WF/dLDPE					
75/20/5 (5 weeks)	107.6 ± 4.1	49.3 ± 2.1	43.9	91.6 ± 0.3	-50.3 ± 0.8
75/20/5 (5.5 weeks)	109.7 ± 3.6	48.7 ± 2.3	44.6	91.2 ± 1.5	-47.0 ± 3.9
75/20/5 (6 weeks)	108.4 ± 0.4	35.9 ± 6.5	-	91.7 ± 0.1	-36.8 ± 0.3
75/20/5 (6.5 weeks)	107.6 ± 0.3	45.9 ± 2.1	-	91.6 ± 0.3	-47.6 ± 1.4
75/20/5 (7 weeks)	107.4 ± 4.5	47.5 ± 2.5	43.7	91.8 ± 1.3	-46.3 ± 1.1
75/20/5 (9 weeks)	106.6 ± 0.1	52.8 ± 3.9	-	91.5 ± 0.2	-48.5 ± 2.1

$T_{p,m}$ and $T_{p,c}$ are the melting and crystallization peak temperatures; ΔH_m^{obs} and ΔH_c^{obs} are the observed melting and crystallization enthalpies; ΔH_m^{calc} is the theoretically calculated melting enthalpy

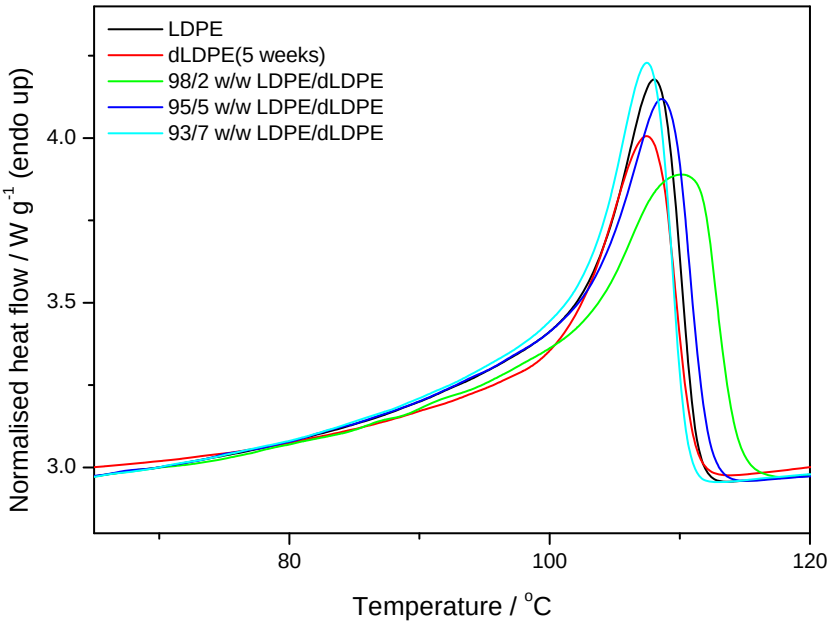

Figure B.1 DSC heating curves of LDPE and 5 weeks dLDPE and blends

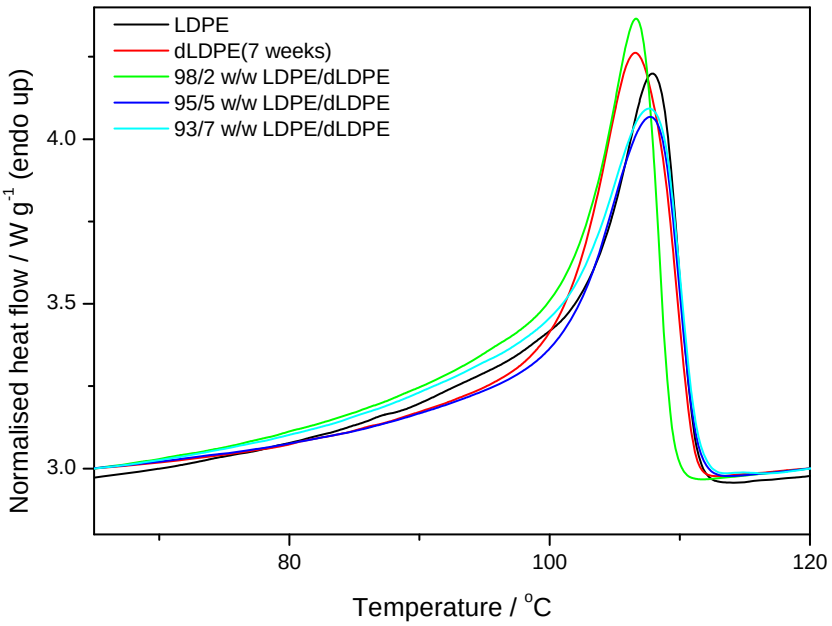

Figure B.2 DSC heating curves of LDPE and 7 weeks dLDPE and blends

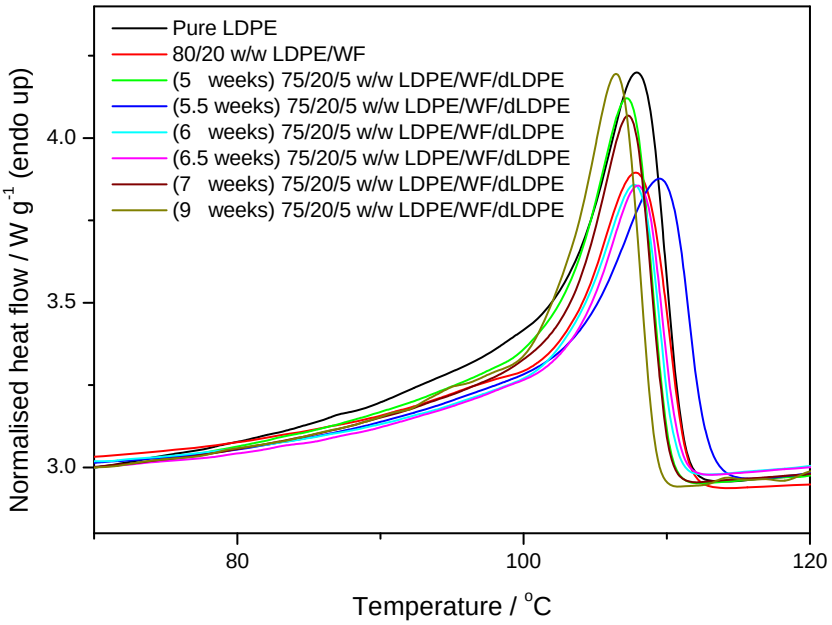

Figure B.3 DSC heating curves showing the effect of different dLDPEs compatibilizers in 20% WF containing composites

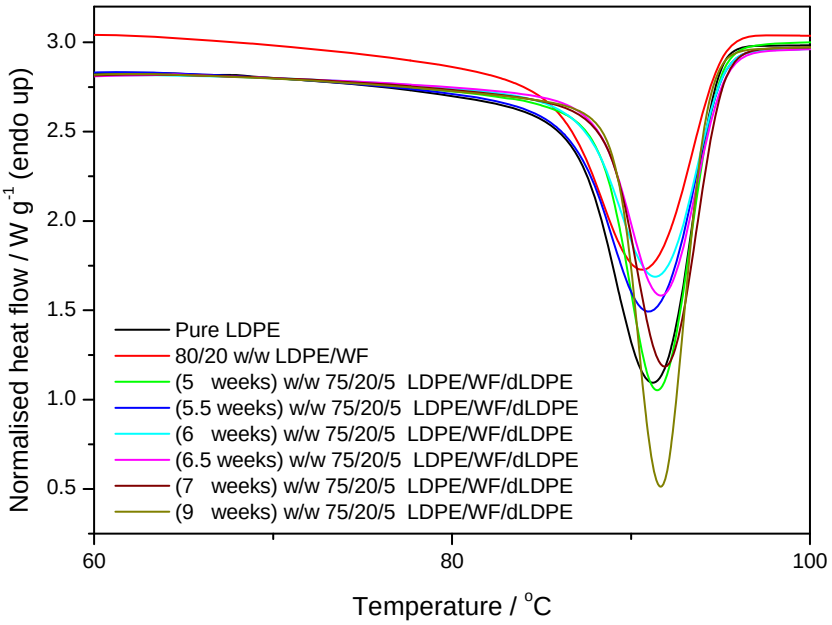

Figure B.4 DSC cooling curves showing the effect of different dLDPEs compatibilizers in 20% WF containing composites

APPENDIX C

TGA analysis

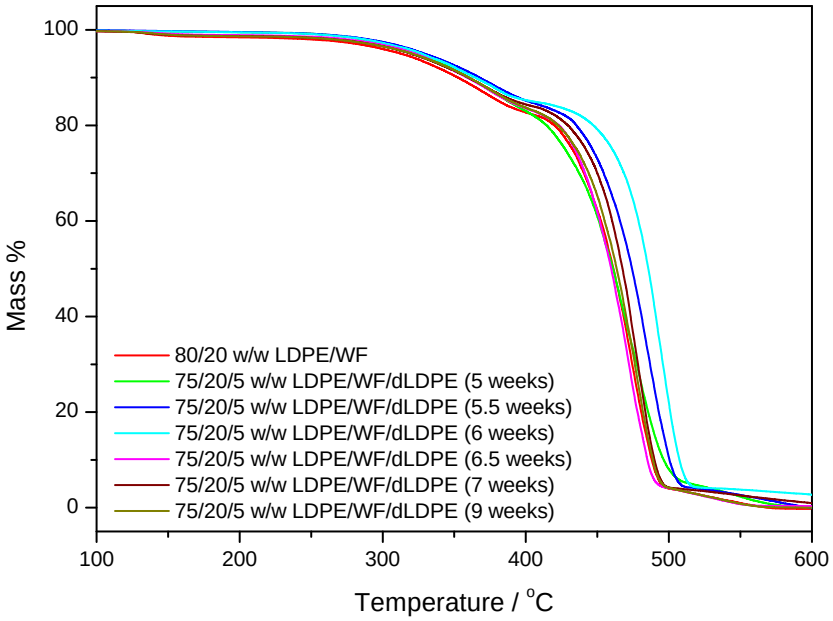

Figure C.1 TGA curves of uncompatibilized as well as compatibilized polymer wood fibre composites

APPENDIX D

Tensile testing analysis

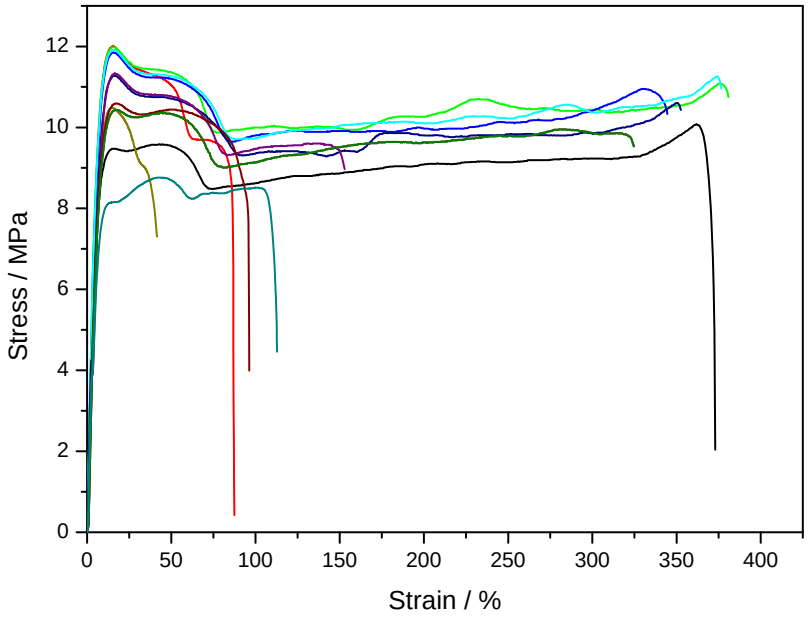

Figure D.1 Stress strain curves of LDPE

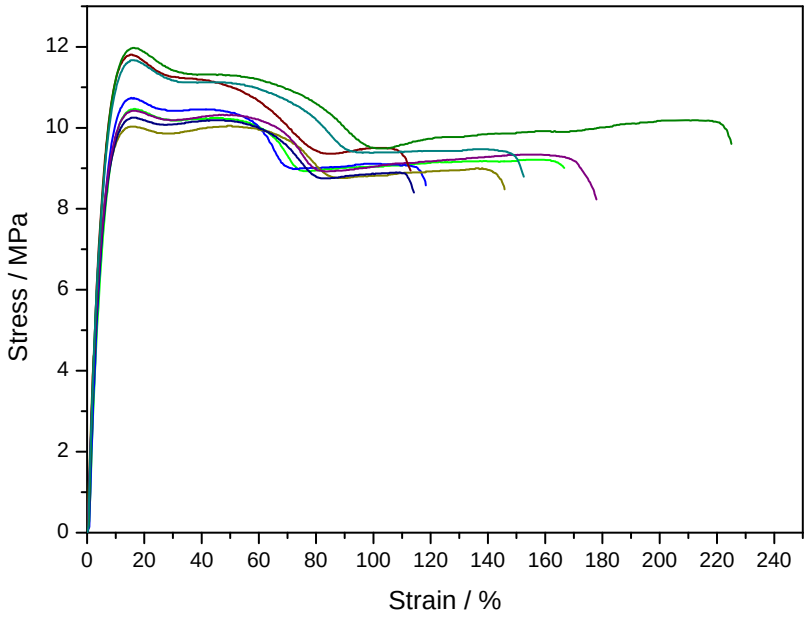

Figure D.2 Stress strain curves of 98/2 w/w LDPE/dLDPE

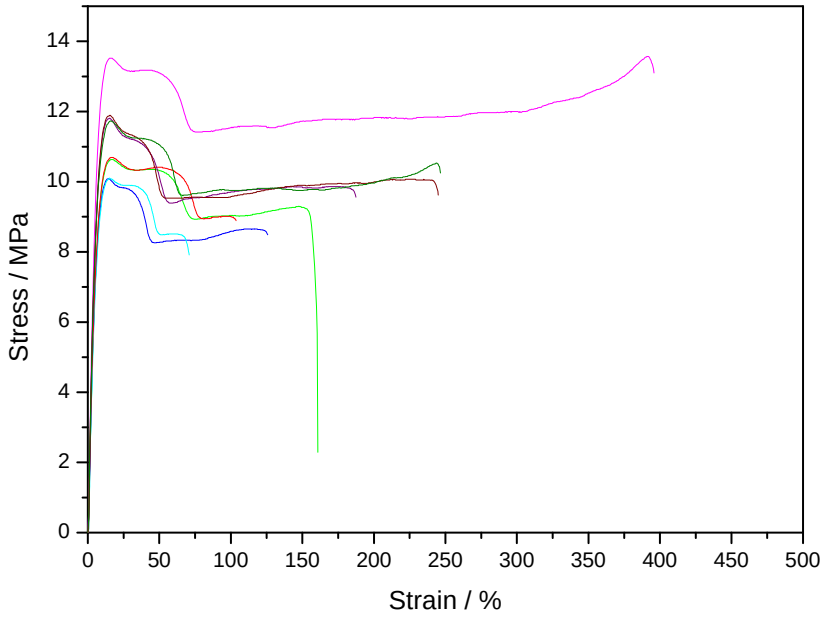

Figure D.3 Stress-strain curves of 95/5 w/w LDPE/dLDPE

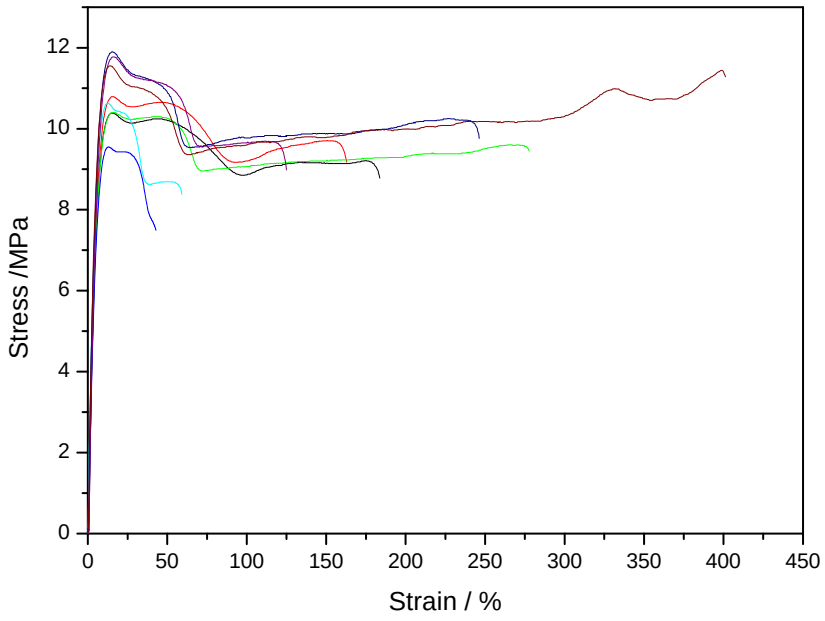

Figure D.4 Stress-strain curves of 93/7 w/w LDPE/dLDPE

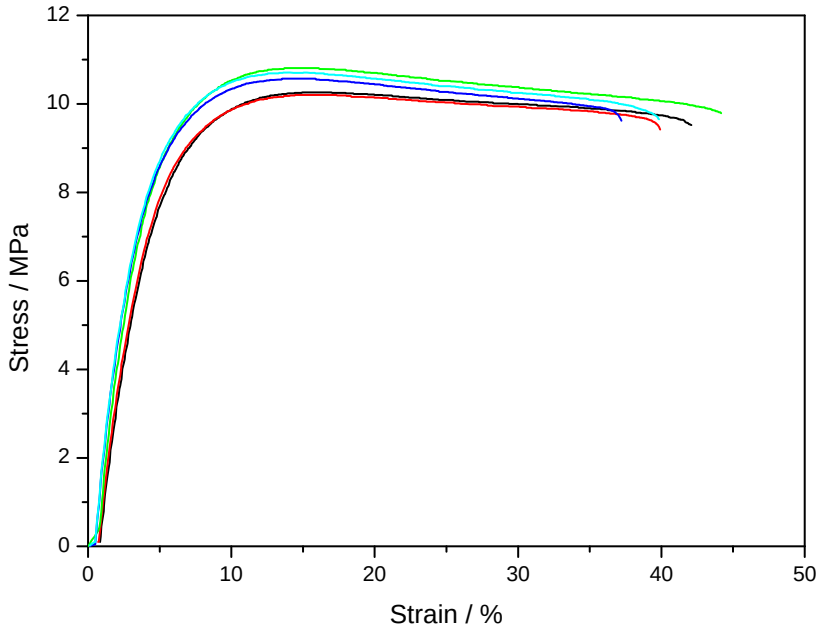

Figure D.5 Stress-strain curves of 90/10 w/w LDPE/WF

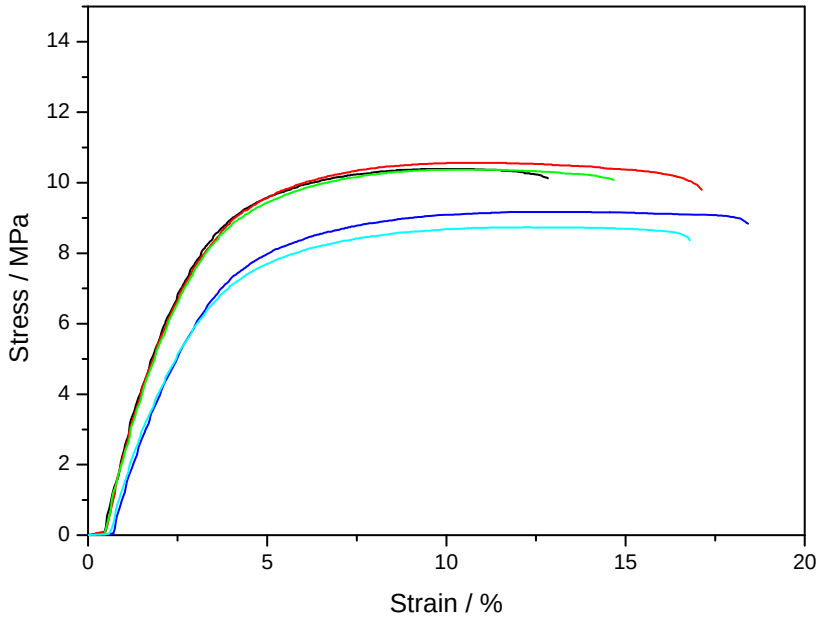

Figure D.6 Stress-strain curves of 80/20 w/w LDPE/WF

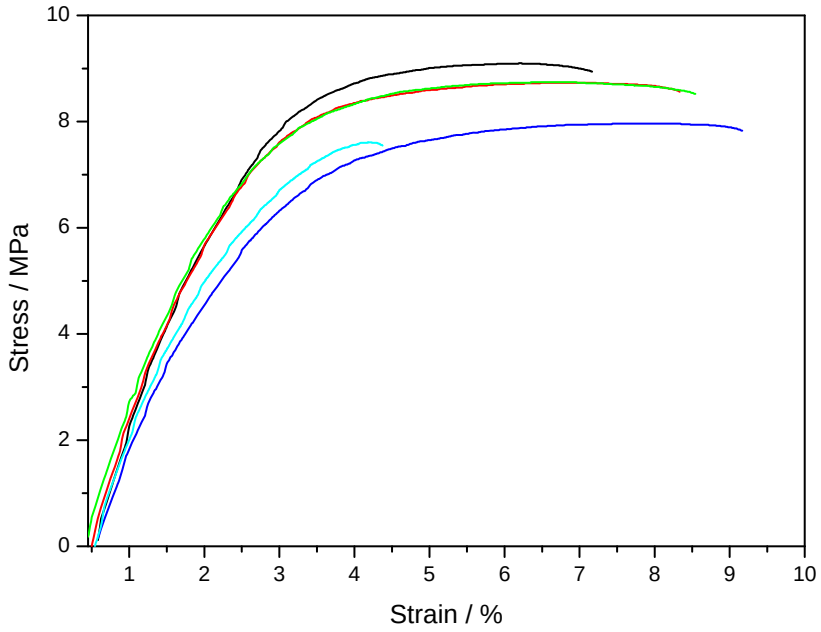

Figure D.7 Stress-strain curves of 70/30 w/w LDPE/WF

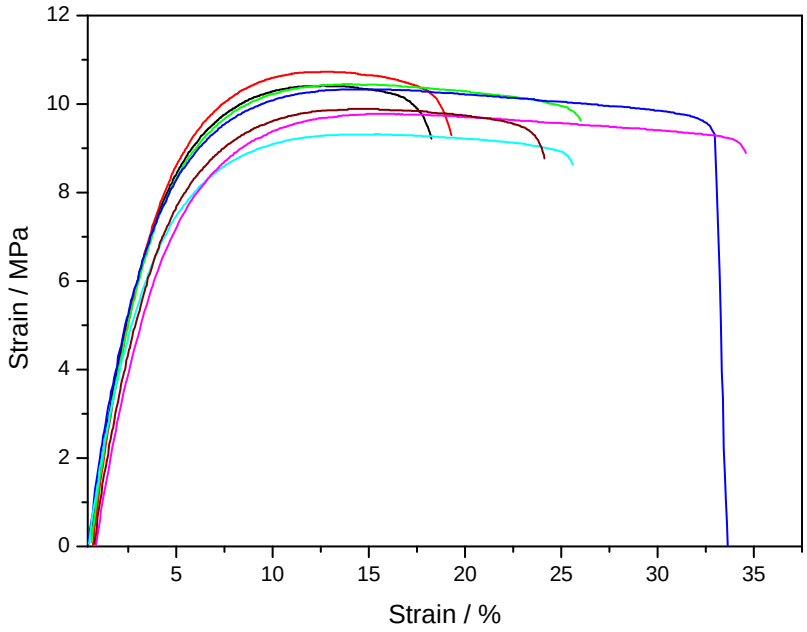

Figure D.8 Stress-strain curves of 88/10/2 w/w LDPE/WF/dLDPE using 5 weeks dLDPE as a compatibilizer

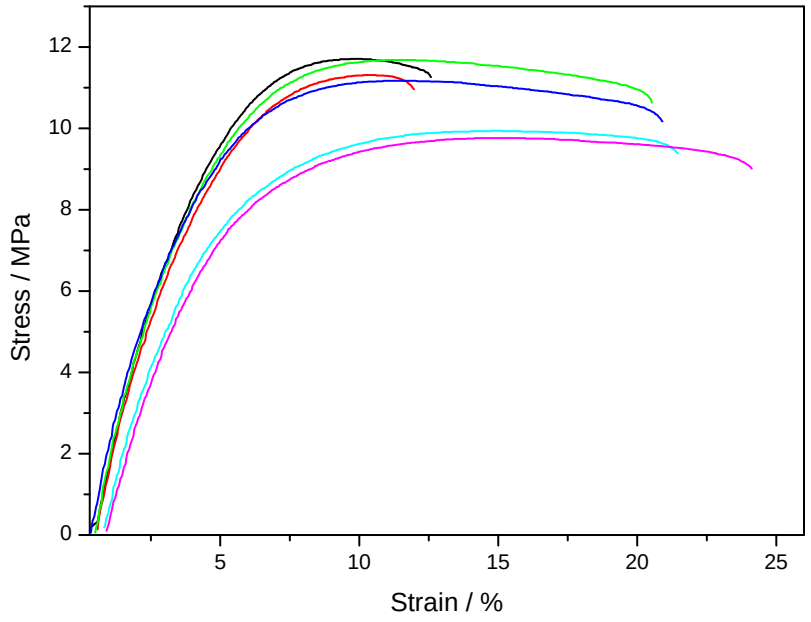

Figure D.9 Stress-strain curves of 85/10/5 w/w LDPE/WF/dLDPE using 5 weeks dLDPE as a compatibilizer

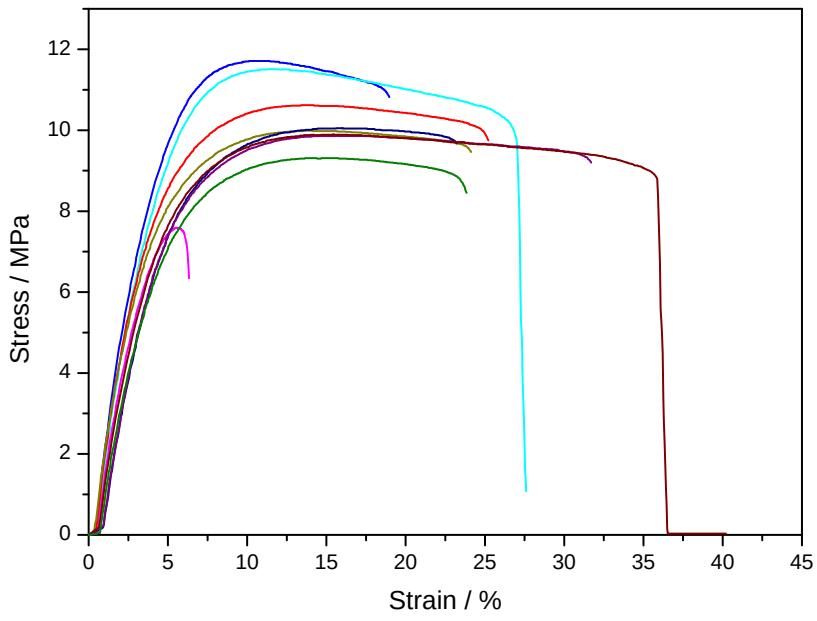

Figure D.10 Stress-strain curves of 83/10/7 w/w LDPE/WF/dLDPE using 5 weeks dLDPE as a compatibilizer

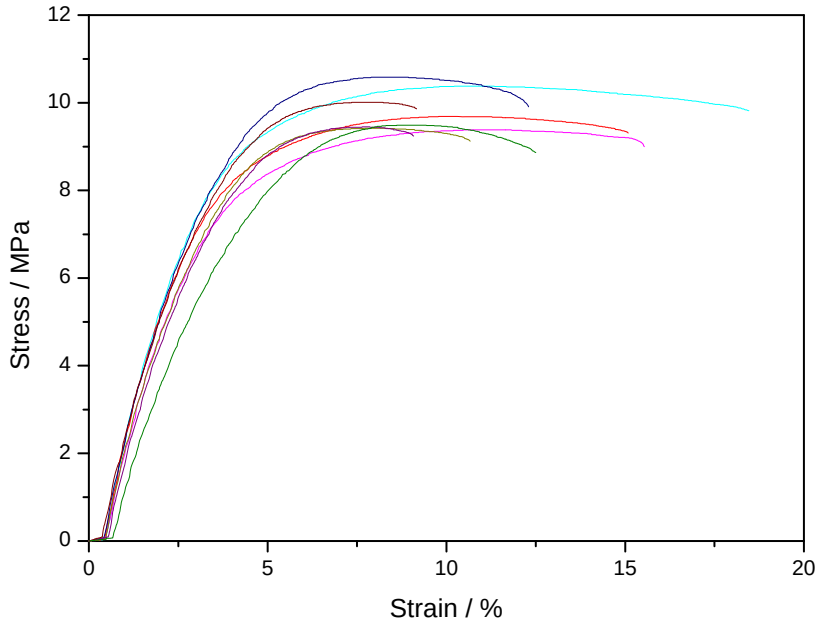

Figure D.11 Stress-strain curves of 78/20/2 w/w LDPE/WF/dLDPE using 5 weeks dLDPE as a compatibilizer

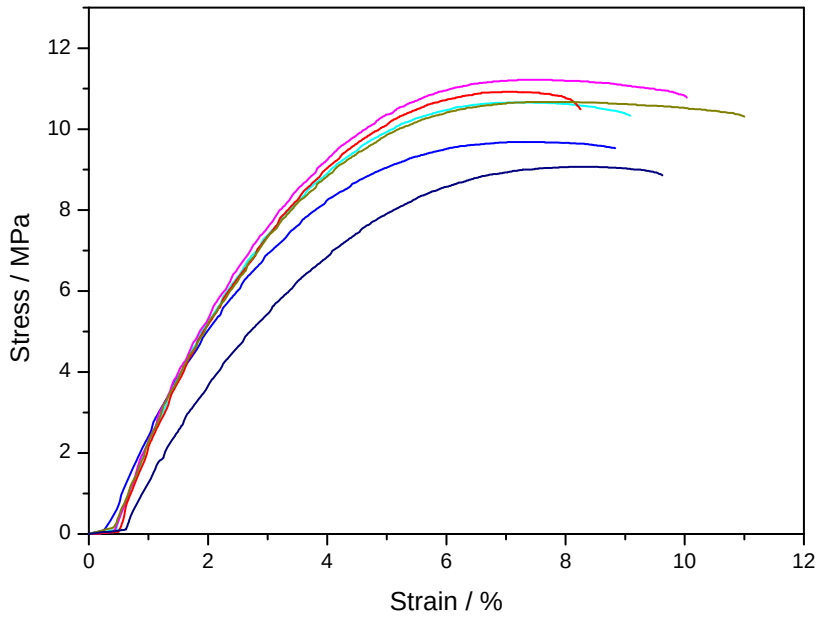

Figure D.12 Stress-strain curves of 75/20/5 w/w LDPE/WF/dLDPE using 5 weeks dLDPE as a compatibilizer

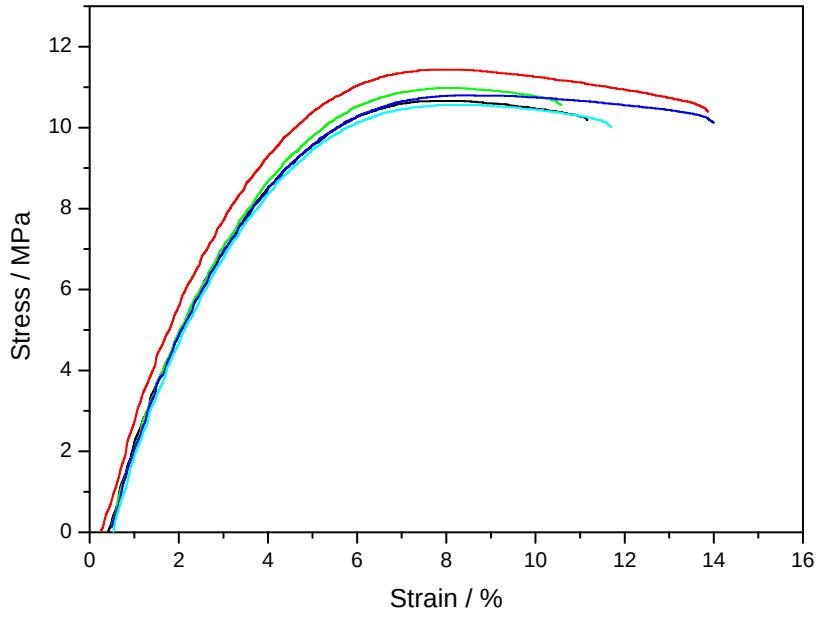

Figure D.13 Stress-strain curves of 73/20/7 w/w LDPE/WF/dLDPE using 5 weeks dLDPE as a compatibilizer

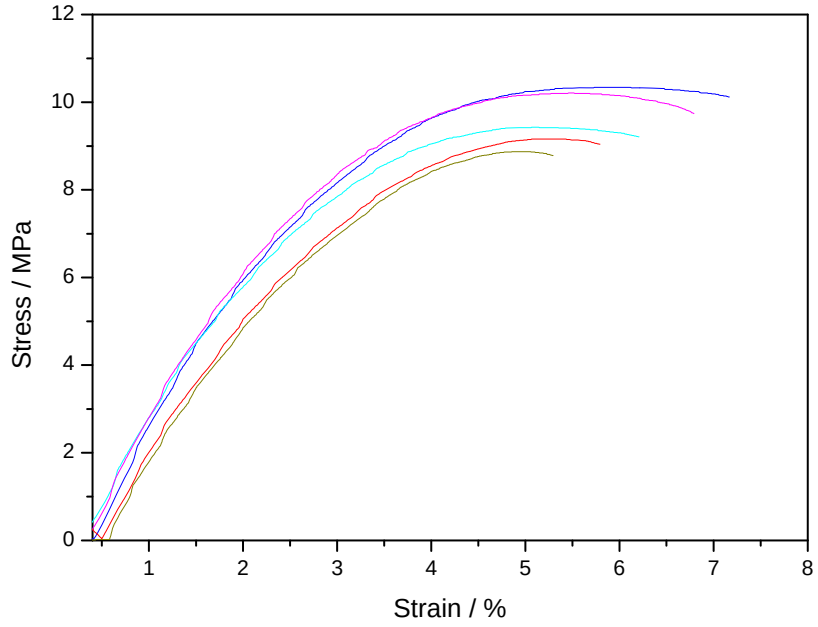

Figure D.14 Stress-strain curves of 68/30/2 w/w LDPE/WF/dLDPE using 5 weeks dLDPE as a compatibilizer

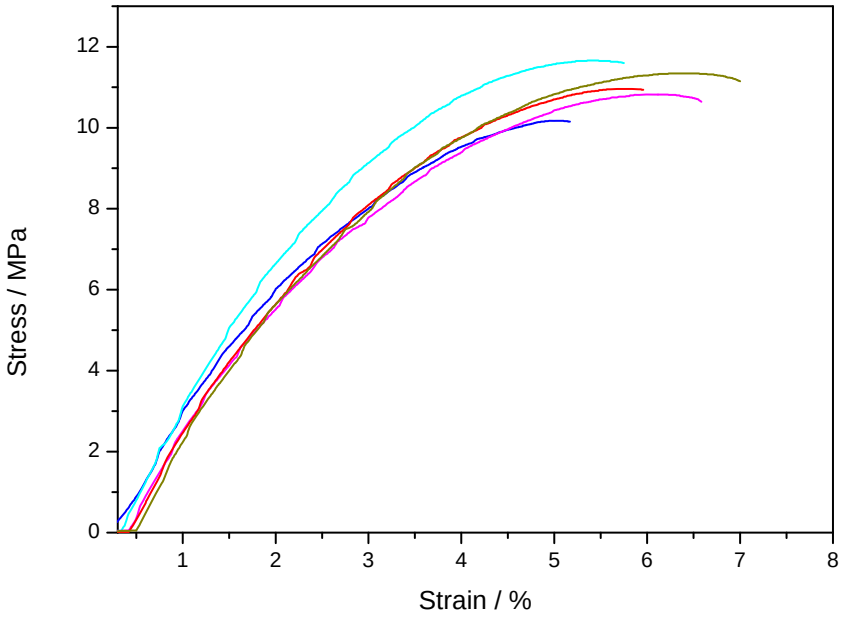

Figure D.15 Stress-strain curves of 65/30/5 w/w LDPE/WF/dLDPE using 5 weeks dLDPE as a compatibilizer

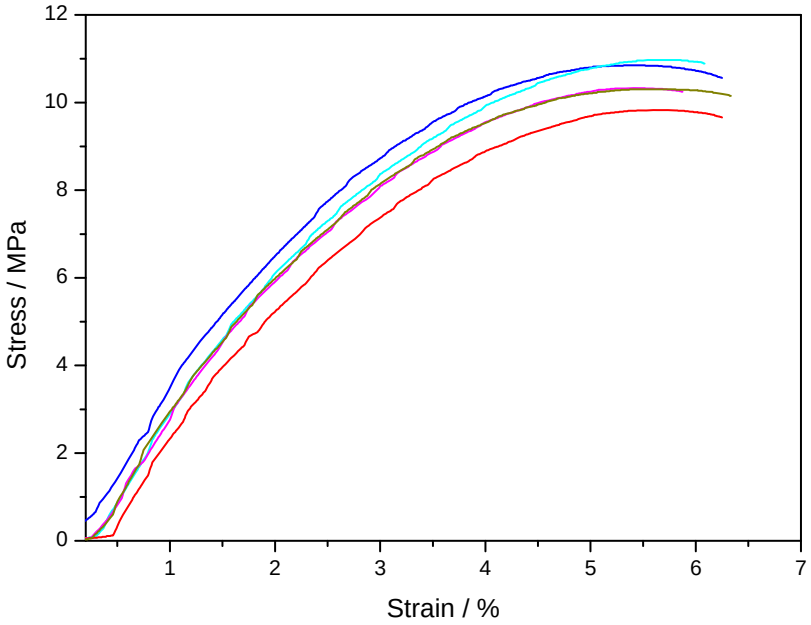

Figure D.16 Stress-strain curves of 63/30/7 w/w LDPE/WF/dLDPE using 5 weeks dLDPE as a compatibilizer